USGS-OFR-93-276

U.S. DEPARTMENT OF THE INTERIOR
U.S. GEOLOGICAL SURVEY

ONSHORE-OFFSHORE WIDE-ANGLE SEISMIC RECORDINGS OF THE SAN FRANCISCO BAY AREA SEISMIC IMAGING EXPERIMENT (BASIX): THE FIVE-DAY RECORDER DATA

By

Thomas M. Brocher[1] and Michael J. Moses[1]

Open-File Report 93-276

[1]345 Middlefield Road, M/S 977, Menlo Park, CA 94025

Menlo Park, California
1993

ABSTRACT

Wide-angle seismic reflection and refraction data were obtained in the vicinity of the San Andreas, Hayward, and Calaveras faults during the Bay Area Seismic Imaging eXperiment (BASIX) to define the crustal structure in the San Francisco Bay Area of California. In September, 1991, the U.S. Geological Survey's (USGS's) R/V **S.P. Lee**'s airgun array, totalling 96 liters (5824 cu. in.), was used as a seismic source for a marine reflection survey of the lower Sacramento River delta, San Francisco Bay, and the continental margin. This source was recorded on a temporary onshore seismic recorder array deployed by investigators from Stanford University, the USGS, the University of California at Berkeley, and Woods Hole Oceanographic Institution. The USGS deployed 18 three-component and 5 vertical-component land stations which continuously recorded the airgun signals on analog tape. The seismic stations (five-day recorders), deployed by the USGS to record the airgun signals, stretched from Golden Gate Park in San Francisco 160 km east to Copperopolis in the Sierran foothills. In this report, we describe the experiment, provide the locations and times of operation of all the onshore BASIX recorders, present the scheme followed to reduce the USGS five-day recorder data to seismic sections, and illustrate the wide-angle seismic data obtained by the five-day recorders.

CONTENTS

FIGURES

TABLES

INTRODUCTION

The Loma Prieta magnitude 7.1 earthquake of October 17, 1989 served both as a reminder of the active transpression along the San Andreas fault system and as a catalyst for studies aimed at better understanding the crustal structure in its vicinity (U.S. Geological Survey Staff, 1990). Results from seismicity and trenching studies indicate that the San Andreas fault is not the only major earthquake hazard in the San Francisco Bay Area. Recent seismicity compilations (e.g., Hill and others, 1990) show that the Hayward, Calaveras, and Greenville faults are seismically active, and the historical record indicates that these faults are capable of generating large-magnitude earthquakes (Ellsworth, 1990).

To date, seismicity, potential field data, and surface mapping have not revealed the nature of the subsurface connections of these faults, if any. Subsurface connections have been proposed to accommodate the fault-normal compression occuring across the San Andreas fault (Namson and Davis, 1988). Active transpression across the San Andreas and East Bay fault systems has been inferred from stress and geodetic measurements, focal mechanism studies, and other data (Zoback and others, 1987). The ongoing transpressional tectonics requires subhorizontal decollements to accommodate both the compressional and strike-slip motion (Namson and Davis, 1988), but the geometry of these surfaces in the San Francisco Bay Area, and their relation to the San Andreas and East Bay faults, is currently unknown.

A subsurface connection between the San Andreas and East Bay faults has also been proposed on the basis of thermal and mechanical modeling of the lithospheric slab window generated by the Mendocino triple junction (Furlong, 1984; Furlong and others, 1989). Either decollement or thermo-mechanical mechanisms for connecting faults beneath San Francisco Bay may explain the observed temporal pairing of large earthquakes occuring on the San Andreas and Hayward-Calaveras faults (Kerr, 1990).

Onshore wide-angle profiling by Catchings and Fuis (1991) support the hypothesis that large-amplitude reflections from the mid-to-lower crust and upper mantle may have increased

ground motions produced by the 1989 Loma Prieta earthquake at some distant sites (Somerville and Yoshimura, 1990), and provide additional motivation for the delineation of subhorizontal structures in the middle- to lower-crust. Given that reflections from the top of the upper mantle are frequently the most energetic arrivals at larger ranges, obtaining a better understanding of these focusing effects is critical for predicting strong ground motion patterns from expected earthquakes in the Bay Area.

In the following we describe and present the primary wide-angle seismic data resulting from an onshore-offshore seismic reflection/refraction investigation of the crustal structure beneath San Francisco Bay. These profiles were acquired as part of the Bay Area Seismic Imaging eXperiment (BASIX), whose core program included deep seismic reflection profiling conducted in September, 1991, using a marine airgun array and a telemetered hydrophone array (Furlong and others, 1991; Hart and Clymer, 1991; McCarthy and Hart, 1993). The wide-angle profiles were obtained to look for structures in the middle and lower crust which may accommodate the observed fault-normal compression as well as to place constraints on the subsurface dips of the major faults in the Bay Area. The wide-angle data were also acquired to obtain a better understanding of wave propagation characteristics in the Bay Area.

DATA ACQUISITION

Operations on the S. P. Lee

BASIX provided an opportunity to obtain wide-angle seismic reflection/refraction profiles in the vicinity of the San Andreas, Hayward, Calaveras, and Green Valley faults. The 12-element airgun array towed by the R/V **S.P. Lee**, totalled 96 liters (5858 cu. in.), generated seismic signals for a reflection profile along the northern half of San Francisco Bay (fig. 1). Due to shallow water depths in the Sacramento River and San Francisco Bay, each airgun was buoyed at a depth of 7.6 meters (25 feet) by a separate Norwegian buoy (McCarthy and Hart, 1993). The seismic reflection profile stretched along the Sacramento River from Rio Vista in the western Great

Valley through the Carquinez Strait to the San Francisco Bay and seaward to the Golden Gate. Because up to 120 telemetered moored hydrophones were used to obtain the seismic reflection data, the seismic profile was acquired in 13 separate, overlapping, segments (lines), each about 27 km long (figs. 2 and 3; Table 1).

Lines 101 to 109 form a continuous E-W profile across the Hayward-Rodgers Creek, Concord-Green Valley, and Antioch faults. The narrow navigatable channel along lines 101 to 109 caused these overlapping lines to be essentially coincident (fig. 2). Lines 110 to 113 were acquired to provide information on the crustal block between the San Andreas and Hayward faults. Lines 110 to 113 were acquired along a NW-SE trend in San Francisco bay proper and the **S.P. Lee** tracklines for these lines show greater divergence (fig. 3). Lines 201 and 202 constitute a short ENE-WSW transect from Alcatraz Island through the Golden Gate to beyond the San Andreas and San Gregorio faults (figs. 1 and 3).

The field operations for the reflection profiling resembled those of an onshore profile (McCarthy and Hart, 1993). Each day the moored hydrophones were shifted along the profiles; at night the **S. P. Lee** steamed along the hydrophone array while firing the airguns. The seismic reflection lines were acquired at night between 8 PM and 6 AM (local time) to minimize cultural and wind noise and interference from ship traffic. Along 10 of the 13 lines the **S.P. Lee** fired the airgun array while steaming along the line, then reversing course, duplicated the line by steaming in the opposite direction, further doubling the number of airgun shots available for stacking seismic signals. The nominal shot interval along all the reflection profiles was 50 m except along lines 201 and 202, which were obtained using 75 m shot intervals. More than 15,000 separate airgun shots were recorded during BASIX.

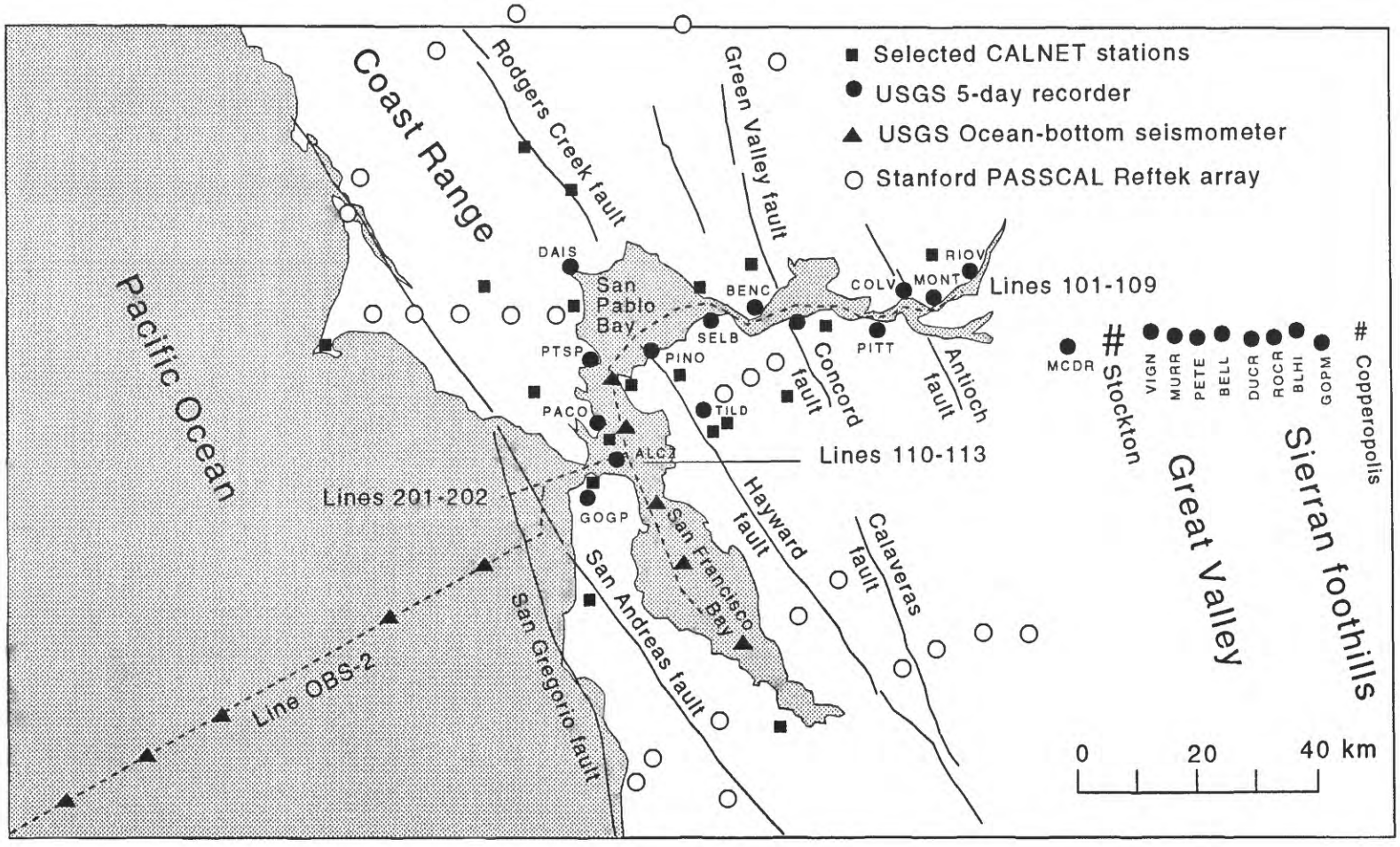

Figure 1. Index map showing location of BASIX seismic reflection lines (dashed lines) and wide-angle recorders. Selected CALNET stations, which also recorded the BASIX airgun signals, are also shown in this figure.

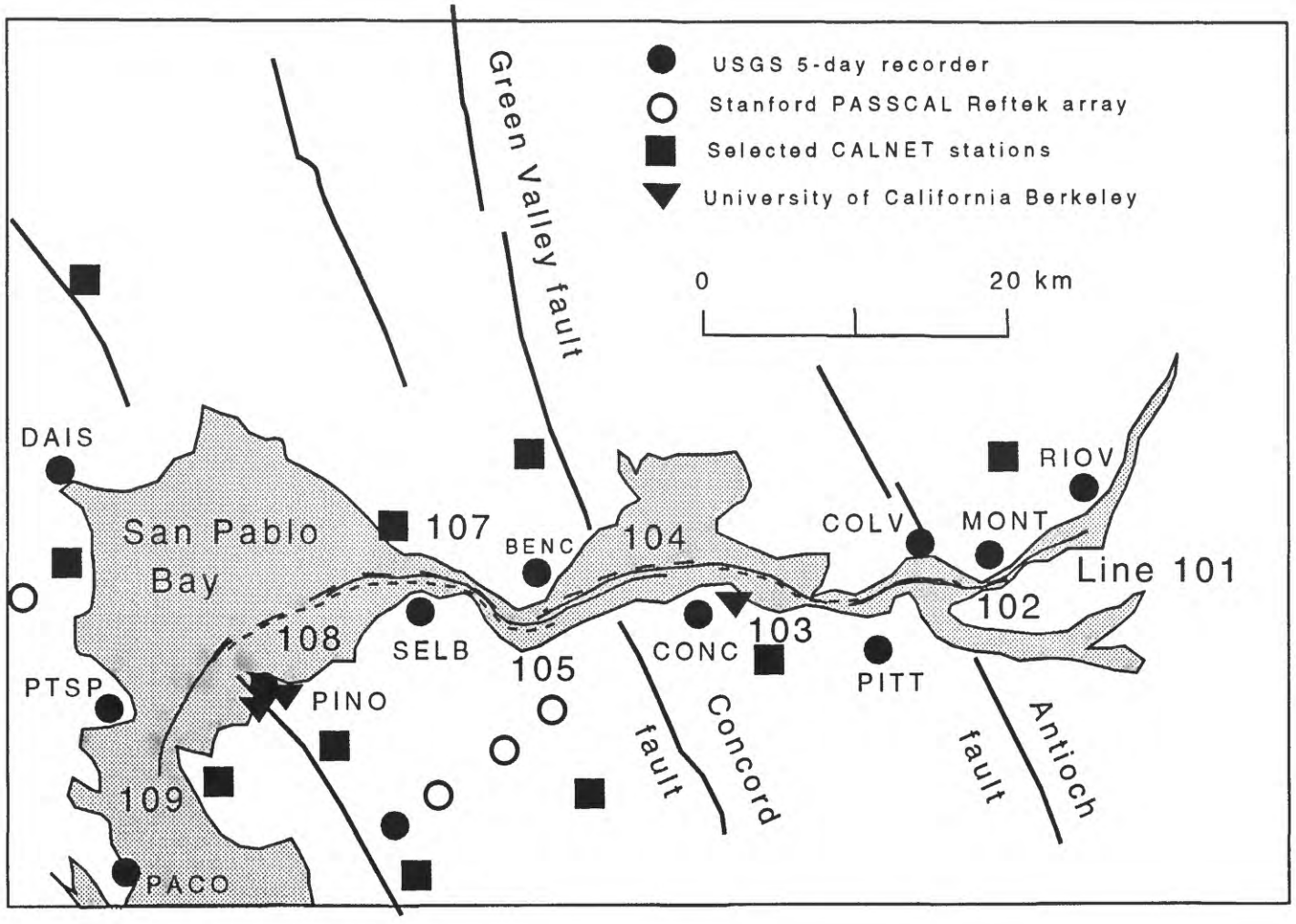

Figure 2. Expanded view of study area showing BASIX seismic reflection lines 101-109 (shown in various patterns) and the locations of wide-angle recorders.

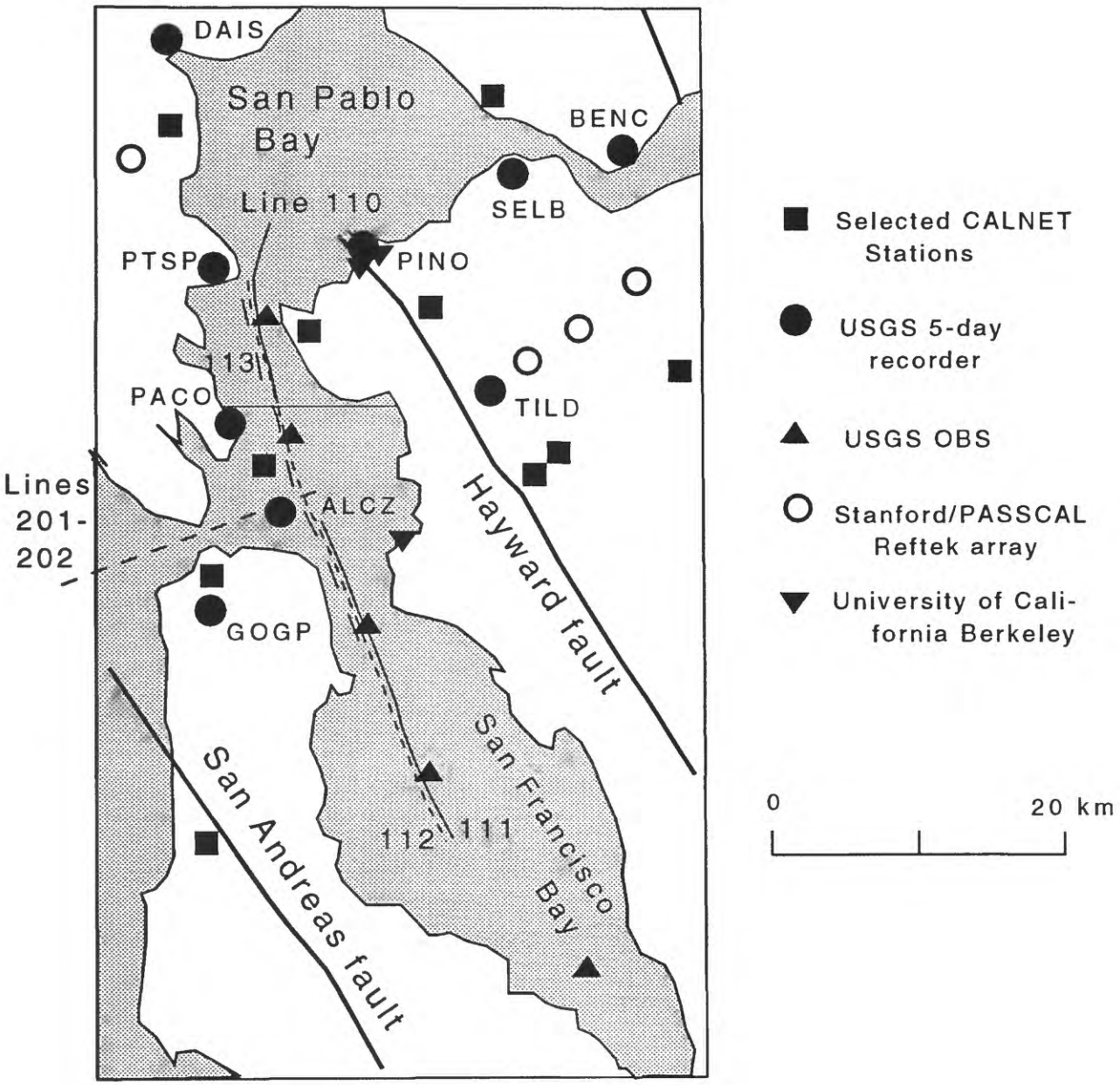

Figure 3. Expanded view of study area showing BASIX lines 110-113 and 201-202 (in various patterns) and wide-angle stations used to record these lines.

TABLE 1. R/V **S.P. Lee** Airgun Firing Times and Locations

Line	UCT Begin Day HRMIN	Lat. (N) Deg. Min.	Long. (W) Deg. Min.	UCT End Day HRMIN	Lat. (N) Deg. Min.	Long. (W) Deg. Min.
101	248 0424	38 05.24	121 44.75	248 1215*	38 02.85	121 53.43
102	249 0706	38 04.98	121 45.17	249 1045	38 03.60	121 59.47
103	250 0901	38 03.60	121 47.90	250 1300	38 02.20	122 07.50
104	251 0518	38 02.76	122 06.22	251 0712	38 03.94	122 03.15
105	252 0213	38 03.46	122 17.39	252 1227*	38 03.89	122 02.11
107	254 0250	38 00.15	122 22.00	254 1017*	38 02.76	122 10.57
108	255 0350	37 57.04	122 57.75	255 1048*	38 03.67	122 14.66
109	256 0330	37 53.29	122 25.77	256 1100*	38 03.24	122 18.63
110	257 0500	37 52.78	122 24.66	257 1152*	38 01.34	122 23.13
111	258 0609	37 45.54	122 21.64	258 1230*	37 36.46	122 17.04
112/ OBS-1#	259 0346	37 36.47	122 17.02	259 1053	37 57.58	122 26.69
113	260 0518	37 47.14	122 20.40	260 1217*	37 57.10	122 26.40
201	261 0512	37 47.55	122 31.92	261 1030*	37 50.79	122 24.83
202	262 0330	37 49.04	122 23.39	262 1115*	37 45.83	122 48.19
TR1#	262 1311	37 46.08	122 32.52	262 1417	37 40.80	122 32.80
OBS2#	262 1417	37 40.80	122 32.80	263 0430	37 12.52	123 31.22

#These lines were intended solely for recording by wide-angle recorders, no reflection profiles were obtained along these lines.
*The **S. P. Lee** reversed course along these lines and stopped approximately where it began; thus, the end time indicates when the **S.P. Lee** ceased firing the airgun array, and the end latitude and longitude indicate the location of the **S. P. Lee** at the farthest distance it reached from the beginning of the line.

In addition to the 13 reflection lines, the airgun array on the **S.P. Lee** was used solely as a seismic source for wide-angle profiles along three other lines: these include the NW-SE trending Line 112/OBS-1 in San Francisco Bay; a short transit leg, Line TR-1, south of the Golden Gate; and the E-W trending Line OBS-2 on the continental margin (fig. 1; Table 1). Lines OBS-1 and OBS-2 were obtained along two separate deployments of 6 USGS ocean bottom seismometers deployed by investigators from the USGS Branch of Atlantic Marine Geology and Woods Hole Oceanographic Institution (Holbrook and ten Brink, 1991; Brocher and others, 1991). The shot interval along Line 112/OBS-1 was 50 m. The shot interval for Lines TR-1 and OBS-2 was doubled to 100 m; Line OBS-2 was located coincident to seismic reflection Line 13 of Lewis

(1990) in order to provide deep structural control on the continental margin west of the San Andreas fault (figs. 1 and 4).

Within San Francisco Bay, navigation of the **S.P. Lee** and the airgun array was accomplished using a combination of GPS and land-based high-resolution Del Norte radio navigation, and is considered accurate to a few meters. Only the GPS positions were used during the reduction of the wide-angle data, yielding source location accuracy of a few tens of meters. Navigation for Lines 202 and OBS-2 seaward of the San Andreas fault was accomplished using a combination of GPS operated in a selected availability mode and rho-rho Loran-C, and is considered accurate to within 150 to 200 m. Shot instant times for the airgun array on the **S.P. Lee** were written to the seismic trace headers and recovered from these headers as described by Brocher and others (1992). A Kinemetrics True Time Satellite Clock Receiver (Model 468), set for the local delay appropriate for the GOES satellite, and stabilized using a high-precision Cesium oscillator, provided the absolute time base recorded on the **S.P. Lee**. The shot instant times are thus considered accurate to the nearest millisecond. These shot instant times were recovered from the seismic trace headers when the data were demultiplexed at the DISCO data processing center, and were merged into one computer file per seismic line along with the final navigation for the **S. P. Lee.**

Operation of the Onshore Array of Temporary Seismic Stations

A temporary array of 23 seismic stations, consisting of 18 three-component five-day recorders and 5 vertical-component seismometers telemetered to the 3-component recorders (Table 2), was used to record the entire set of seismic reflection lines acquired by the **S. P. Lee**. The analog three-component, five-day seismic recorders are described by Criley and Eaton (1978). These instruments have been used primarily for recording aftershock sequences and teleseismic studies of the lithosphere and record continuously using 1/2 inch analog magnetic tape. The combined frequency response of the 1 Hz geophones and internal five-day recorder electronics is heavily weighted to frequencies less than 15 Hz.

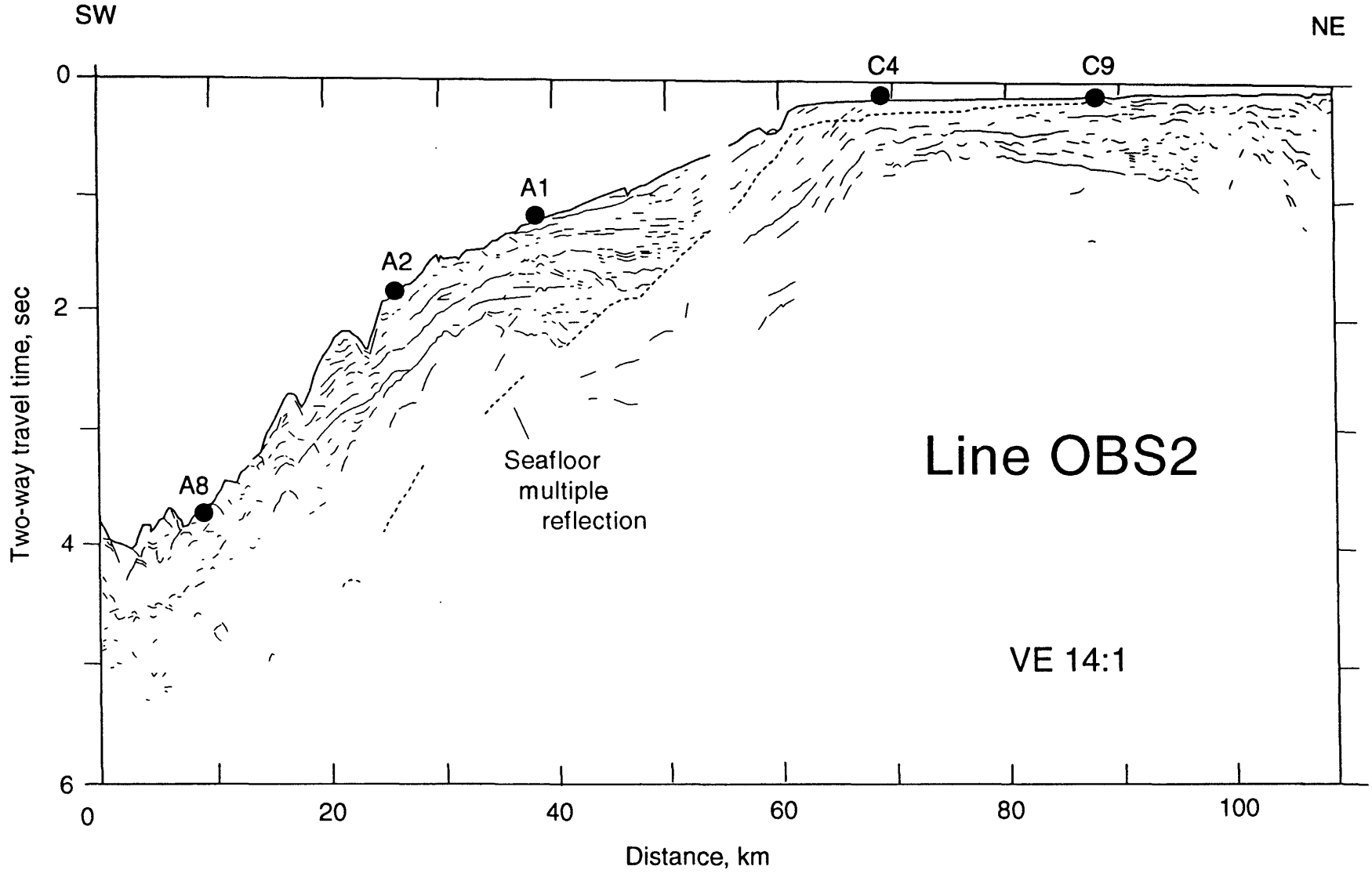

Figure 4. Line drawing of the unmigrated, single-fold reflection line OBS2, showing OBS locations as solid, labelled circles.

The field procedures used to deploy the five-day recorders were identical to those described for a similar experiment in north-central California (Brocher and others, 1992). Recorders were deployed near roads and were turned on prior to the commencement of the acquisition of the seismic reflection lines. At five sites in the eastern Great Valley and Sierran foothills west of Stockton (Figure 1), seismic signals from a vertical-component seismometer were telemetered to an adjacent five-day recorder. These sites were chosen for telemetry because of the dense station coverage telemetry provided there and because minimal radio interference was expected in this location. Recovery of data from the 5-day recorders for the BASIX study averaged about 90%.

TABLE 2. 5-day Recorder Station Locations and Elevations

Station Abbrev.	Station Name	Latitude (N) Deg. Min. Sec.	Longitude (W) Deg. Min. Sec.	Elevation (m)
GOGP	Golden Gate Park	37 46 14.503	122 28 33.928	99
ALCZ	Alcatraz Island	37 49 37.152	122 25 30.084	39
TILD	Tilden Park	37 54 31.192	122 15 16.713	261
PACO	Paradise Cove	37 53 49.139	122 27 49.220	46
PTSP	Pt. San Pedro	37 59 01.060	122 27 21.226	106
PINO	Pt. Pinole	38 00 34.106	122 21 50.306	9
DAIS	Day Island	38 06 11.854	122 29 20.724	39
SELB	Selby	38 03 16.689	122 14 30.752	64
BENC	Benecia	38 03 43.348	122 08 26.564	42
CONC	Concord	38 02 22.384	122 01 45.292	7
PITT	Pittsburg	38 00 31.457	121 54 38.691	35
COLV	Collinsville	38 04 58.344	121 51 12.702	0
MONT	Montezuma Hills	38 04 14.636	121 48 09.276	15
RIOV	Rio Vista	38 07 34.636	121 40 11.983	18
MCDR	MacDonald Road	37 57 52.517	121 28 15.961	-3
VIGN	Vignolo Road	38 00 14.238	121 10 59.749	17
MURR*	Murray Road	37 59 39.470	121 06 56.574	26
PETE*	Peters	37 58 48.146	121 02 20.808	38
BELL	Bellota Road	37 59 26.225	120 58 53.148	81
DUCR*	Duck River	37 58 20.993	120 54 25.947	91
ROCR*	Rock River	37 58 17.351	120 51 19.805	83
BLHI	Black Hill	37 59 01.722	120 47 22.479	204
GOPM*	Gopher Hill Mine	37 56 51.258	120 46 29.499	285

*Station consisted of a transmitter broadcasting signals from a vertical seismometer only.

Of the 23 stations deployed during the experiment (Table 2), a set of 3 stations in Golden Gate Park (GOGP), on Alcatraz Island (ALCZ), and in Tilden Park (TILD) were deployed to record reflection lines 201-202 and OBS-2 in an in-line and off-end geometry. Three other stations, at Paradise Cove (PACO), Pt. San Pedro (PTSP), and Pt. Pinole (PINO), all located on the western shore of San Pablo Bay, were deployed to record reflection lines 110-112/OBS-1 in an off-end geometry. The primary focus of our experiment, however, was the deployment of 17 stations along and off-end to reflection lines 101-109. As indicated in Figure 1 and in Table 2, this later set of stations stretched 160 km eastwards from Day Island (DAIS) on the western shore of the San Francisco Bay to Gopher Hill Mine (GOPM) in the Sierran foothills. Due to fears of signal loss through the peat layer in the Sacramento Delta (Vuillermoz and others, 1987), only one station, at MacDonald Road (MCDR), was deployed in the Great Valley. While a station in the Farallon Islands was desired, available funds did not permit the deployment of a recorder on these islands. We relied on stations in the permanent USGS CALNET earthquake network to fill gaps in our deployment of temporary recorders (Figure 1).

The five-day recorders and transmitter stations were deployed over a period of several days and were turned on prior to the acquisition of seismic reflection lines. Table 3 therefore provides a listing of the times for which each five-day recorder actually recorded data. Short (1-hour-long) gaps in the recording not shown in Table 3 were caused by the need to change tapes and refurbish the 5-day recorders at 4 to 5 day intervals. These short gaps occurred during daylight hours, when the **S.P. Lee** was not firing its airgun array. Thus, no wide-angle data were lost by the need to maintain the 5-day recorders. Where possible, we attempted to deploy the seismometers on hard rock to improve signal quality. The locations and elevations of the temporary seismic stations shown in Table 2 were determined from USGS topographic quadrangle sheets and are thought be accurate to within several tens of meters.

TABLE 3. 5-day Recorder Times of Operation

Station Abbrev.	Station Name	Time On JD Hr. Min.	Time Off JD Hr.Min.
GOGP	Golden Gate Park	247 2159	265 1830
ALCZ	Alcatraz Island	242 2007	266 1900
TILD	Tilden Park	246 2059	263 1822
PACO	Paradise Cove	246 2235	266 2300
PTSP	Pt. San Pedro	246 2124	267 2300
PINO	Pt. Pinole	246 1753	266 1846
DAIS	Day Island	246 1933	266 2000
SELB	Selby	246 2218	249 2300
		252 2236	263 1942
BENC	Benecia	247 2320	263 2128
CONC	Concord	247 2350	252 2300
		254 0220	263 2021
PITT	Pittsburg	247 1914	263 2231
COLV	Collinsville	249 2145	266 2127
MONT	Montezuma Hills	246 0045	251 1200
		253 0124	262 0000
		262 2305	266 2015
RIOV	Rio Vista	246 2206	247 0030
		252 2148	261 1900
		262 1935	266 1850
MCDR	MacDonald Road	249 2145	251 2007
		252 0136	267 0010
VIGN	Vignolo Road	244 0010	267 1720
MURR*	Murray Road	245 2144	249 0700
		250 2055	266 2220
PETE*	Peters	245 2144	249 0700
		250 2055	266 2220
BELL	Bellota Road	245 2144	249 0700
		250 2055	266 2220
DUCR*	Duck River	245 2144	249 0700
		251 0358	266 1800
ROCR*	Rock River	245 0216	266 1800
BLHI	Black Hill	245 0216	266 1800
GOPM*	Gopher Hill Mine	245 0216	266 1800

*Transmitter station consisting of vertical component seismometer only.

Additional wide-angle seismic profiles were recorded onshore throughout the Bay Area by permanent seismic network stations of the CALNET earthquake array and by temporary arrays of Reftek recorders deployed by Stanford University and by the University of California, Berkeley

(Figures 1-3). Investigators from Stanford University deployed PASSCAL Reftek recorders mainly in a fan geometry with respect to the reflection lines to determine whether there exist offset of crustal and Moho reflections across the major strike slip faults in the area (Klemperer and BASIX Working Group, 1991). The locations of the 38 stations occupied by researchers at Stanford University are provided in Table 4 and Figure 1. The Stanford University investigators deployed 5 PASSCAL recorders in-line to reflection lines 101-108 on the Marin Headland (stations A1-A5), 3 recorders in-line to reflection lines 201-202 (B2-B5), and 14 east-west (E-W) pairs of recorders in fan geometry north of the Bay (stations N1-N6) and south of the Bay (stations S7-S14). The CALNET, University of California, Berkeley, and Stanford University/PASSCAL recordings are described elsewhere. Table 5 provides the locations of ocean-bottom seismometers deployed during BASIX by investigators from USGS/Woods Hole and the Woods Hole Oceanographic Institution. Table 6 provides the locations of Reftek recorders deployed by the University of California, Berkeley.

TABLE 4. Stanford University PASSCAL Recorder Locations and Elevations

Station Abbrev.	Station Name	Latitude (N) Deg. Min. Sec.	Longitude (W) Deg. Min. Sec.	Elevation (m)
A1	D Ranch, Pt. Reyes	38 02 15	122 57 45	79
A2	Drake's Bay Beach	38 04 30	122 52 26.5	29
A3	Samuel Taylor State Park	38 02 20.5	122 42 56.5	73
A4	Lucas Valley Ranch	38 03 00	122 40 29.5	85
A5	Ignacio	38 03 43	122 34 38.5	73
B2	San Pablo Reservoir	37 56 47	122 14 25.5	104
B4	Martinez	37 58 26	122 07 51.5	98
B5	Pacheco	37 58 51.5	122 04 43.5	27

TABLE 4. Continued.

Station Abbrev.	Station Name	Latitude (N) Deg. Min. Sec.	Longitude (W) Deg. Min. Sec.	Elevation (m)
N1W	Salt Point	38 34 25.5	123 21 07.5	145
N1E	Seaview Ranch	38 32 56	123 13 50	431
N2W	Geyserville	38 44 08	122 58 59	111
N2E	Geyser Peak	38 45 49.5	122 50 32.5	1020
N3W	Jerusalem Grade	38 49 47	122 29 49	291
N3E	Knoxville	38 45 58	122 16 13	261
N4W	Pt. Reyes	38 10 34.5	122 56 22.5	180
N4E	Tomales	38 14 30	122 55 58	113
N5W	Windsor	38 32 57	122 50 24	50
N5E	Franz Valley	38 36 44	122 41 31	114
N6W	Iron Mt.	38 33 43	122 15 58	533
N6E	Rocky Ridge	38 31 45	122 05 38.5	506
S7W	Pescadero	37 17 16	122 23 14	178
S7E	Arata Ranch, Pomponio	37 17 52.5	122 21 48	216
S8W	Russian Ridge	37 19 18	122 13 02.5	591
S8E	Jasper Ridge	37 23 59	122 12 54.5	183
S9W	Coyote Hills	37 33 23	122 05 47.5	6
S9E	Rancho Arroyo	37 36 02.5	121 58 06	393
S10W	Mill Creek Road	37 31 48	121 52 19	486
S10E	Sunol Wilderness	37 32 53.5	121 49 31	265
S11W	Del Valle	37 32 58	121 39 59	276
S11E	Arroyo Mocho, Mines Road	37 33 11.5	121 34 00	750
S12W	Cascade Ranch, Año Nuevo	37 08 05	122 19 19	32
S12E	Last Chance Road, Big Basin	37 06 10.5	122 15 54	265
S13W	Bear Creek	37 09 41	122 01 34	671
S13E	Soda Springs, Lexington Res.	37 10 03.5	121 55 49	951
S14W	Silver Creek	37 17 19	121 46 43	108
S14E	Jos. Grant County Park	37 20 13	121 40 55.5	799

Note: Deployments A1-A5 and B2-B5 were located inline to the seismic reflection lines 101-108. Deployments N1-N6 and S7-S14 have a fan geometry to the seismic reflection lines, and were located to the north and south of the San Francisco Bay, respectively.

TABLE 5. USGS Ocean-bottom Seismometer Locations and Depths

OBS ID	Latitude (N) Deg. Min.	Longitude (W) Deg. Min.	Depth (m)
	OBS-1 Deployment		
A1	37 33.4046	122 11.7081	15
A2	37 40.5028	122 18.9071	10
C4	37 46.1819	122 20.8038	17
A8	37 52.1990	122 24.2006	16
C9	37 57.5991	122 26.9887	--
	OBS-2 Deployment		
A8	37 14.962	123 25.21	2710
A2	37 19.185	123 15.684	1330
A1	37 22.36	123 08.30	860
C4	37 31.60	122 50.94	100
C9	37 37.008	122 40.469	80

TABLE 6. Locations of Reftek Recorders Deployed by University of California Berkeley

Channel	Latitude (N)* Degrees	Longitude (W)* Degrees	Elevation (m)
		Concord Naval Weapons Station	
East Array (recorded lines 101, and 103-5)			
3	38.04054	121.98863	18
2	38.04054	121.98977	21
1	38.04054	121.99091	21
4	38.04054	121.99205	18
5	38.04054	121.99319	15
6	38.04054	121.99433	13
West Array (recorded lines 103 and 105)			
3	38.04054	121.99569	12
2	38.04054	121.99683	12
1	38.04054	121.99797	15
4	38.04054	121.99911	16
5	38.04054	122.00025	17
6	38.04054	122.00139	17
		Point Pinole	
South Array (recorded lines 108-110)			
3	37.97802	122.36200	18
2	37.98133	122.36147	18
1	37.98209	122.36093	18
4	37.98285	122.36039	18
5	37.98362	122.35985	18
6	37.98438	122.35930	18
North Array (recorded lines 107-110)			
3	37.99657	122.34690	3
2	37.99731	122.34627	3
1	37.99804	122.34563	3
4	37.99878	122.34500	3
5	37.99771	122.34438	3
6	38.00025	122.34373	3
		Bay Bridge	
East Array (recorded lines 113 and 201)			
3	37.83226	122.31532	2
2	37.82215	122.31645	2
1	37.82204	122.31760	2
4	37.82192	122.31874	2
5	37.82181	122.31989	2
6	37.82170	122.32103	2

TABLE 6 continued.

Channel	Latitude (N)* Degrees	Longitude (W)* Degrees	Elevation (m)
		Bay Bridge	
West Array (recorded lines 113 and 202)			
3	37.82159	122.32217	2
2	37.82147	122.32331	2
1	37.82136	122.32446	2
4	37.82124	122.32560	2
5	37.82113	122.32675	2
6	37.82102	122.32788	2

*Coordinates are for the North American Datum of 1927.

DATA REDUCTION

Data Playback

The playback and digitization of the five-day recorder tapes, the formating of the digitized data into SEG-Y format, and the subsequent processing of the record sections were nearly identical to those described by Brocher and others (1992). We digitized the analog five-day recorder data at 100 samples/sec by running the software program called xdetectv using an Everex 386/25 MHz computer with 4 Mbytes of internal memory and 330 Mbytes of hard disk memory. Xdetectv is a version of xdetect, described by Tottingham and Lee (1989). The analog tape drive was manually positioned to the desired time on the tape for the start of digitizing with the aid of an IRIG-C clock code reader. Up to 260-minute-long blocks of analog data were digitized in a single pass requiring about 13 minutes of playback time. The digitized data were temporarily stored in Seismic Unified Data System (SUDS) format on the Everex computer (Ward and Williams, 1992), then transfered to a 2 GByte disk drive on the VAX 11/785, where the data were demultiplexed into two different time code channels and 6 seismometer channels (three low-gain channels and three high-gain channels).

The time of the digitized files were determined using recorded WWVB time code broadcast from Denver, Colorado, in addition to a recorded internal IRIG-C clock code, both of which were recorded continuously at each station. Because WWVB time is accurate to a few milliseconds, we used the WWVB clock code to determine the time on 99% of the digitized files. When WWVB code could not be used, however, we relied on the internal clock code in IRIG-C format.

We converted the digitized WWVB clock code to a binary signal by equating the largest positive values (generally in the range of +3000 to +5000 counts) as equal to one and all smaller values (generally in the range of +1000 to +2000 counts) as zero. We filtered this binary code to remove short (1 to 3 sample long) noise pulses in the time code. A software program, SUDIRIGTOVB.FOR, decoded the times of the minute marks on the time code and determined the sample number at the beginning of each minute mark. A second software program, SUDTOSEGY.FOR, counted second marks (where the binary code changes from zero to one) to determine the time within the digitized file; this time was verified and updated using the sample numbers of the minute marks. The digitized file was broken into individual traces for each airgun shot based on the reduced travel time for that receiver using a velocity of 6 or 8 km/s. The reduced travel time was calculated from a list of shot times and locations, the receiver location, and the reduction velocity (6 or 8 km/s). Twenty-three seconds of data were saved for each trace. The individual traces were then written in SEG-Y format to a 9-track digital tape (see below).

Most of the software used for this processing sequence was described by Brocher and others (1992). The record sections were then filtered and plotted using DISCO Processing Software as described by Brocher and Moses (1990). On many of the sections shown here, a predictive deconvolution, based on the Wiener-Levinson algorithm, has been applied. We used a 0.5 s operator length, a 0.01 s gap, and a 4 s design window centered on the first arrivals for the deconvolution of the entire trace.

The redundancy of airgun shotpoints caused by the overlapping and reshooting of lines allowed us to determine whether features observed in the data result from complexities introduced by the geology or whether they resulted from equipment malfunctions or digitizing problems. The

relatively high-fold of the wide-angle data (up to 5-6 fold along lines 101-109) and high-coherence of the data also allowed us to stack the wide-angle data to improve signal to noise levels. For the two line segments defined by lines 101-109 and 110-113, we binned the data according to range and stacked the data within bins 50 m wide after reduction to 8 km/s. Reduced record sections plotted with a scale of 4 to 5 inches per second suggest that there is little relative moveout for arrivals within this short range bin.

SEG-Y Tape Format

The wide-angle seismic reflection/refraction profiles were written to 9-track tapes in SEG-Y format. For most recorders three traces were written for each shot: trace 1 contains the high-gain N/S horizontal seismometer component; trace 2 contains the high-gain vertical seismometer component; and trace 3 contains the high-gain E/W horizontal seismometer component. Each trace contains a 240-byte trace header of 2- and 4-byte integers describing the specific trace and 2301 2-byte integer data samples. For stations consisting solely of a transmitter, only a single trace is written for each shot and receiver pair; trace 1 contains a high-gain vertical seismometer component. The location of each value in the SEG-Y trace header as described by Barry and others (1975) was slightly modified as described by Luetgert and others (1990). All trace integer values were byte swapped from DEC to SEGY-IBM format and are written in SEGY-IBM 16INT format. An End of Tape (EOT) mark was written at the end of each 12-inch, 6250 BPI, SEG-Y tape.

DESCRIPTION OF THE DATA

In the following section we describe the data in terms of the four major lines acquired during the BASIX experiment in the order the lines were collected. In general, the quality of data acquired by stations in the Coast Range (ALCZ, PACO, PTSP, PINO and DAIS), East Bay Hills (TILD), and eastern Sierra foothills (DUCR, ROCR, BLHI, and GOPM) are superior to those acquired east of Concord and in the Great Valley. A peat layer underlying the Sacramento Delta

east of Concord (Vuillermoz and others, 1987) is thought to account for the lower signal levels of the stations in the middle of our array (CONC, PITT, COLV, MONT, RIOV, and MCDR). Data from stations in the Great Valley (VIGN, MURR, PETE, and BELL) near Stockton (Figure 1) were probably adversely affected by cultural noise and poor propagation characteristics of the Great Valley fill. The quality of the recorded data is generally highest for those stations nearest the airgun source and decreases as the distance of the five-day station to the airgun line increases. Table 7 presents a list of the source-receiver ranges recorded by each station for each of these lines, and indicates the closest approach of the airgun array to the recorder.

TABLE 7. Offset Ranges of Wide-angle Seismic Profiles

Station Abbrev.	Station Name	Recorded Ranges (km) Lines 101-109	Lines 110-113 (including OBS1)
GOGP	Golden Gate Park	25.9-77.3	26.1-8.5-30.4
ALCZ	Alcatraz Island	34.3-65.6	Not recorded
TILD	Tilden Park	17.9-15.8-52.9	34.1-12.3-18.2
PACO	Paradise Cove	12.1-70.4	36.9-1.6-17.2
PTSP	Pt. San Pedro	3.6-67.0	45.4-1.6-9.6
PINO	Pt. Pinole	5.0-2.1-58.5	46.0-2.1-4.2
DAIS	Day Island	13.5-12.1-68.3	58.9-12.1
SELB	Selby	16.8-0.7-47.1	50.4-11.0
BENC	Benecia	25.5-3.0-38.2	52.4-19.9
CONC	Concord	34.6-2.5-29.1	53.1-29.3
PITT	Pittsburg	44.7-3.8-21.0	55.3-39.8-44.1
COLV	Collinsville	50.6-2.1-13.0	64.9-45.1
MONT	Montezuma Hills	54.8-1.0-9.3	66.5-49.4
RIOV	Rio Vista	67.3-44.2	78.9-61.8
MCDR	MacDonald Road	83.5-50.6	86.3-78.7-85.7

TABLE 7 continued.

Station Abbrev.	Station Name	Recorded Ranges (km) Lines 101-109	Lines 110-113 (including OBS1)
VIGN	Vignolo Road	108.6-47.7	111.8-103.7-108.2
MURR*	Murray Road	114.6-86.6	117.6-109.6-115.0
PETE*	Peters	121.3-86.3	124.3-116.4-122.9
BELL	Bellota Road	126.4-91.5	129.4-121.4-127.1
DUCR*	Duck River	132.9-97.9	135.8-127.0-134.8
ROCR*	Rock River	137.5-76.6	140.3-131.3-139.4
BLHI	Black Hill	143.2-82.0	146.2-137.2-144.5
GOPM*	Gopher Hill Mine	147.6-87.0	150.3-140.1-150.3

Station Abbrev.	Station Name	Recorded Ranges (km) Lines 201-202	Line TR1	Line OBS2
GOGP	Golden Gate Park	17.4-4.5-11.4	5.8-11.5	11.6-111.4
ALCZ	Alcatraz Island	22.7-1.0-3.9	12.4-19.2	19.3-118.6
TILD	Tilden Park	39.8-14.8	29.9-35.8	35.9-136.1
PACO	Paradise Cove	23.0-5.8-11.1	16.7-24.9	24.9-120.6
PTSP	Pt. San Pedro	30.5-14.2-19.4	Not recorded	Not recorded
PINO	Pt. Pinole	37.9-17.1	31.3-39.6	39.7-135.3
DAIS	Day Island	40.6-27.8-33.0	37.8-47.0	47.0-134.6
SELB	Selby	49.2-26.2	41.6-49.2	49.2-146.7
BENC	Benecia	56.8-32.7	48.3-55.1	55.2-154.2
CONC	Concord	63.9-39.1	54.4-60.2	60.3-79.9
PITT	Pittsburg	72.0-47.0	61.7-66.5	66.6-167.5
COLV	Collinsville	79.9-54.9	Not recorded	Not recorded
MONT	Montezuma Hills	70.8-58.4	Not recorded	142.6-179.2
RIOV	Rio Vista	84.5-71.5	Not recorded	91.4-192.4
MCDR	MacDonald Road	107.9-82.3	96.8-99.5	119.4-199.4
VIGN	Vignolo Road	133.6-108.0	122.4-125.0	125.1-224.4
MURR*	Murray Road	139.3-113.7	128.0-130.4	130.5-229.5
PETE*	Peters	145.6-120.1	134.3-136.6	136.7-235.2
BELL	Bellota Road	150.8-125.2	139.5-141.8	141.9-240.4
DUCR*	Duck River	157.0-131.4	145.6-147.7	147.8-245.8
ROCR*	Rock River	161.5-135.9	150.1-152.1	152.2-250.1
BLHI	Black Hill	167.4-141.8	156.1-158.1	158.1-256.0
GOPM*	Gopher Hill Mine	171.1-145.6	159.7-161.5	161.5-258.7

Lines 101-109, which have a combined length of 63 km, were recorded at source-receiver offsets ranging from as little as 0.7 km to as large as 147.6 km. These recordings show a large delay in Pg arrival times across the Hayward fault and between the Green Valley and Antioch faults (figs. 5-26). An observed 0.8 s delay of Pg at a range of about 43 km on Figure 9 is consistent with a down-to-the-east offset across the Green Valley fault. A smaller down-to-the-west offset is observed across the Antioch fault on the same figure at a range of about 60 km. Strong diffractions having a lower phase velocity than Pg can be traced to surface locations of the Green Valley and Antioch faults. Stations in the western Sierran foothills (DUCR, ROCR, BLHI, and GOPM) record arrivals having an apparent velocity close to 8 km/s and are interpreted as upper mantle refractions, or Pn.

The onshore recordings of lines 110-113 (this includes line OBS1), spanning a length of 49 km, range from an inline to distinctly fan configuration. The inline stations (PACO, PTSP, PINO, and DAIS, shown in figs. 27-29) represent single-fold plots of portions of lines 110-113 and display a very linear Pg arrival having an apparent phase velocity of 5.95 km/s. Fan data plotted in Figures 30 to 33 for stations east of Selby (SELB) represent stacks of portions of lines 110-113 (Shots 1-157 and 531-707 of Line 110; Shots 181-520 and 618-798 of Line 111; Shots 97-121 of Line 112; and Shots 7-51 and 687-906 of Line 113). Source-receiver offsets from 1.6 to 150 km were recorded by the five-day recorders. Wide-angle reflections from two-way travel times (twtt) between 6 and 8 s recorded on stations in the vicinity of San Pablo Bay are particularly well-displayed on Figure 28 for station PTSP. Reflections at 9 and 11 s twtt are also observed.

Lines 201-202 span a distance of about 25 km. Onshore recordings of these lines were made at offsets as small as 1 km to as large as 171 km (Figures 34-45). The 6 to 8 s twtt reflections imaged on lines 110-113 are also observed on recordings of lines 201-202 made at stations ALCZ, GOGP, and TILD (Figures 34-35). The onshore recordings of these lines show an abrupt truncation of a wide-angle reflection at the San Andreas fault, as well as diffracted arrivals which originate at the fault zone.

Lines TR1 and OBS2 transit the continental shelf and slope, and for the plots presented here, records obtained from these lines have been merged (figs. 46-66). Wide-angle recordings of line OBS2 are very similar to recordings obtained along the Año Nuevo transect during seismic reflection line 32 by Brocher and others (1992). The quality of the recordings obtained during lines TR1 and OBS2 are generally inferior to those for other lines, probably because OBS2 was obtained during daylight when cultural noise levels are higher, and because the recordings represent only single-fold data. These profiles, which captured source-receiver offsets ranging from 11.6 to 258.7 km, show Pg arrivals having phase velocities close to 6 km/s. The first arrivals are cutoff at offsets greater than about 60 km perhaps by a low-velocity zone (figs. 46-67). Faint but coherent refractions from the upper mantle, Pn, emerge as first arrivals at ranges of about 90 km on the record from Day Island (DAIS). Pg arrivals can be traced as secondary arrivals to distances beyond 130 km.

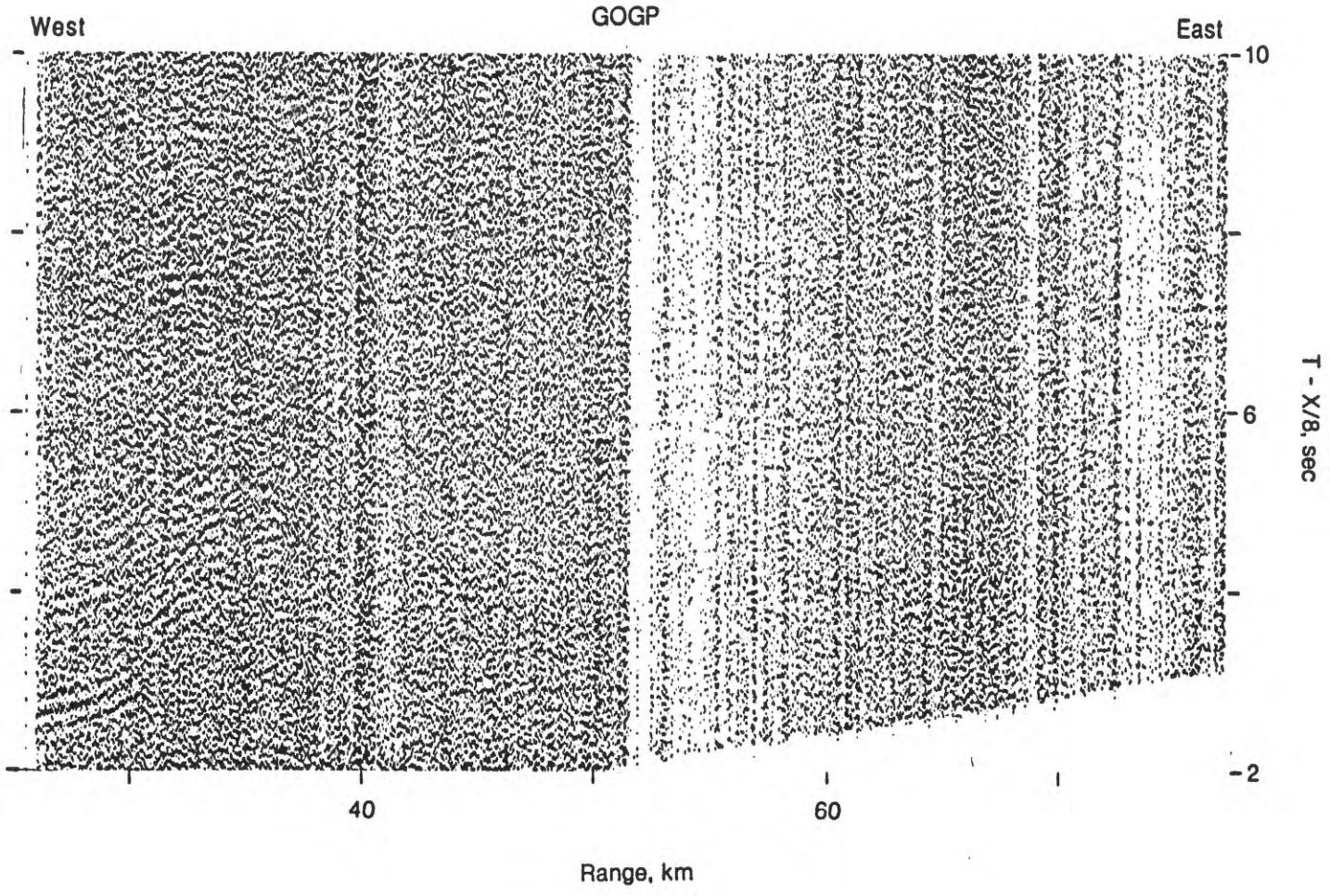

FIGURE 5. Receiver gather for station GOGP from lines 101-109. The record section has been linearly reduced using a velocity of 8 km/s and trace amplitudes have been scaled according to $\text{Range}^{0.7}$.

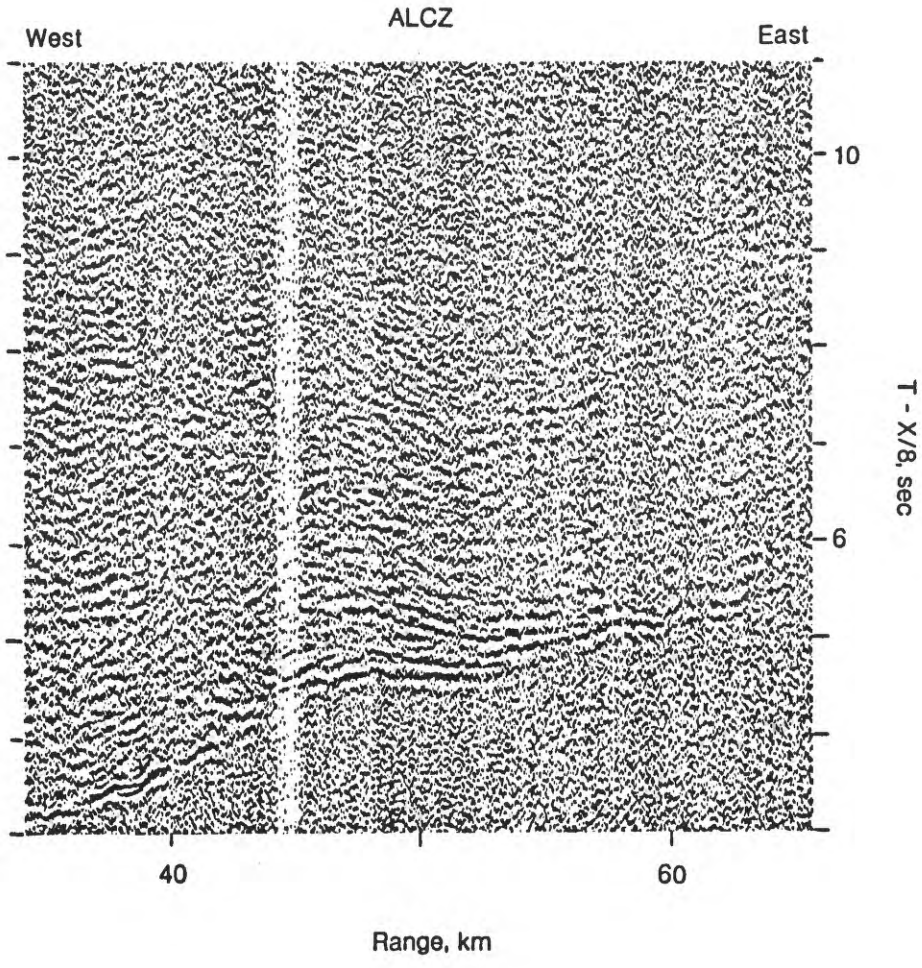

FIGURE 6. Deconvolved receiver gather for station ALCZ from lines 101-105. The record section has been linearly reduced using a velocity of 8 km/s and trace amplitudes have been scaled according to Range$^{0.7}$.

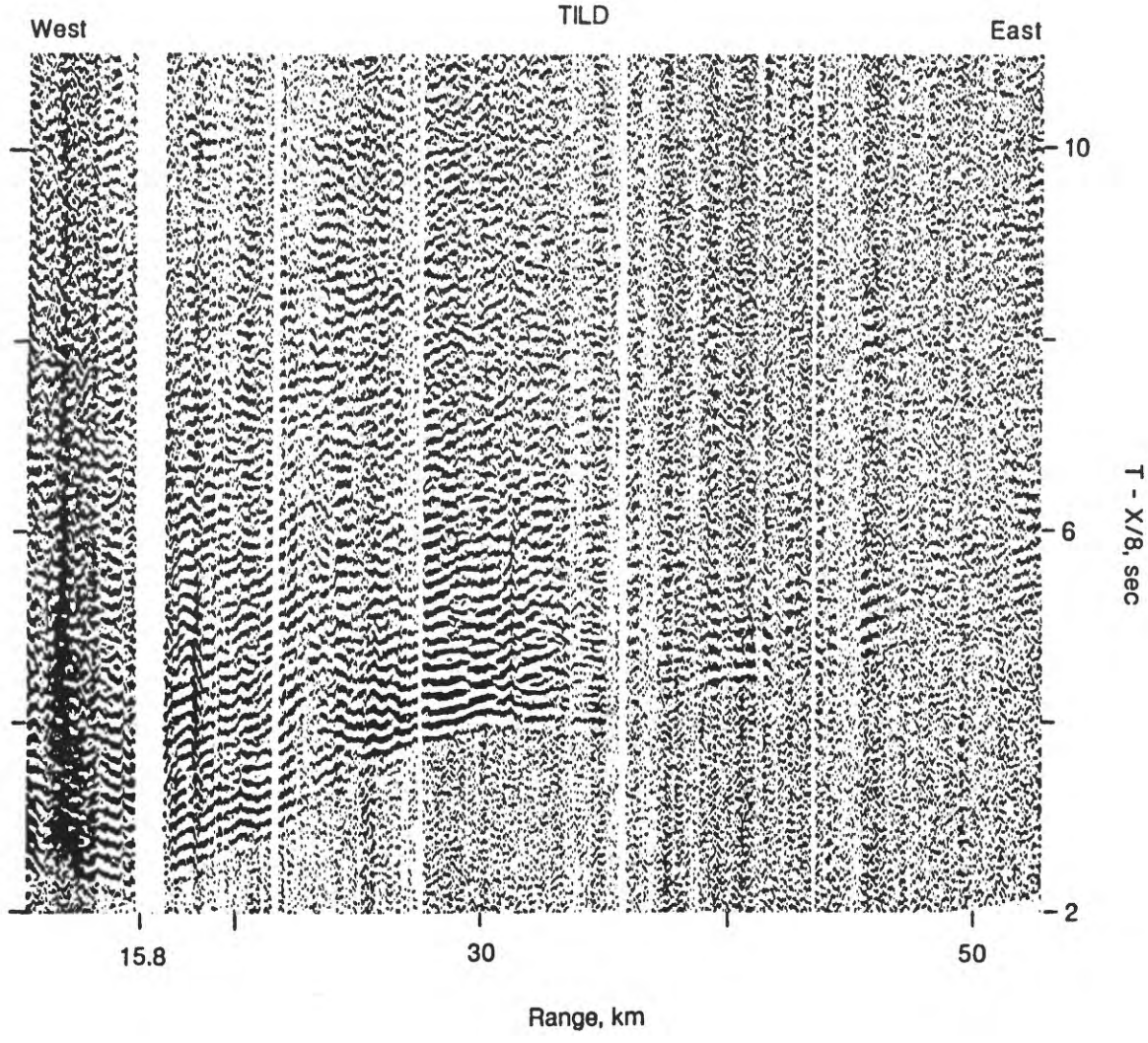

FIGURE 7. Deconvolved receiver gather for station TILD from lines 101-109. The record section has been linearly reduced using a velocity of 8 km/s and trace amplitudes have been scaled according to Range$^{0.7}$.

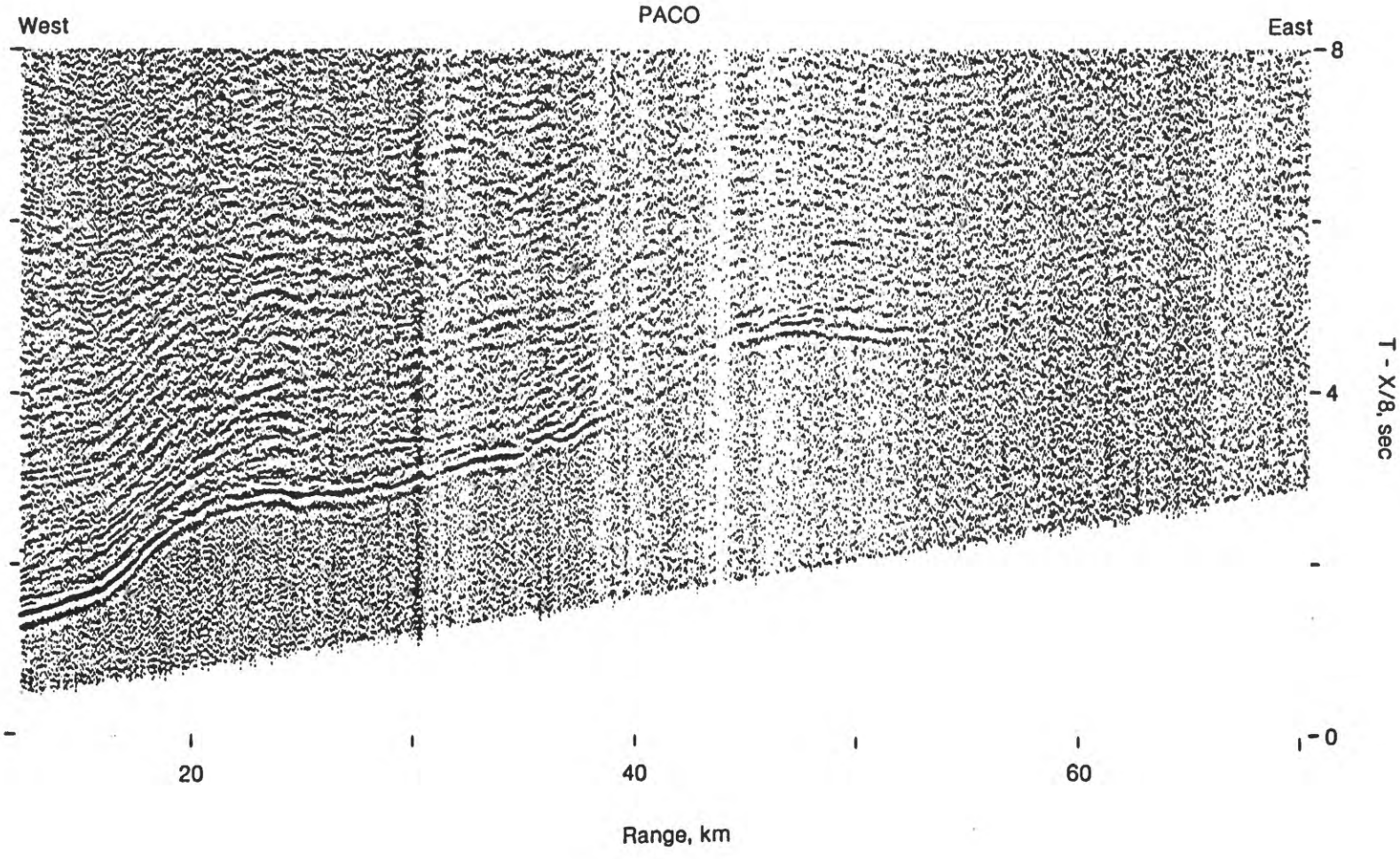

FIGURE 8. Deconvolved receiver gather for station PACO from lines 101-109. The record section has been linearly reduced using a velocity of 8 km/s and trace amplitudes have been scaled according to Range$^{0.7}$.

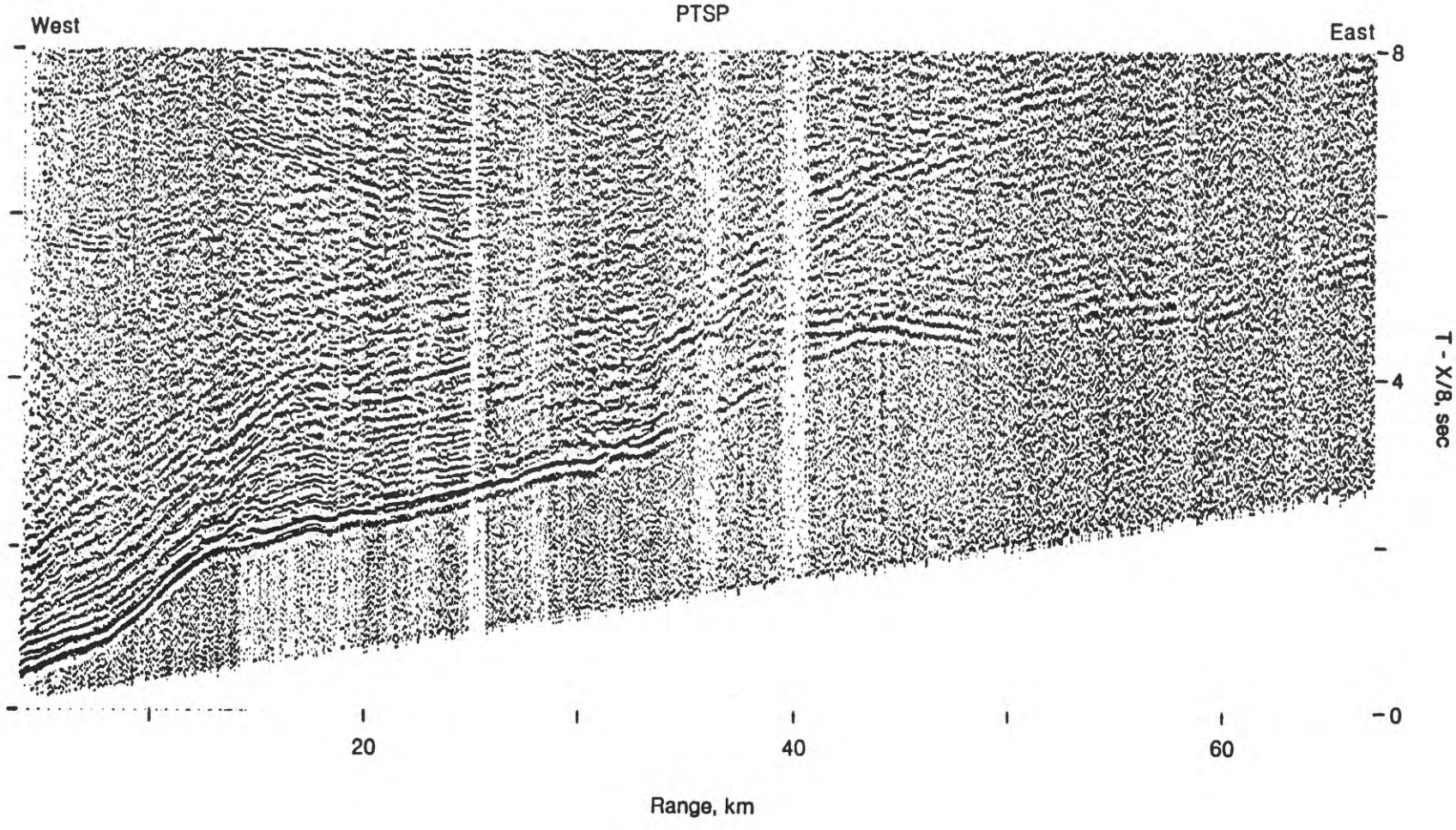

FIGURE 9. Deconvolved receiver gather for station PTSP from lines 101-109. The record section has been linearly reduced using a velocity of 8 km/s and trace amplitudes have been scaled according to Range$^{0.7}$.

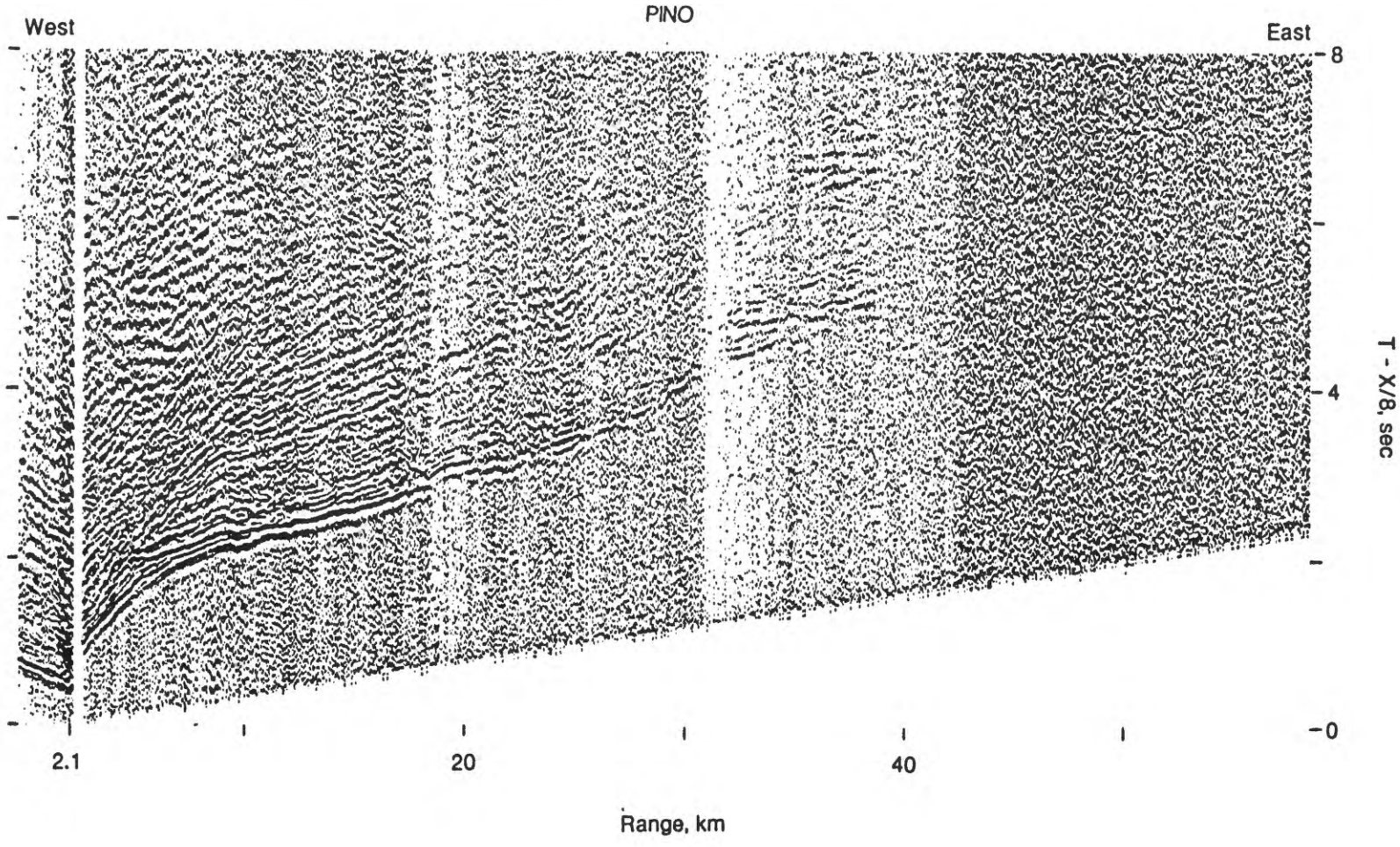

FIGURE 10. Deconvolved receiver gather for station PINO from lines 101-109. The record section has been linearly reduced using a velocity of 8 km/s and trace amplitudes have been scaled according to Range$^{0.7}$.

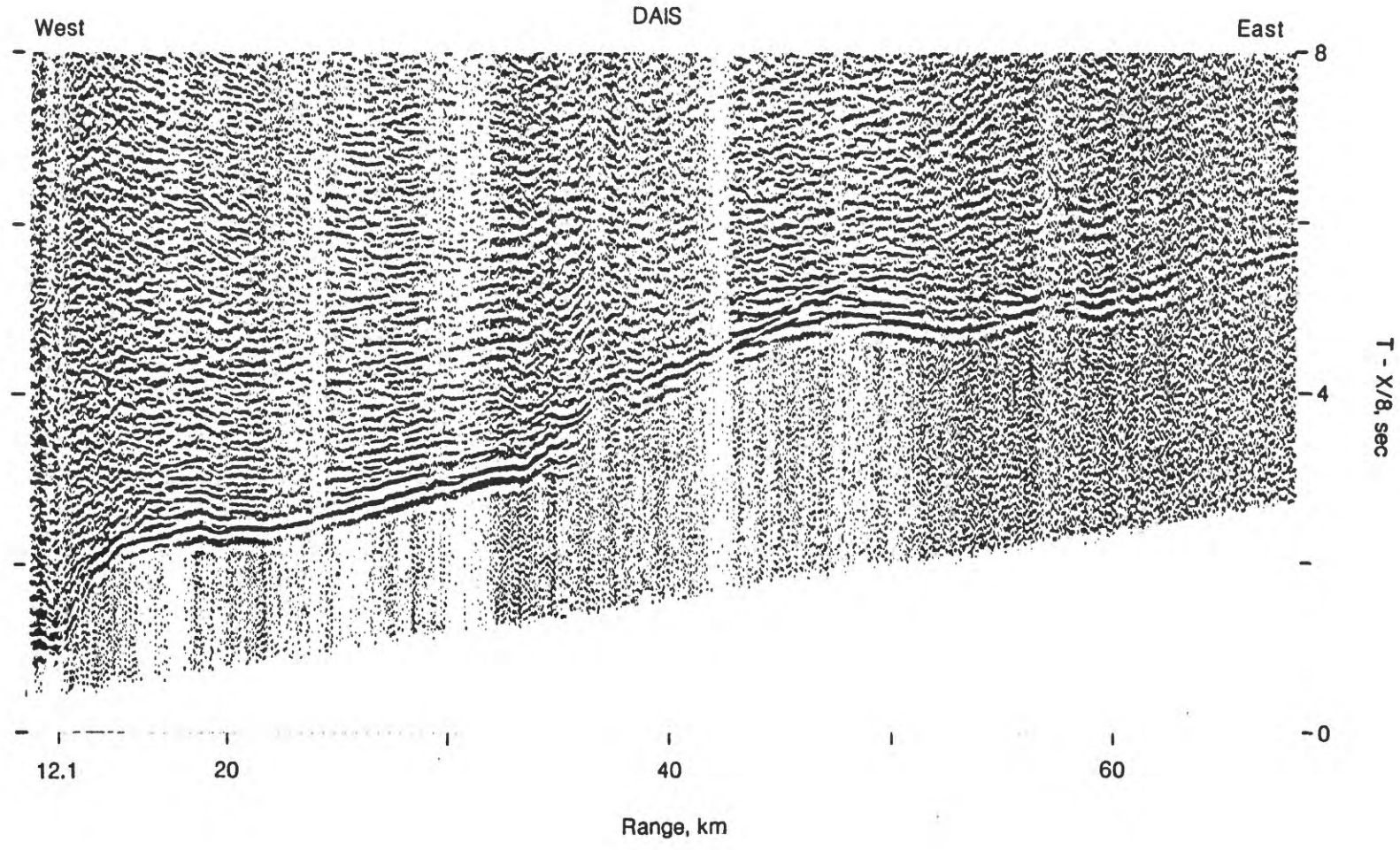

FIGURE 11. Deconvolved receiver gather for station DAIS from lines 101-109. The record section has been linearly reduced using a velocity of 8 km/s and trace amplitudes have been scaled according to Range$^{0.7}$.

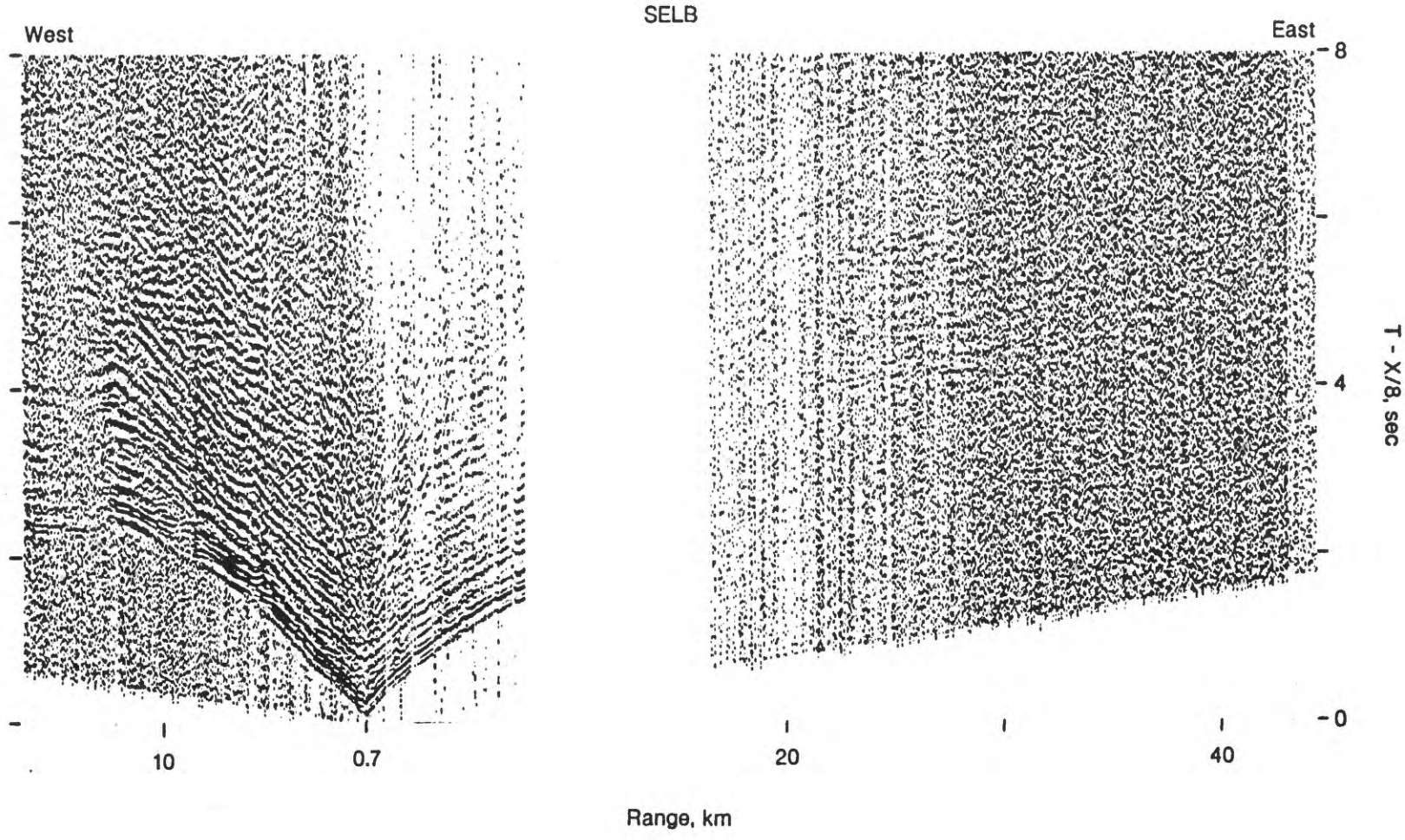

FIGURE 12. Deconvolved receiver gather for station SELB from lines 101-109. The record section has been linearly reduced using a velocity of 8 km/s and trace amplitudes have been scaled according to Range$^{0.7}$.

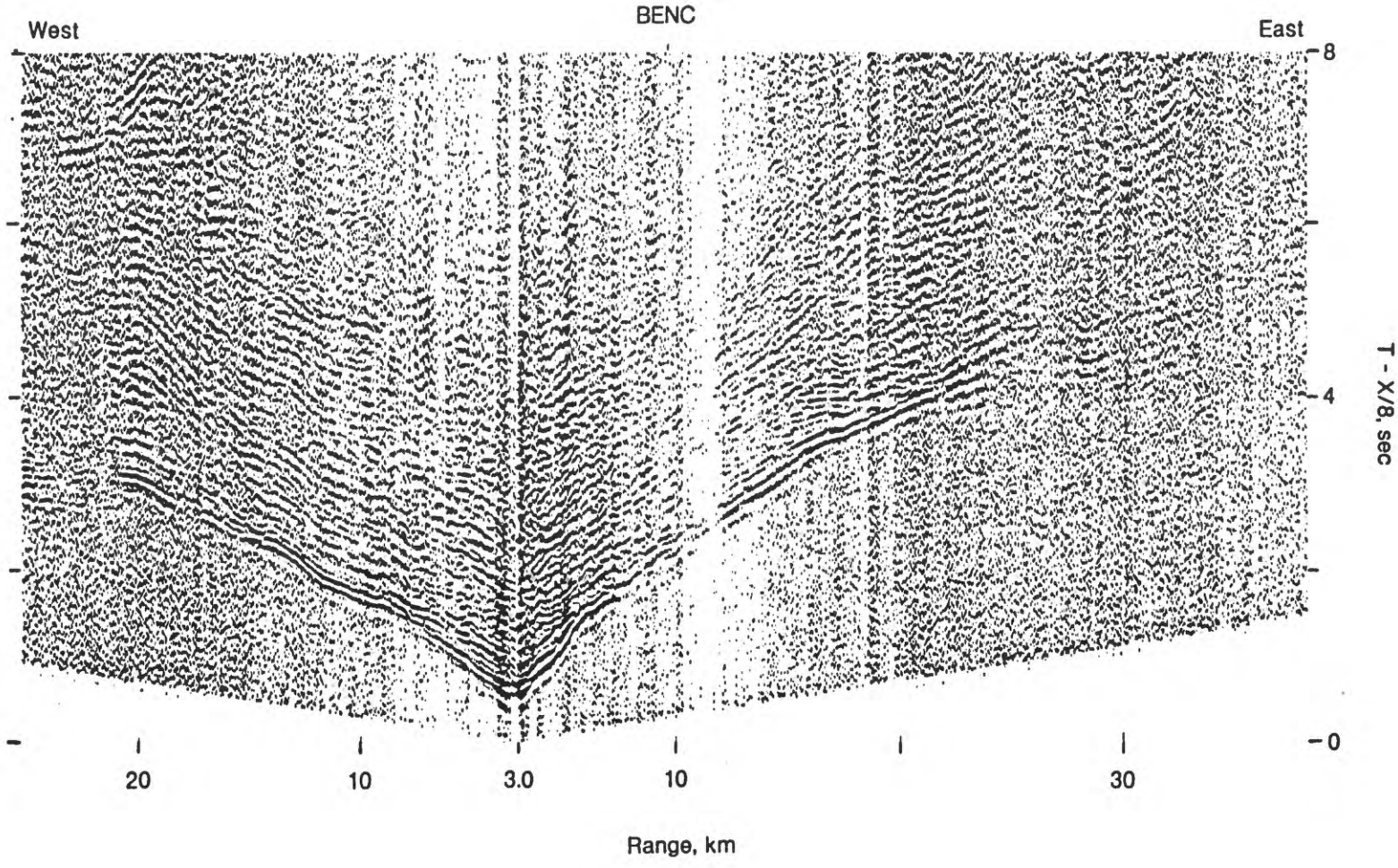

FIGURE 13. Deconvolved receiver gather for station BENC from lines 101-109. The record section has been linearly reduced using a velocity of 8 km/s and trace amplitudes have been scaled according to Range$^{0.7}$.

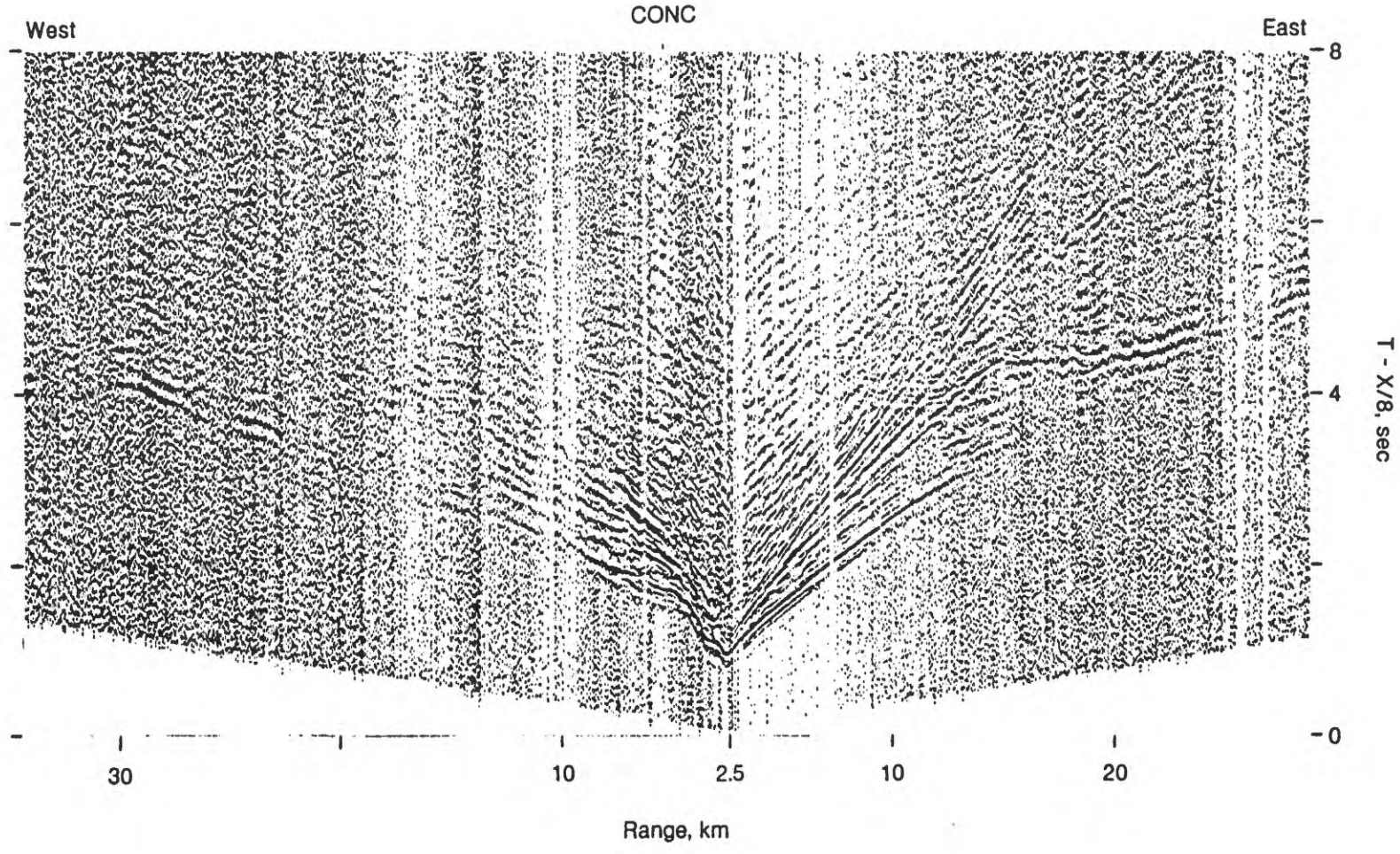

FIGURE 14. Deconvolved receiver gather for station CONC from lines 101-109. The record section has been linearly reduced using a velocity of 8 km/s and trace amplitudes have been scaled according to Range$^{0.7}$.

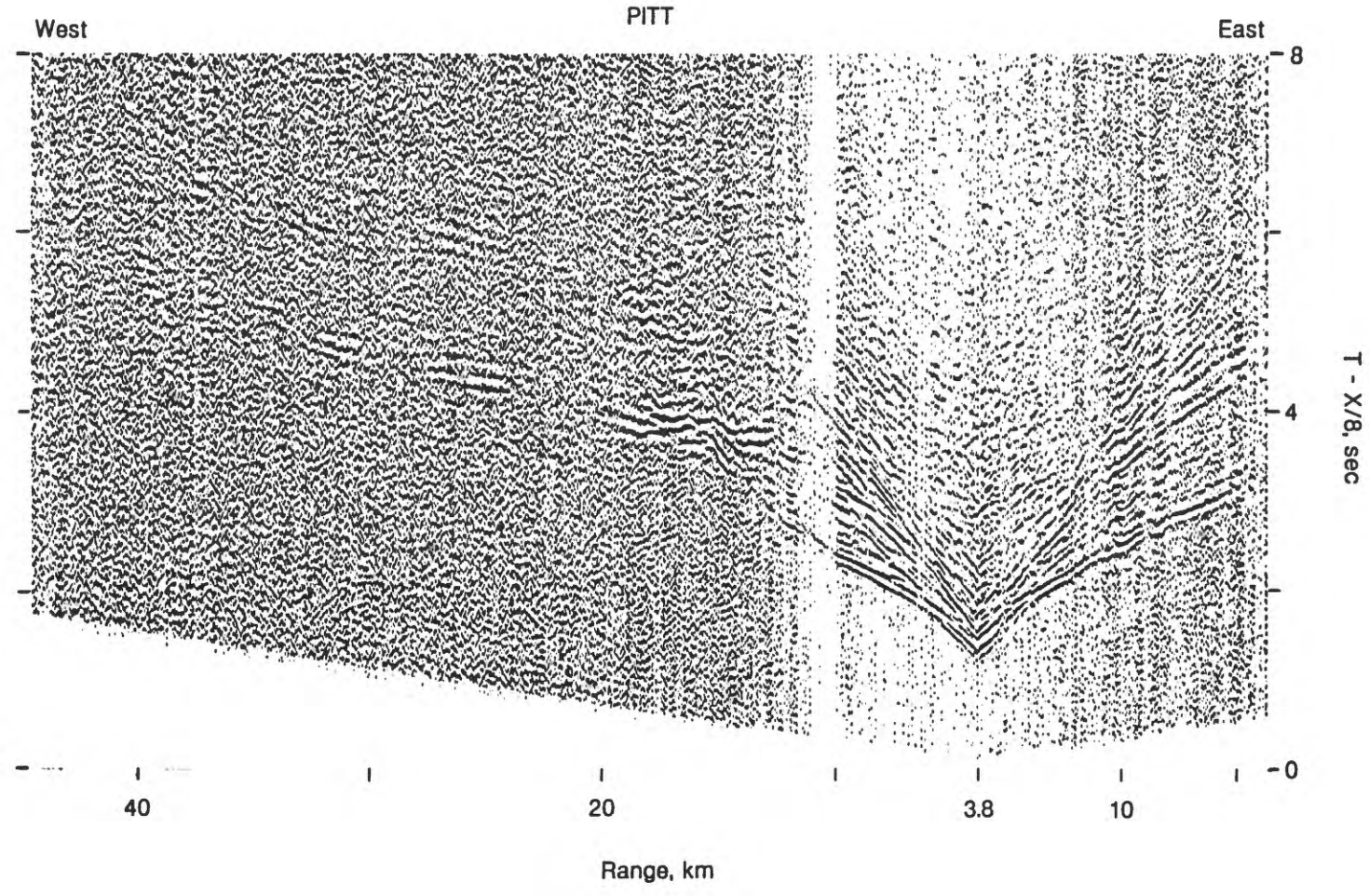

FIGURE 15. Deconvolved receiver gather for station PITT from lines 101-109. The record section has been linearly reduced using a velocity of 8 km/s and trace amplitudes have been scaled according to Range$^{0.7}$.

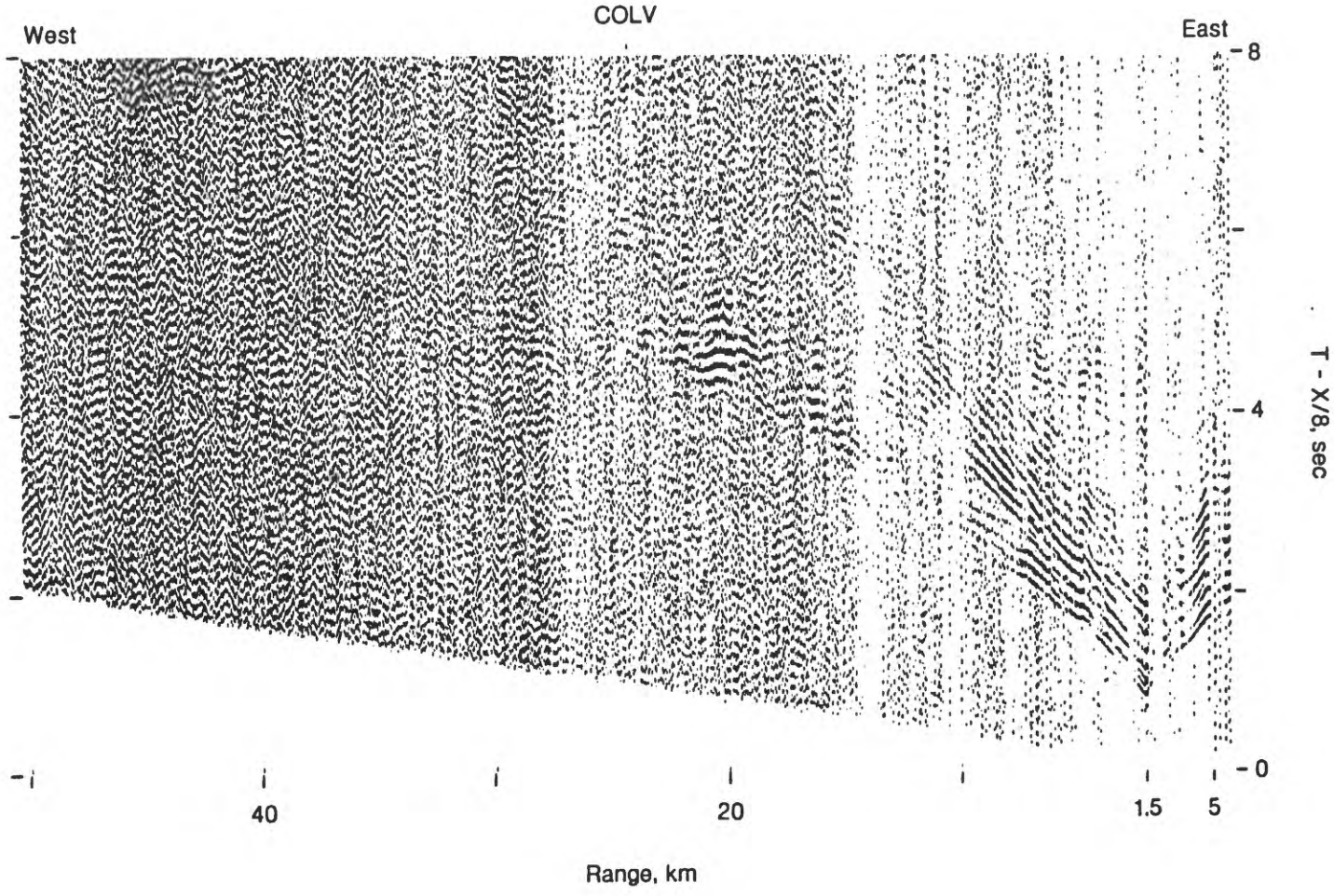

FIGURE 16. Receiver gather for station COLV from lines 103-109. The record section has been linearly reduced using a velocity of 8 km/s and trace amplitudes have been scaled according to Range$^{0.7}$.

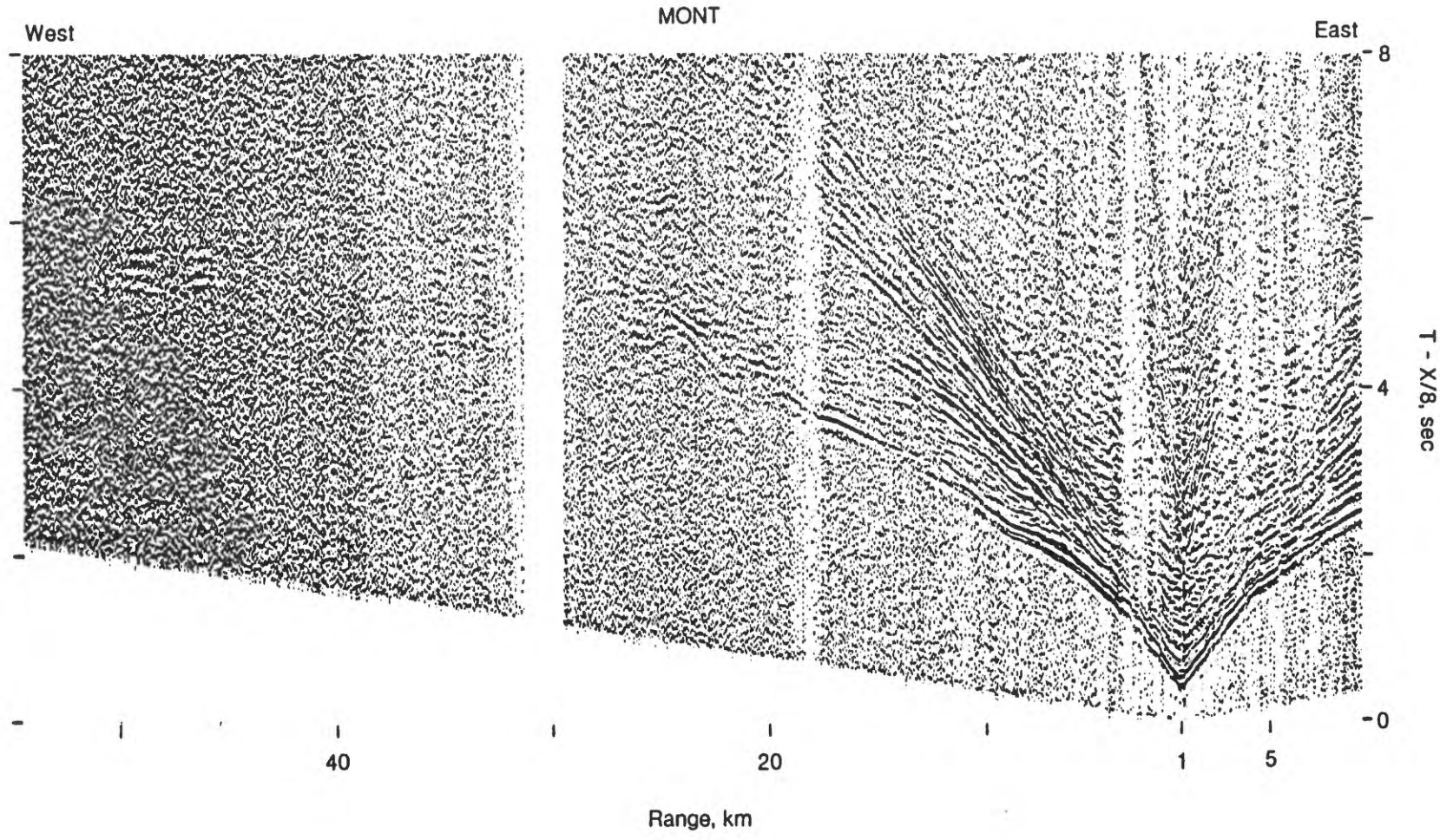

FIGURE 17. Deconvolved receiver gather for station MONT from lines 101-109. The record section has been linearly reduced using a velocity of 8 km/s and trace amplitudes have been scaled according to Range$^{0.7}$.

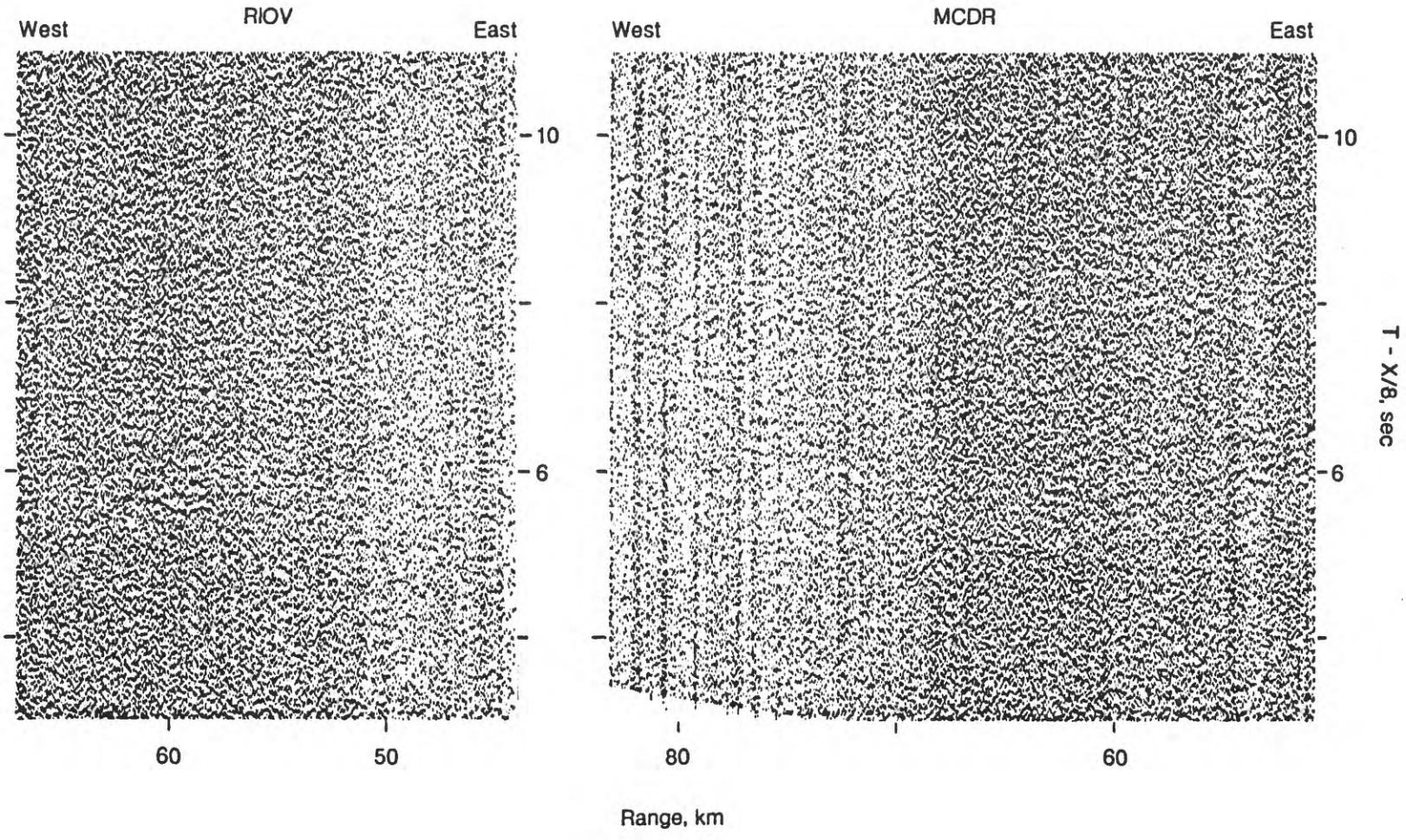

FIGURE 18. Deconvolved receiver gathers for stations RIOV and MCDR from lines 105-109. The record sections have been linearly reduced using a velocity of 8 km/s and trace amplitudes have been scaled according to Range$^{0.7}$.

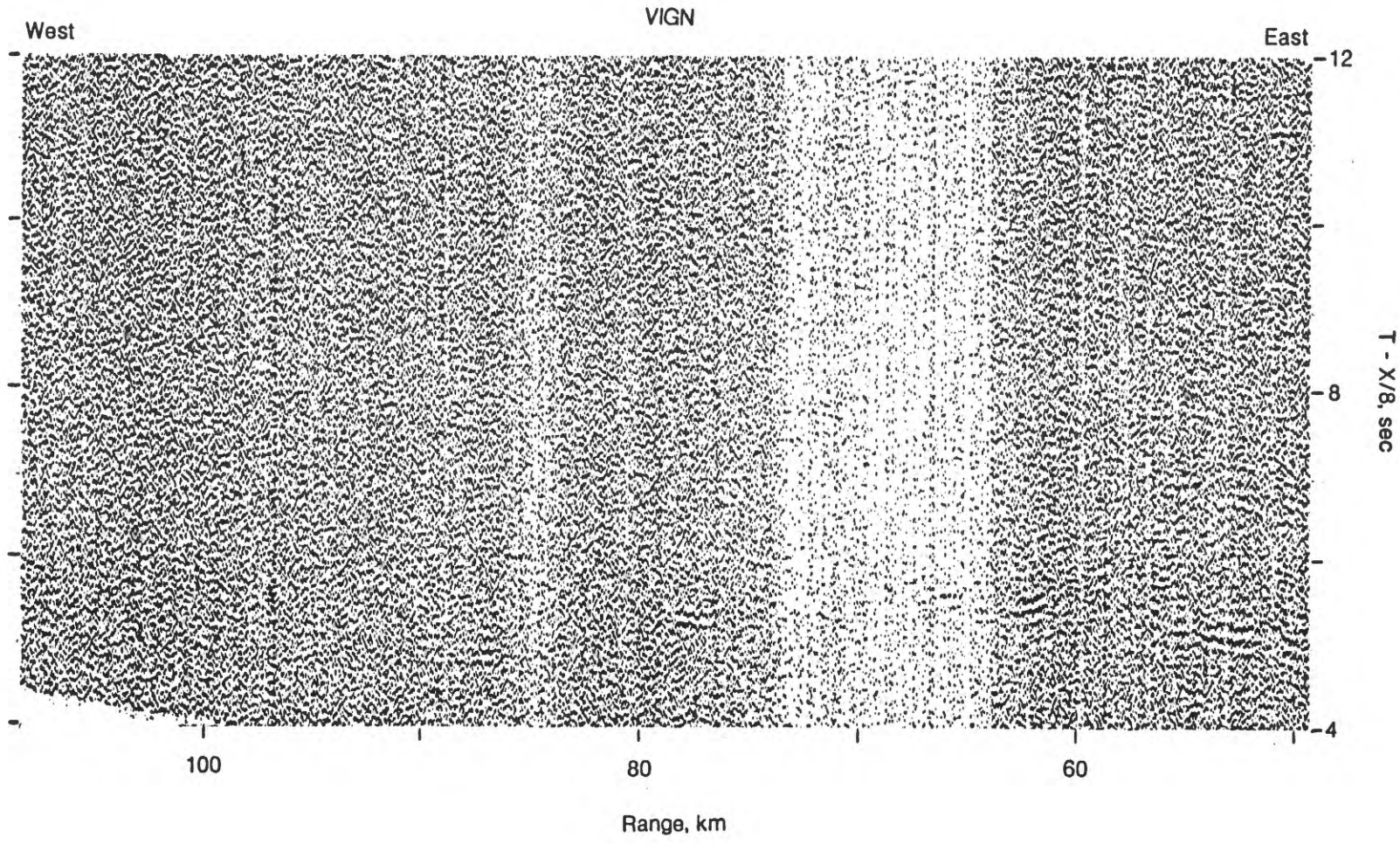

FIGURE 19. Deconvolved receiver gather for station VIGN from lines 101-109. The record section has been linearly reduced using a velocity of 8 km/s and trace amplitudes have been scaled according to Range$^{0.7}$.

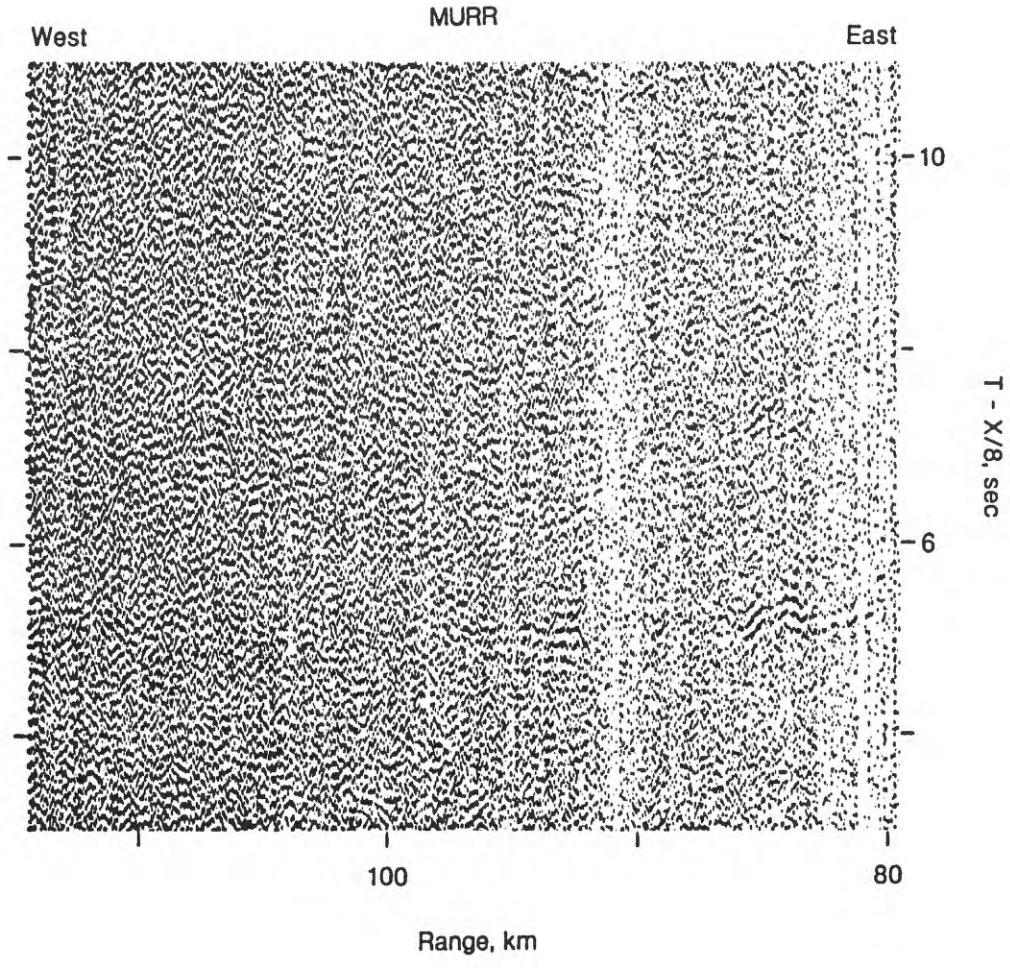

FIGURE 20. Receiver gather for station MURR from lines 104-109. The record section has been linearly reduced using a velocity of 8 km/s and trace amplitudes have been scaled according to Range$^{0.7}$.

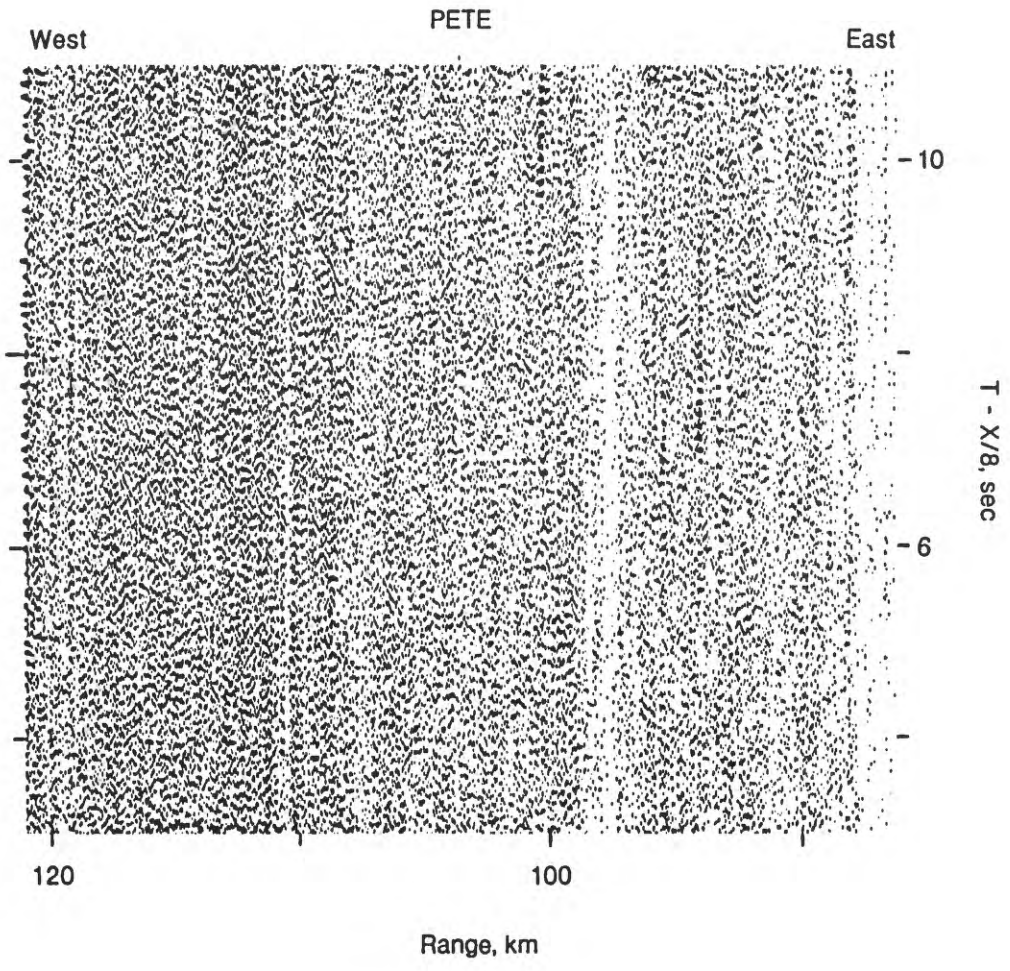

FIGURE 21. Receiver gather for station PETE from lines 104-109. The record section has been linearly reduced using a velocity of 8 km/s and trace amplitudes have been scaled according to Range$^{0.7}$.

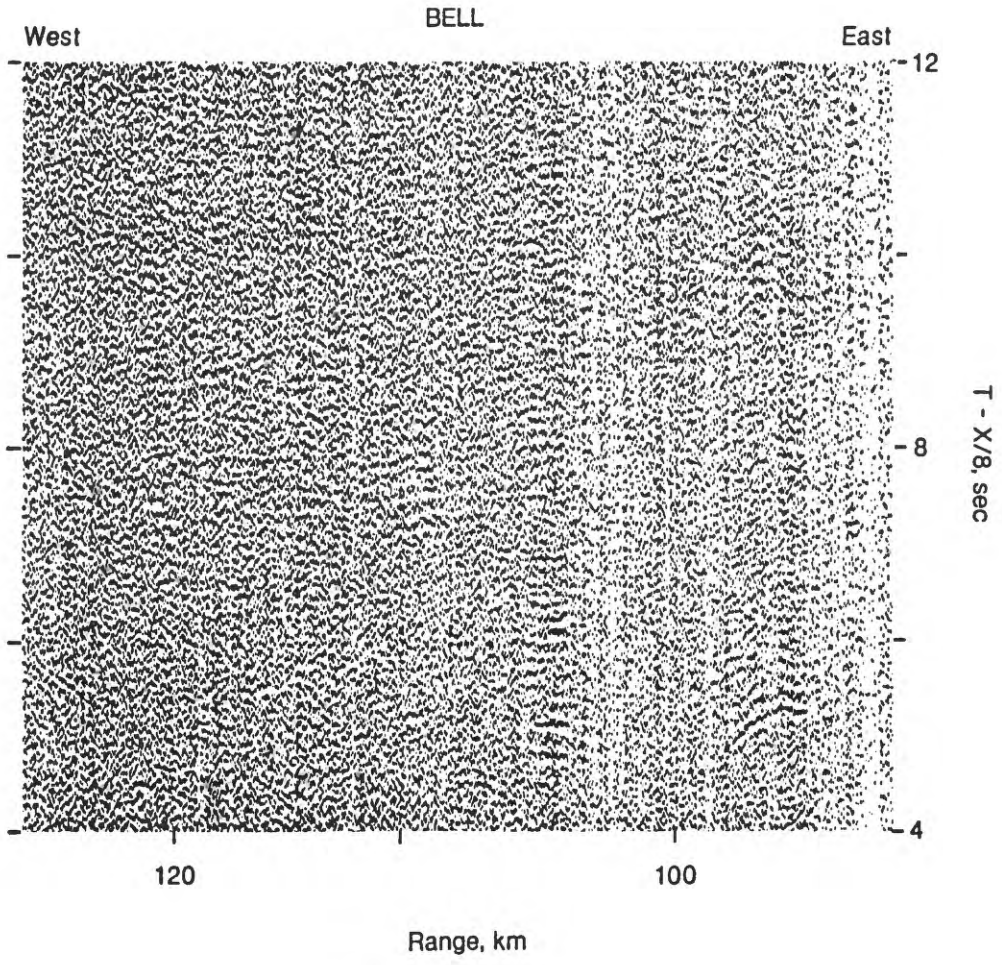

FIGURE 22. Deconvolved receiver gather for station BELL from lines 104-109. The record section has been linearly reduced using a velocity of 8 km/s and trace amplitudes have been scaled according to Range$^{0.7}$.

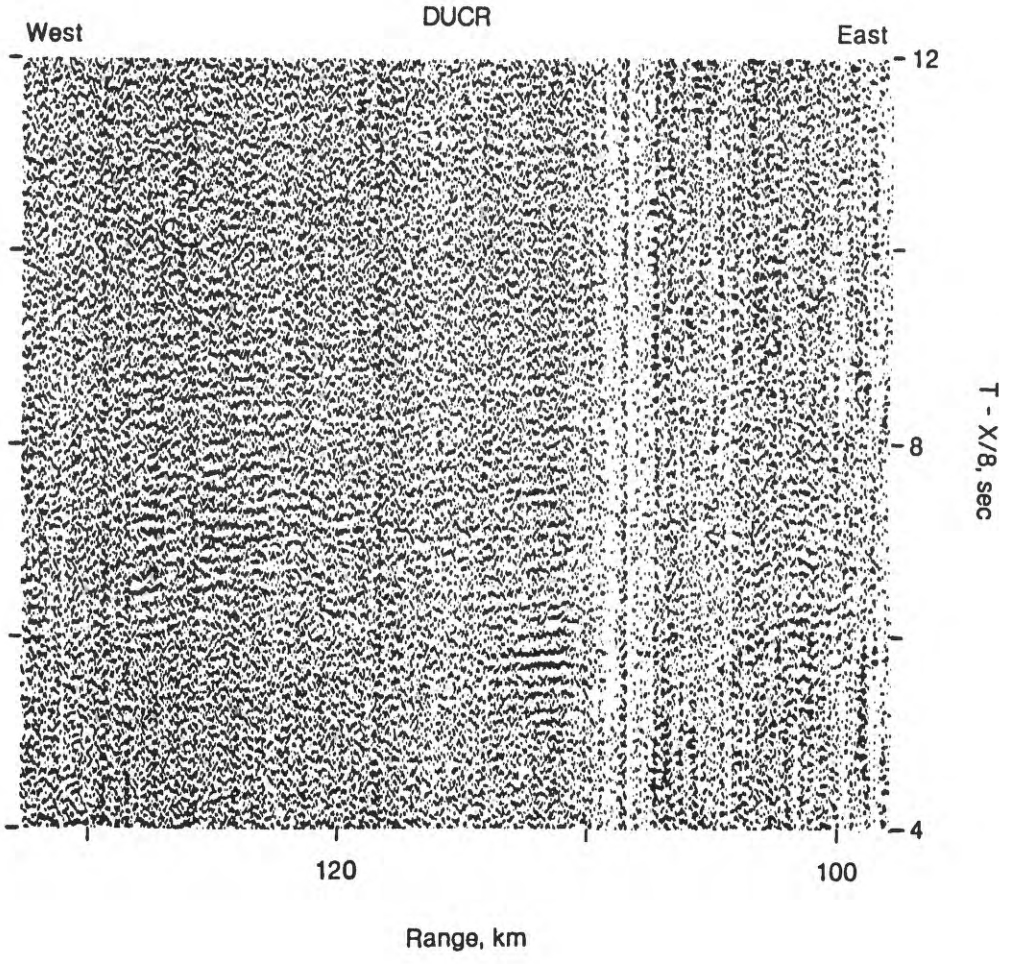

FIGURE 23. Deconvolved receiver gather for station DUCR from lines 101-109. The record section has been linearly reduced using a velocity of 8 km/s and trace amplitudes have been scaled according to Range$^{0.7}$.

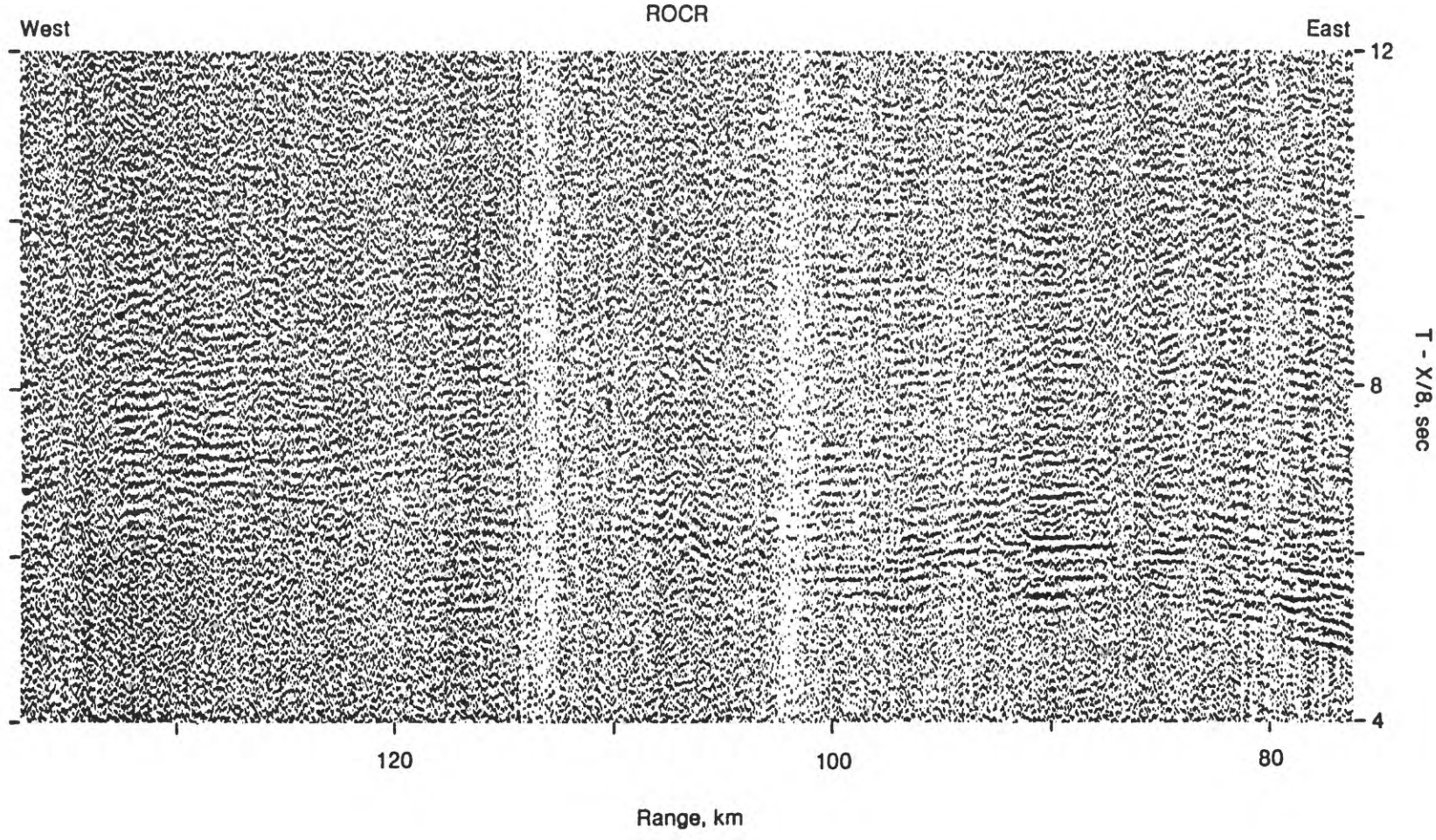

FIGURE 24. Deconvolved receiver gather for station ROCR from lines 101-109. The record section has been linearly reduced using a velocity of 8 km/s and trace amplitudes have been scaled according to Range$^{0.7}$.

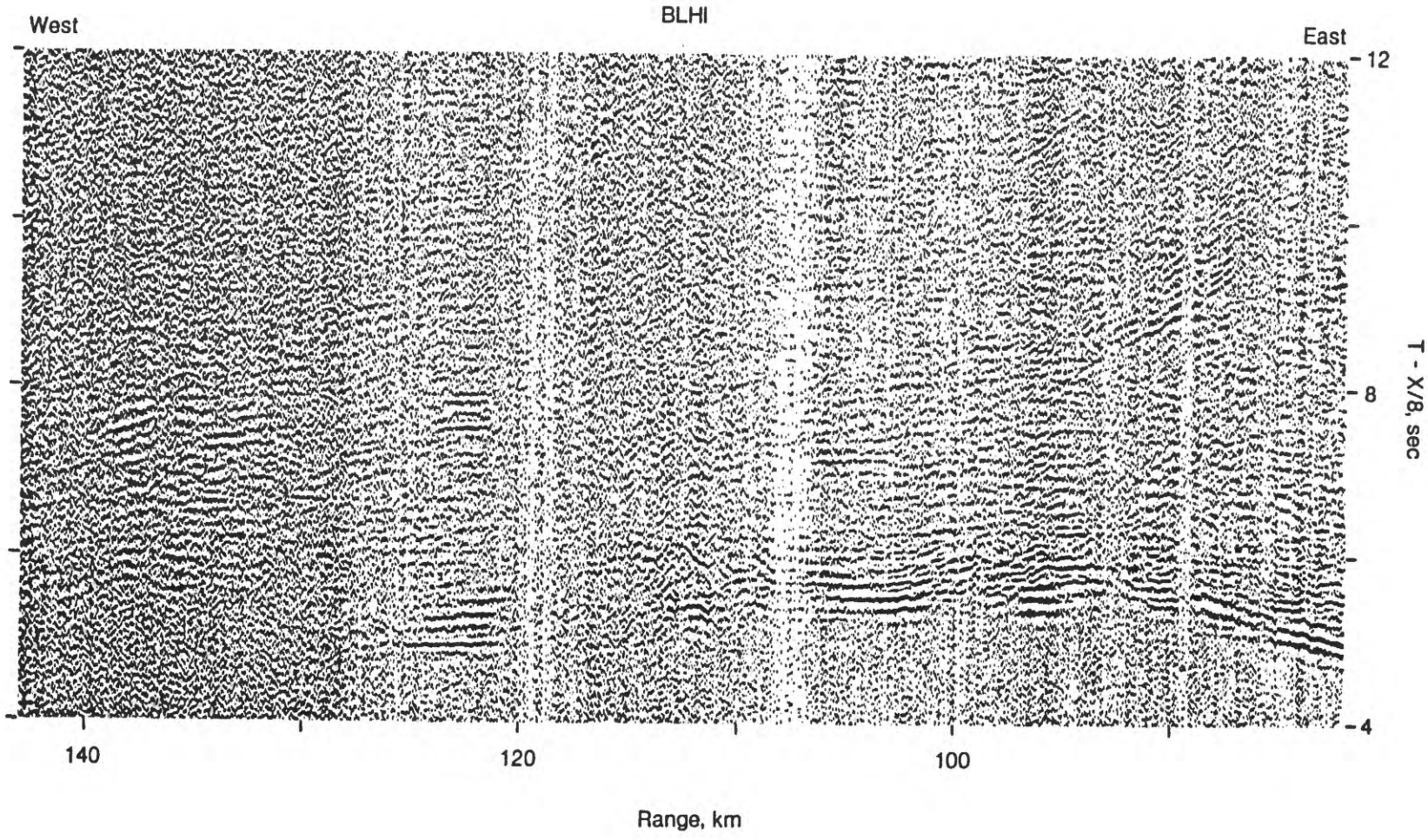

FIGURE 25. Deconvolved receiver gather for station BLHI from lines 101-109. The record section has been linearly reduced using a velocity of 8 km/s and trace amplitudes have been scaled according to Range$^{0.7}$.

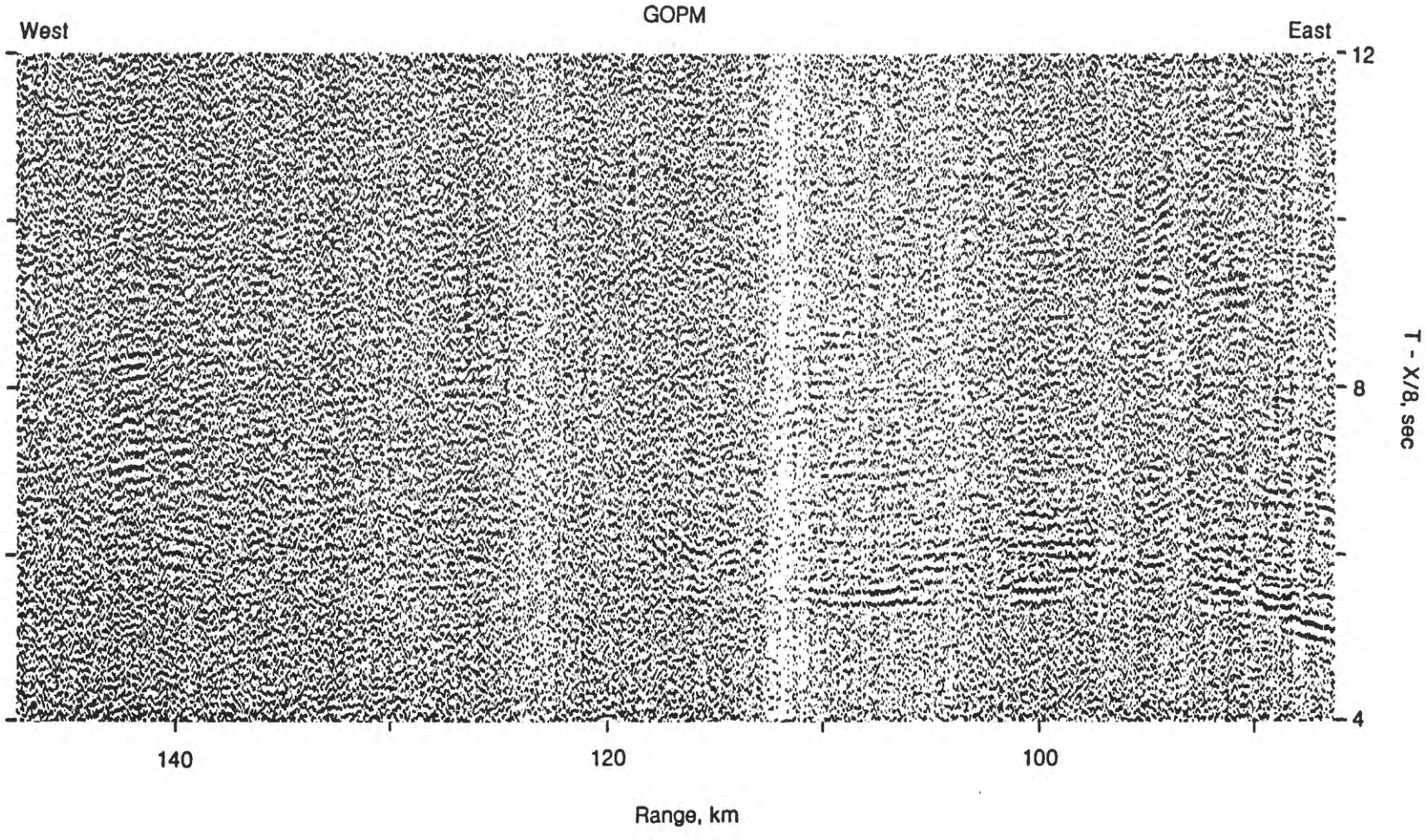

FIGURE 26. Deconvolved receiver gather for station GOPM from lines 101-109. The record section has been linearly reduced using a velocity of 8 km/s and trace amplitudes have been scaled according to Range$^{0.7}$.

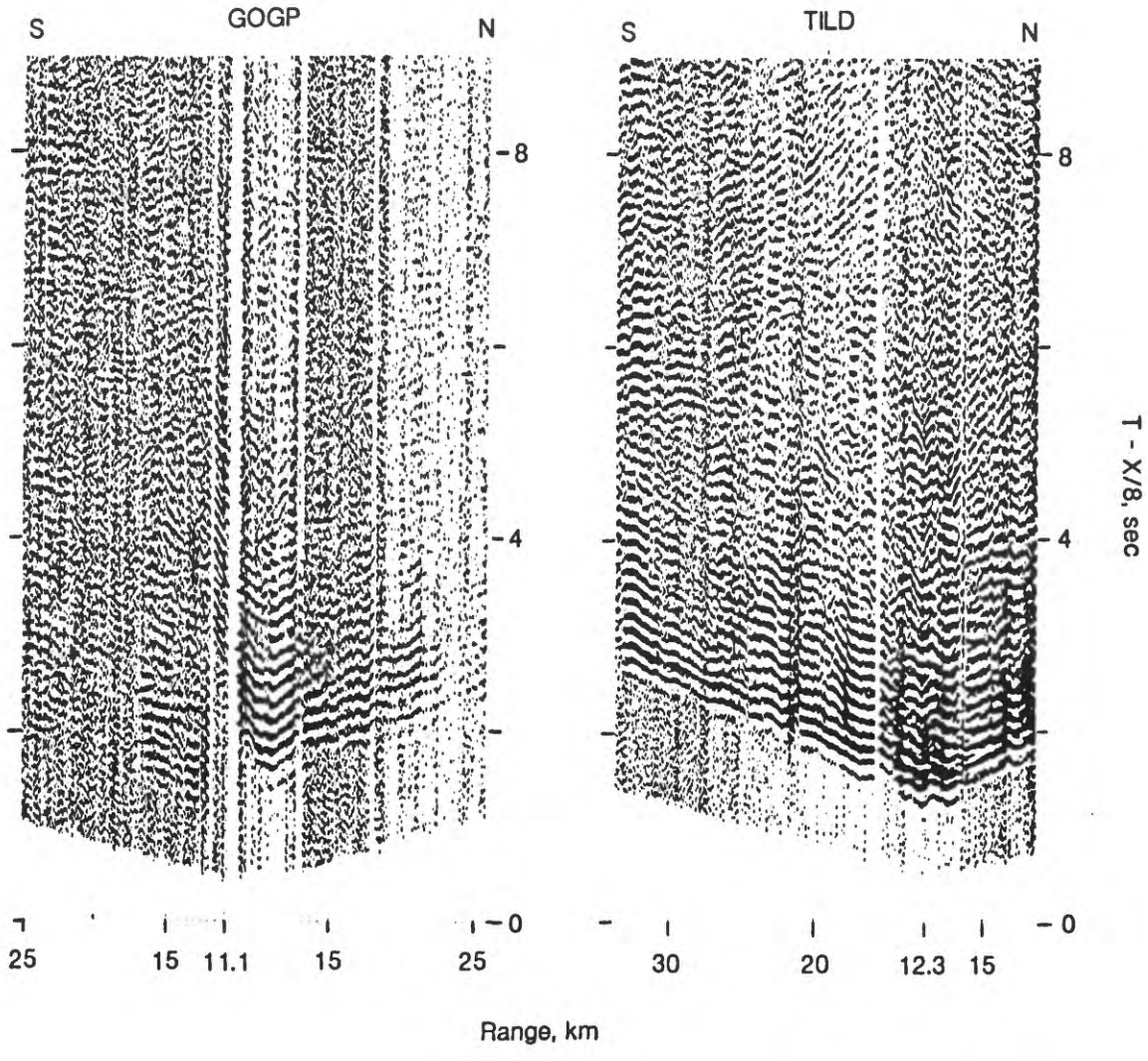

FIGURE 27. Deconvolved receiver gathers for stations GOGP and TILD from lines 110-113. The record sections have been linearly reduced using a velocity of 8 km/s and trace amplitudes have been scaled according to Range$^{0.7}$.

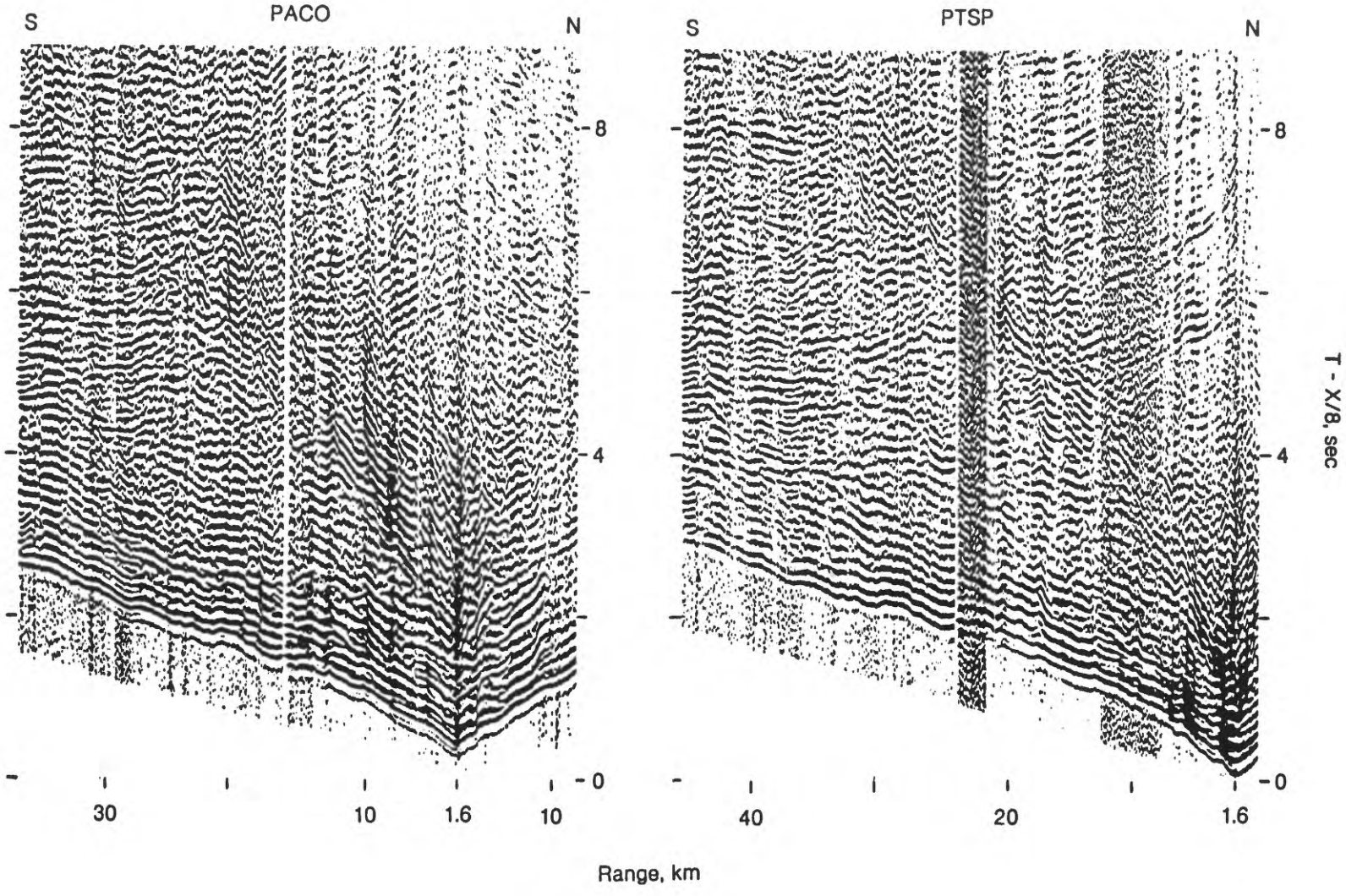

FIGURE 28. Deconvolved receiver gathers for stations PACO and PTSP from lines 110-113. The record sections have been linearly reduced using a velocity of 8 km/s and trace amplitudes have been scaled according to Range$^{0.7}$.

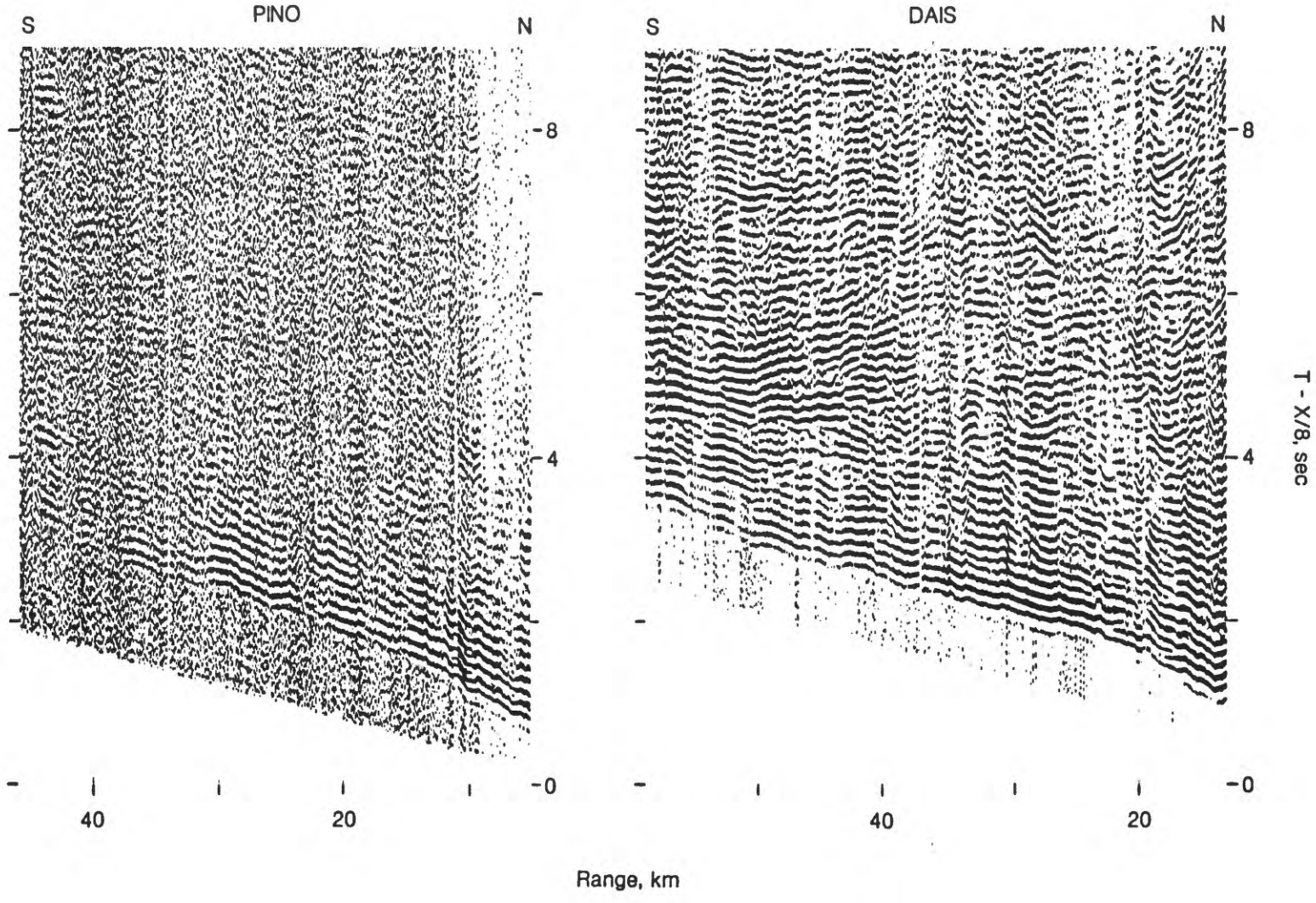

FIGURE 29. Deconvolved receiver gathers for stations PINO and DAIS from lines 110-113. The record sections have been linearly reduced using a velocity of 8 km/s and trace amplitudes have been scaled according to Range$^{0.7}$.

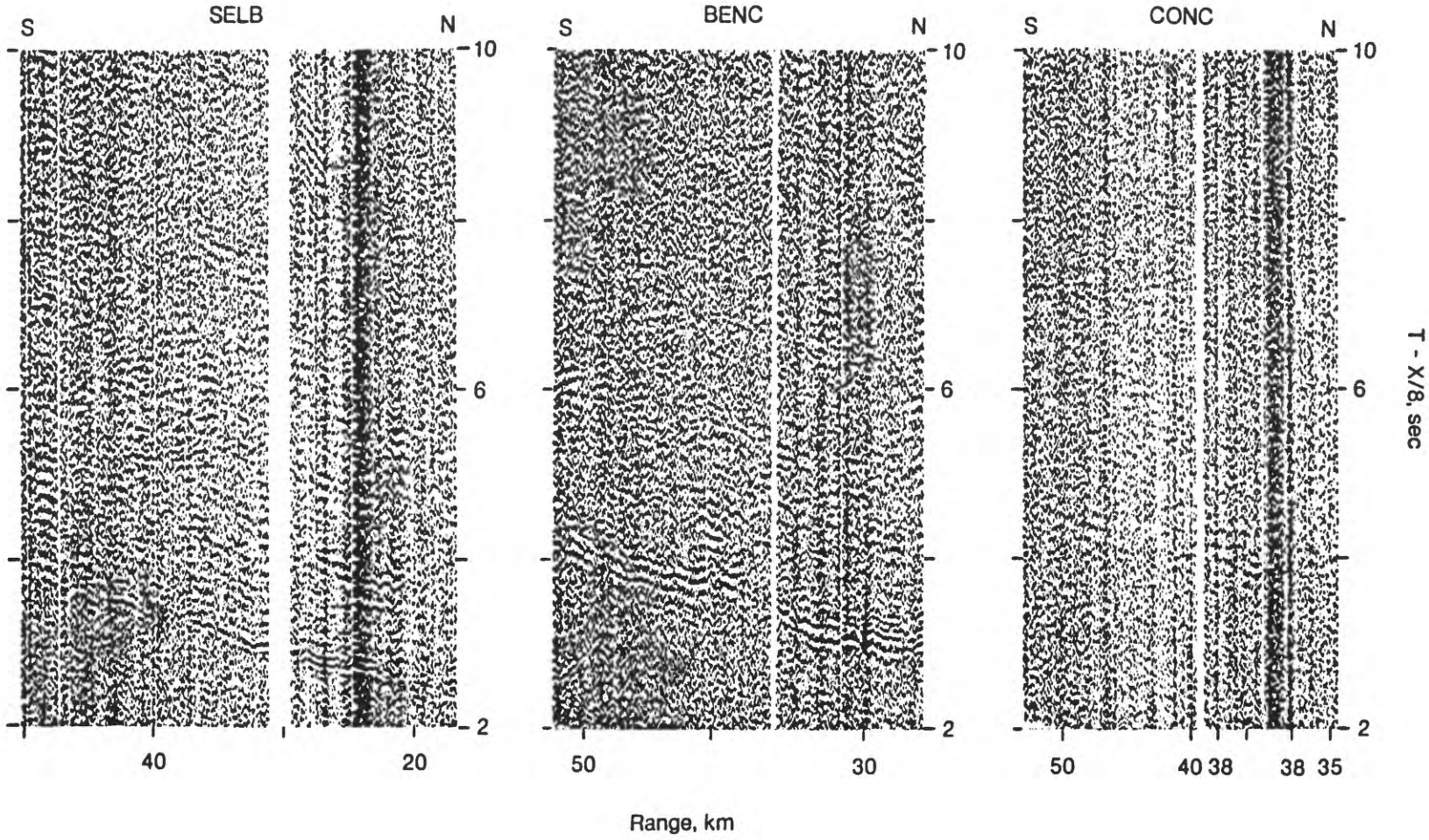

FIGURE 30. Deconvolved receiver gathers for stations SELB, BENC, and CONC from lines 110-113. The record sections have been linearly reduced using a velocity of 8 km/s and trace amplitudes have been scaled according to Range$^{0.7}$.

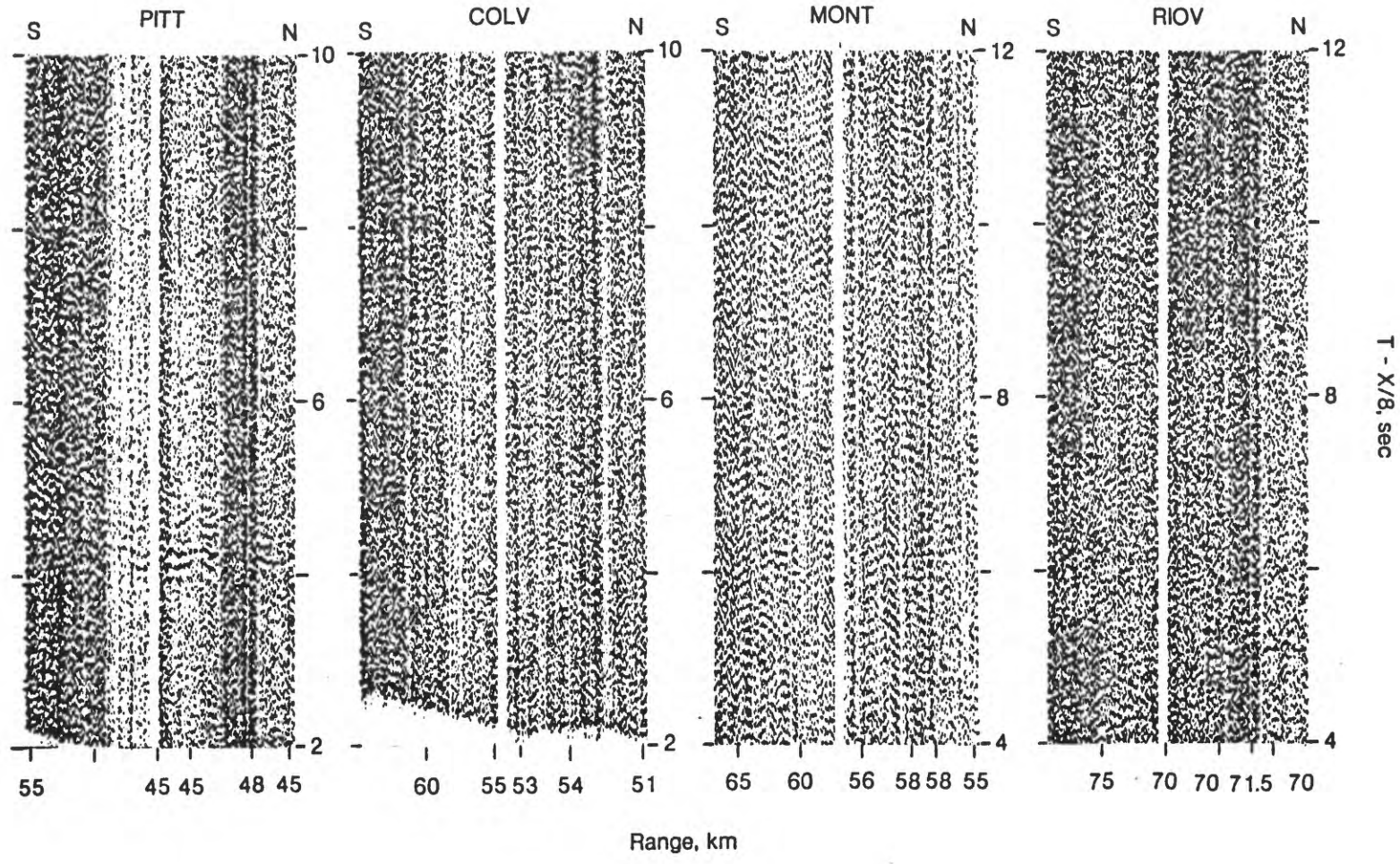

FIGURE 31. Deconvolved receiver gathers for stations PITT, COLV, MONT, and RIOV from lines 110-113. The record sections have been linearly reduced using a velocity of 8 km/s and trace amplitudes have been scaled according to Range$^{0.7}$.

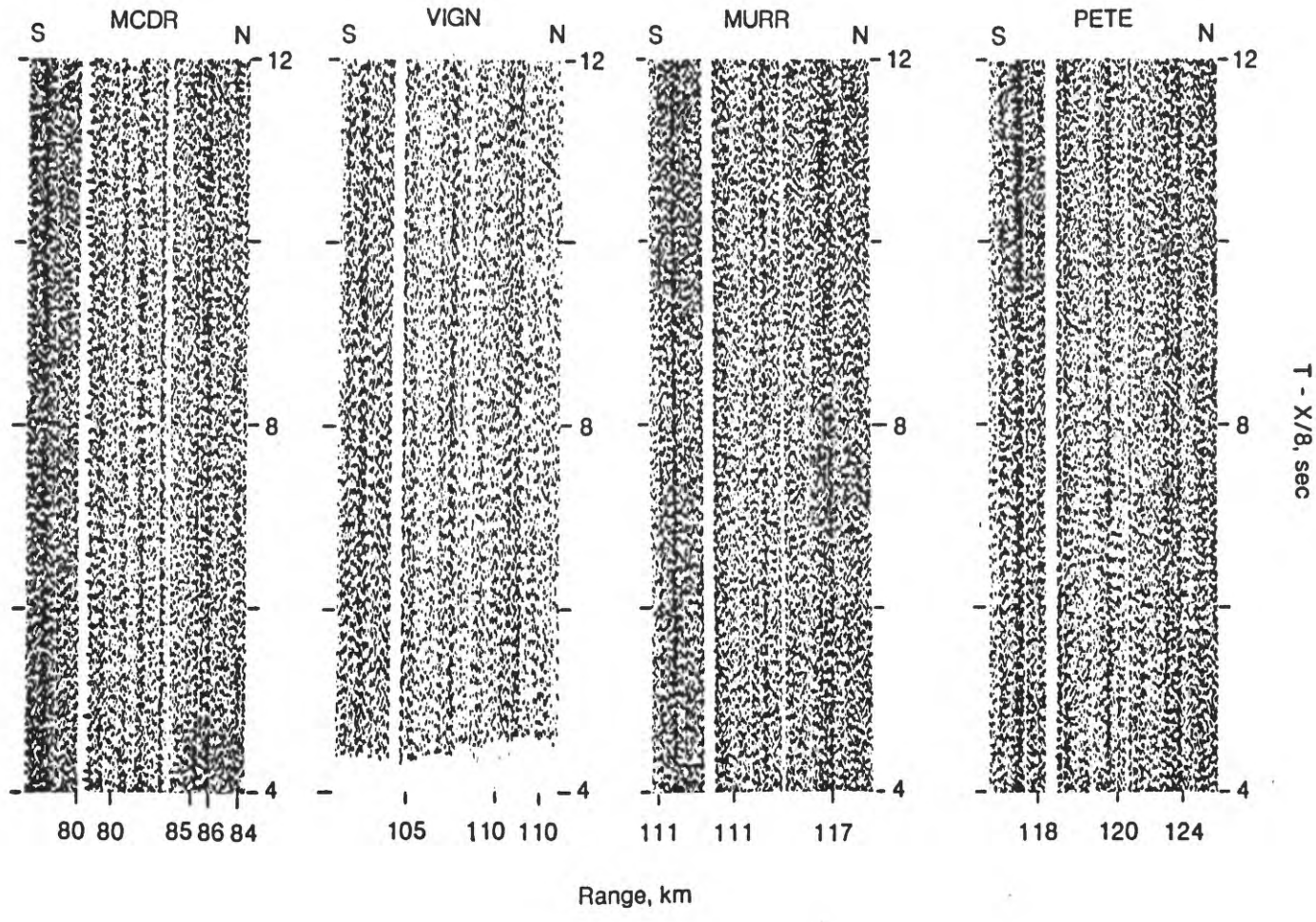

FIGURE 32. Deconvolved receiver gathers for stations MCDR, VIGN, MURR, and PETE from lines 110-113. The record sections have been linearly reduced using a velocity of 8 km/s and trace amplitudes have been scaled according to Range$^{0.7}$.

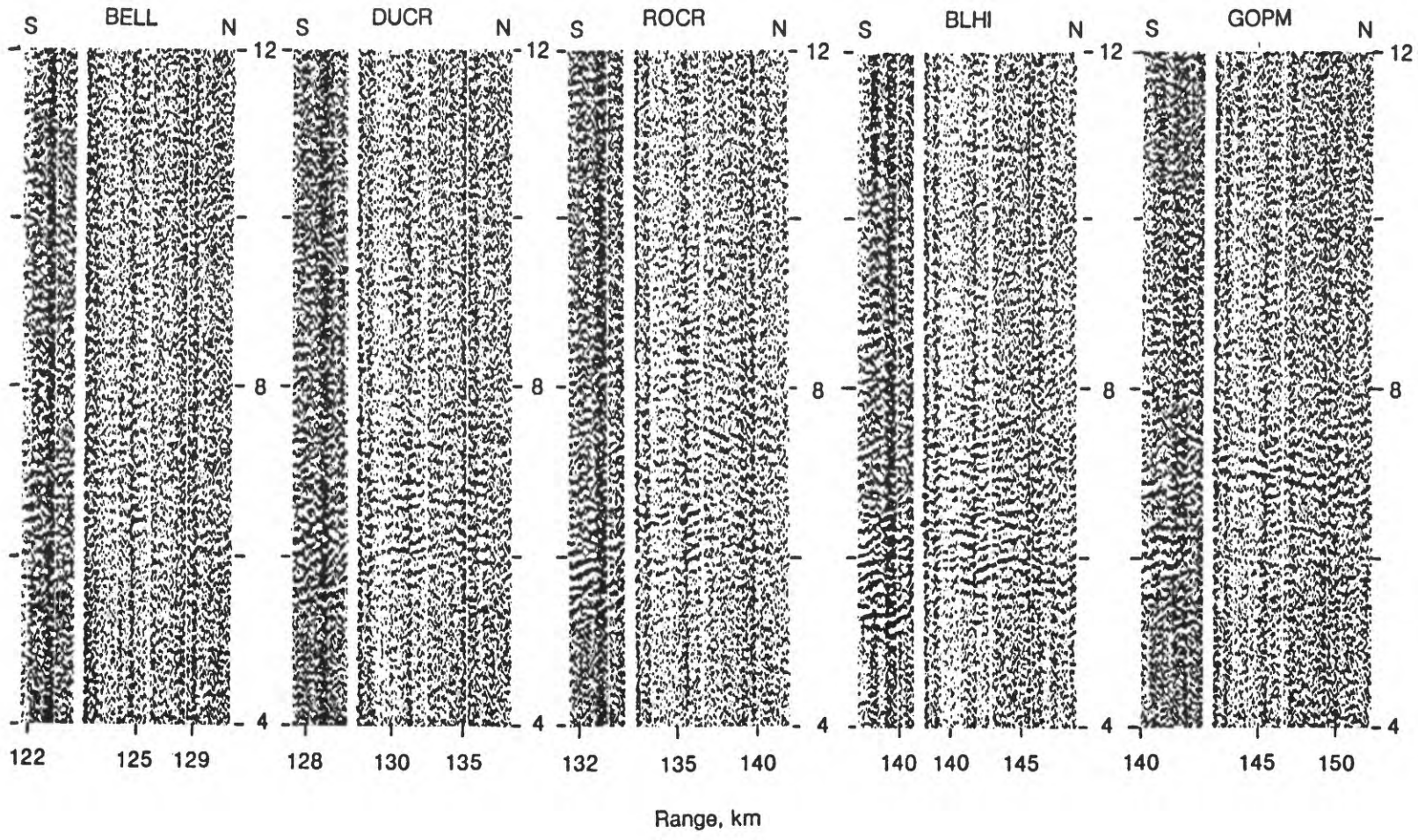

FIGURE 33. Deconvolved receiver gathers for stations BELL, DUCR, ROCR, BLHI, and GOPM from lines 110-113. The record sections have been linearly reduced using a velocity of 8 km/s and trace amplitudes have been scaled according to $\text{Range}^{0.7}$.

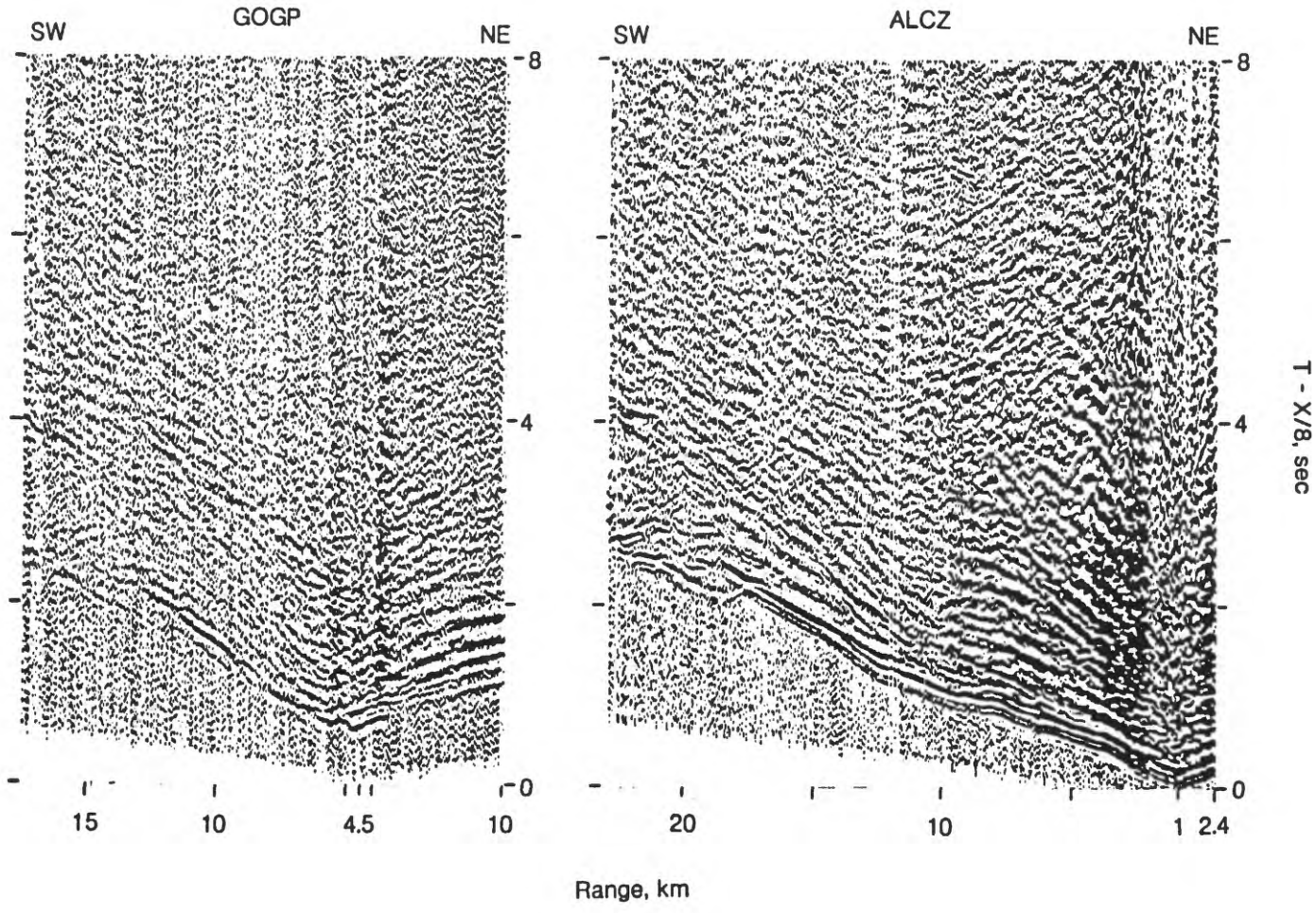

FIGURE 34. Deconvolved receiver gathers for stations GOGP and ALCZ from lines 201-202. The record sections have been linearly reduced using a velocity of 8 km/s and trace amplitudes have been scaled according to Range$^{0.7}$.

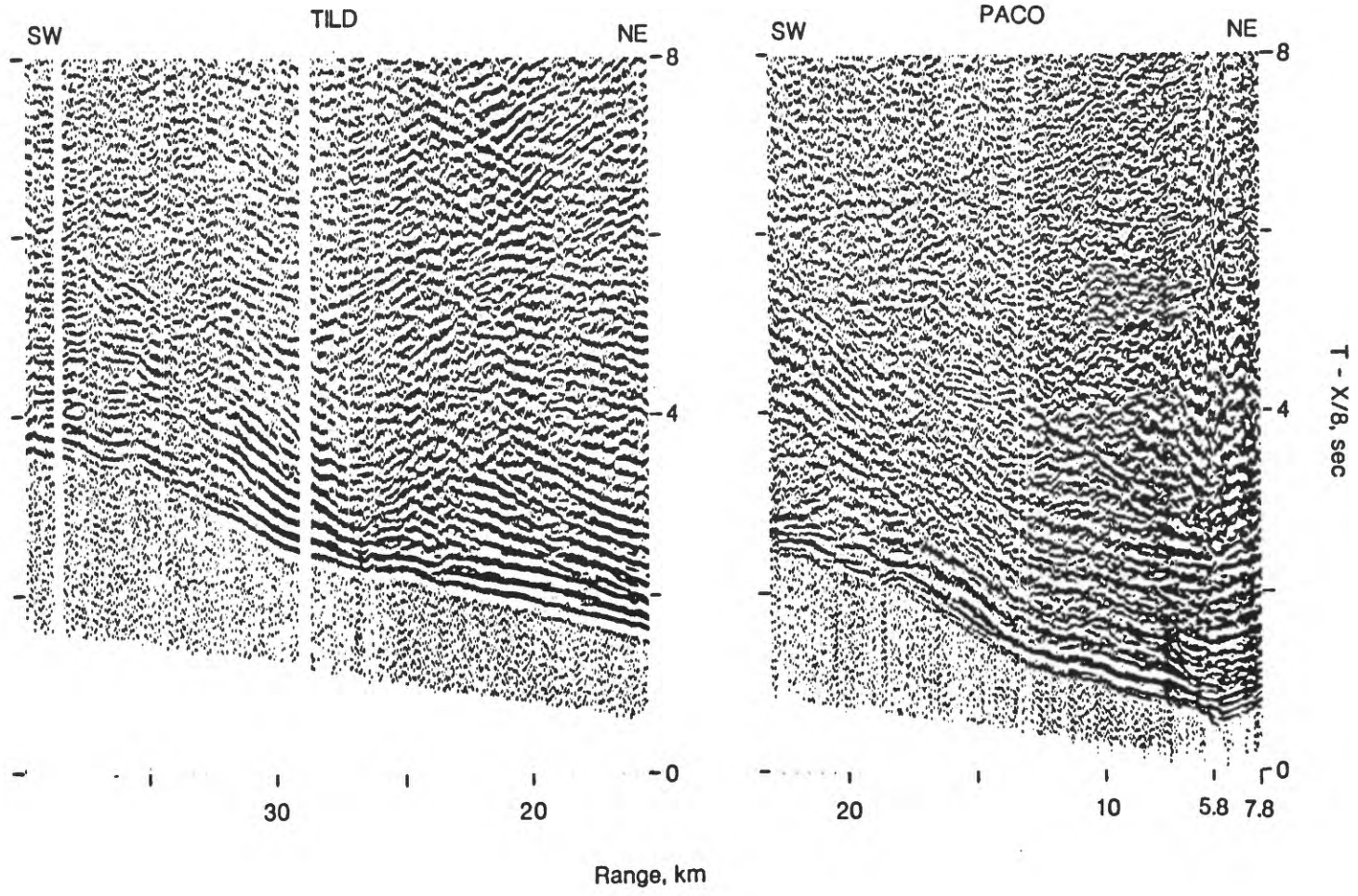

FIGURE 35. Receiver gathers for stations TILD and PACO from lines 201-202. The record sections have been linearly reduced using a velocity of 8 km/s and trace amplitudes have been scaled according to Range$^{0.7}$.

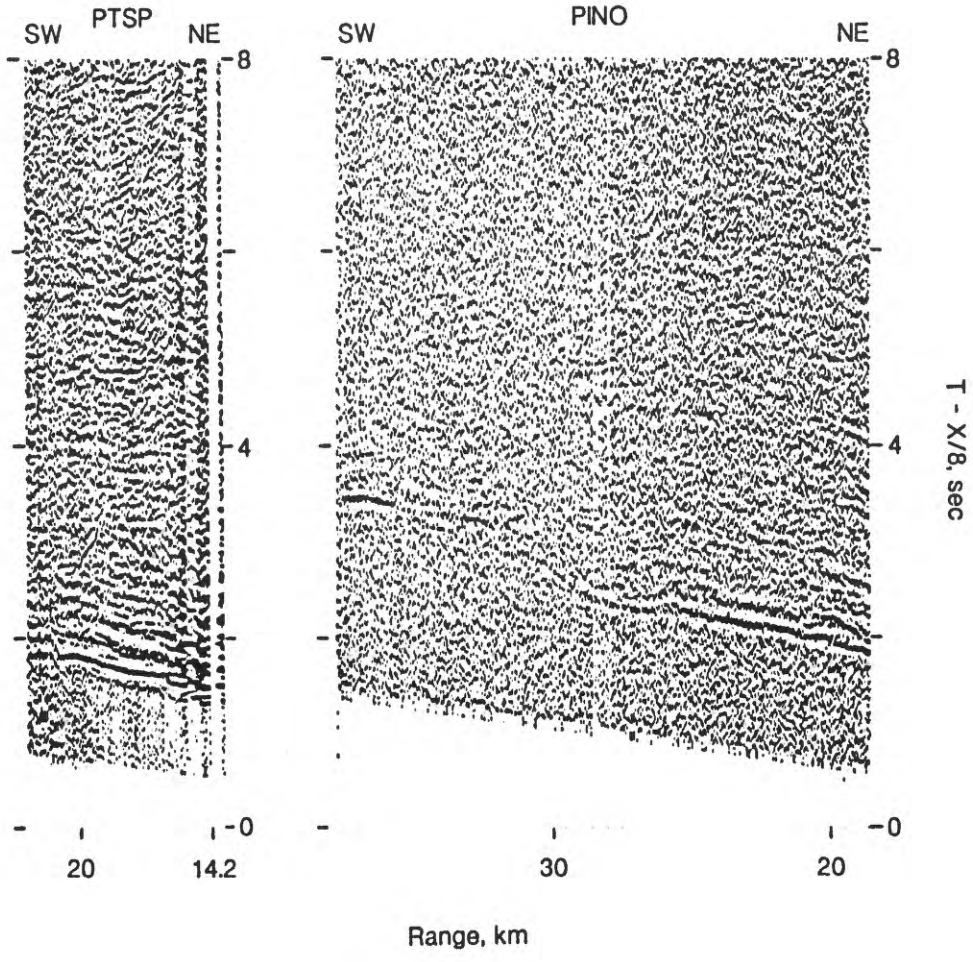

FIGURE 36. Deconvolved receiver gathers for stations PTSP and PINO from lines 201-202. The record sections have been linearly reduced using a velocity of 8 km/s and trace amplitudes have been scaled according to Range$^{0.7}$.

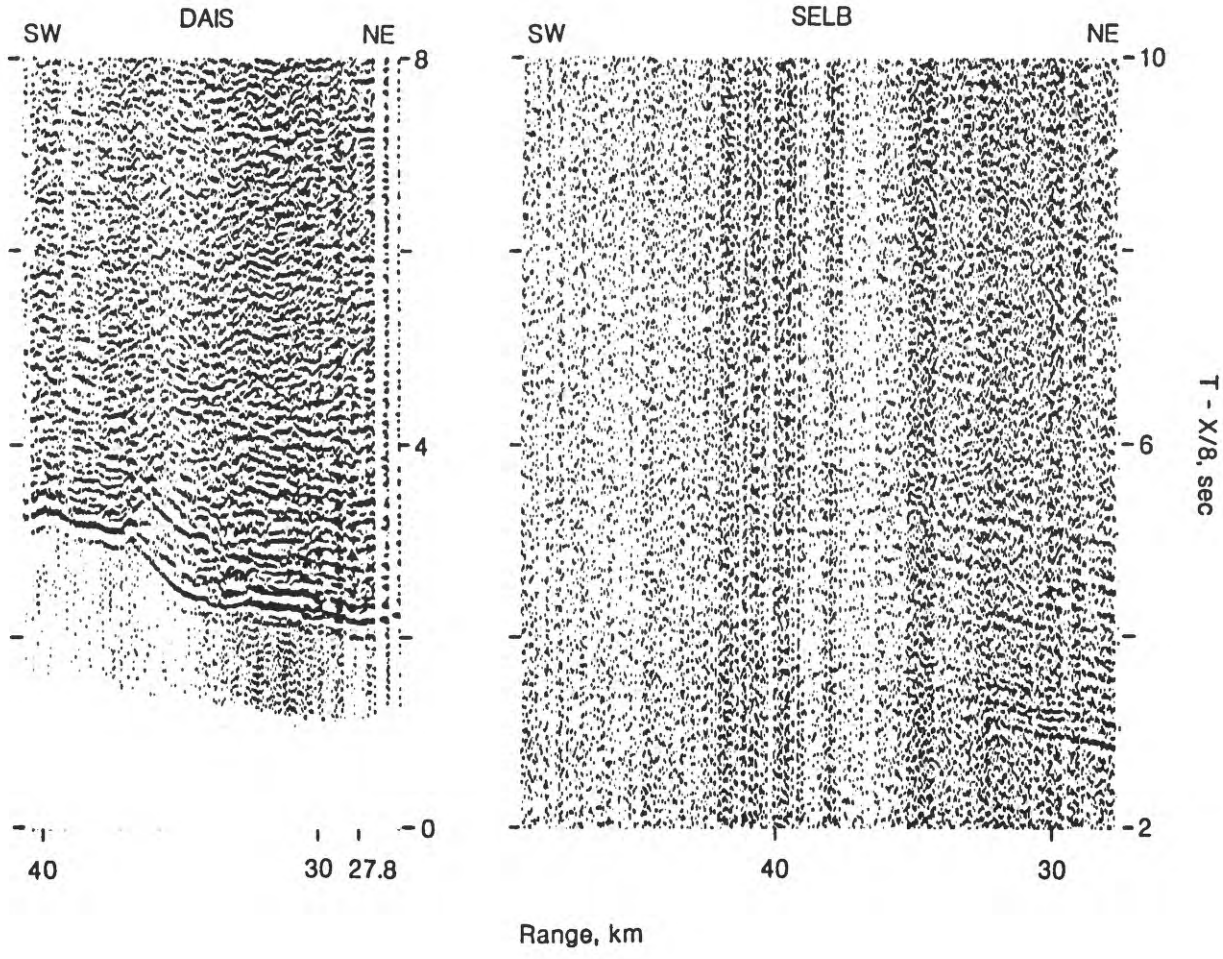

FIGURE 37. Deconvolved receiver gathers for stations DAIS and SELB from lines 201-202. The record sections have been linearly reduced using a velocity of 8 km/s and trace amplitudes have been scaled according to Range$^{0.7}$.

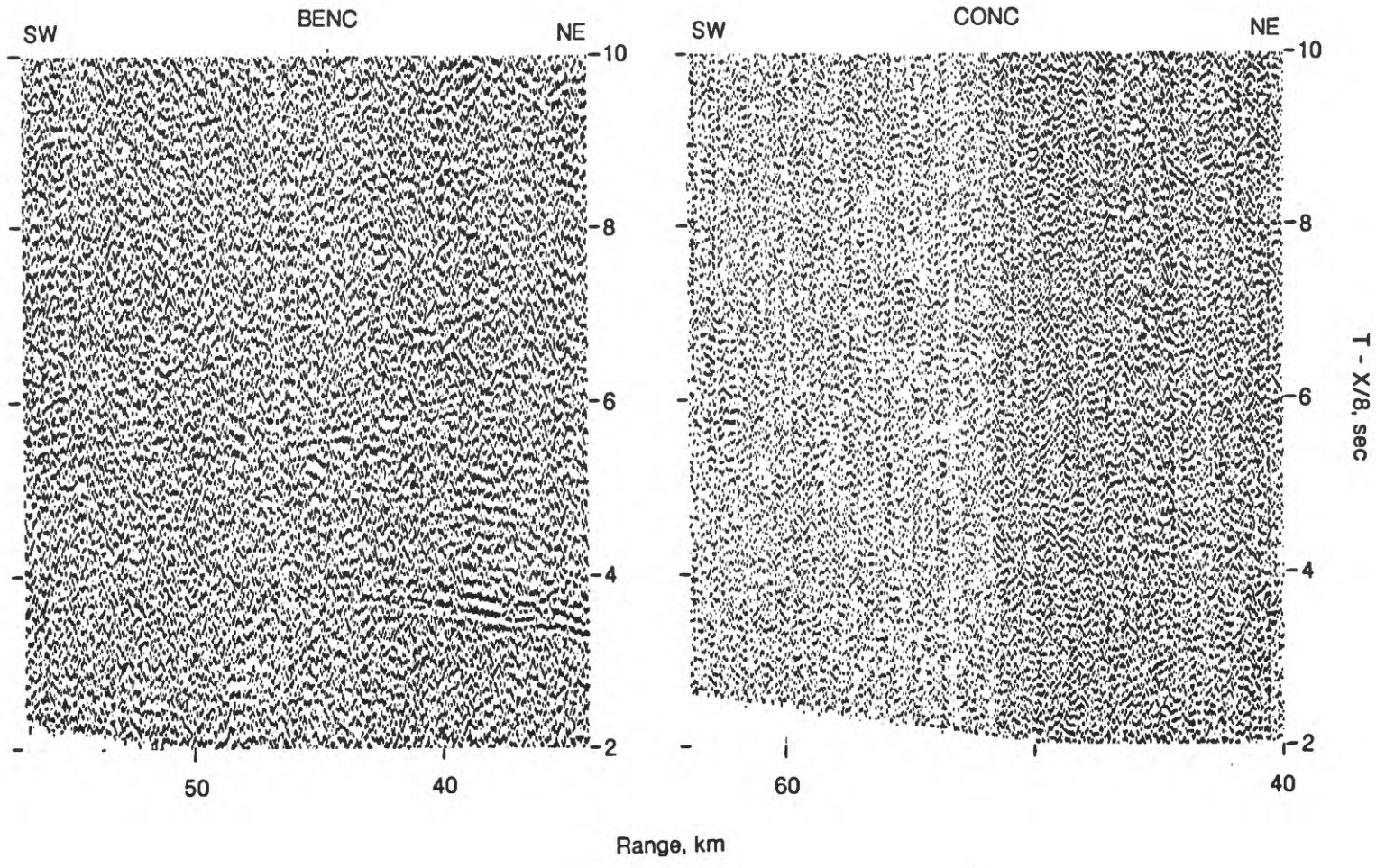

FIGURE 38. Receiver gathers for stations BENC and CONC from lines 201-202. The record sections have been linearly reduced using a velocity of 8 km/s and trace amplitudes have been scaled according to Range$^{0.7}$.

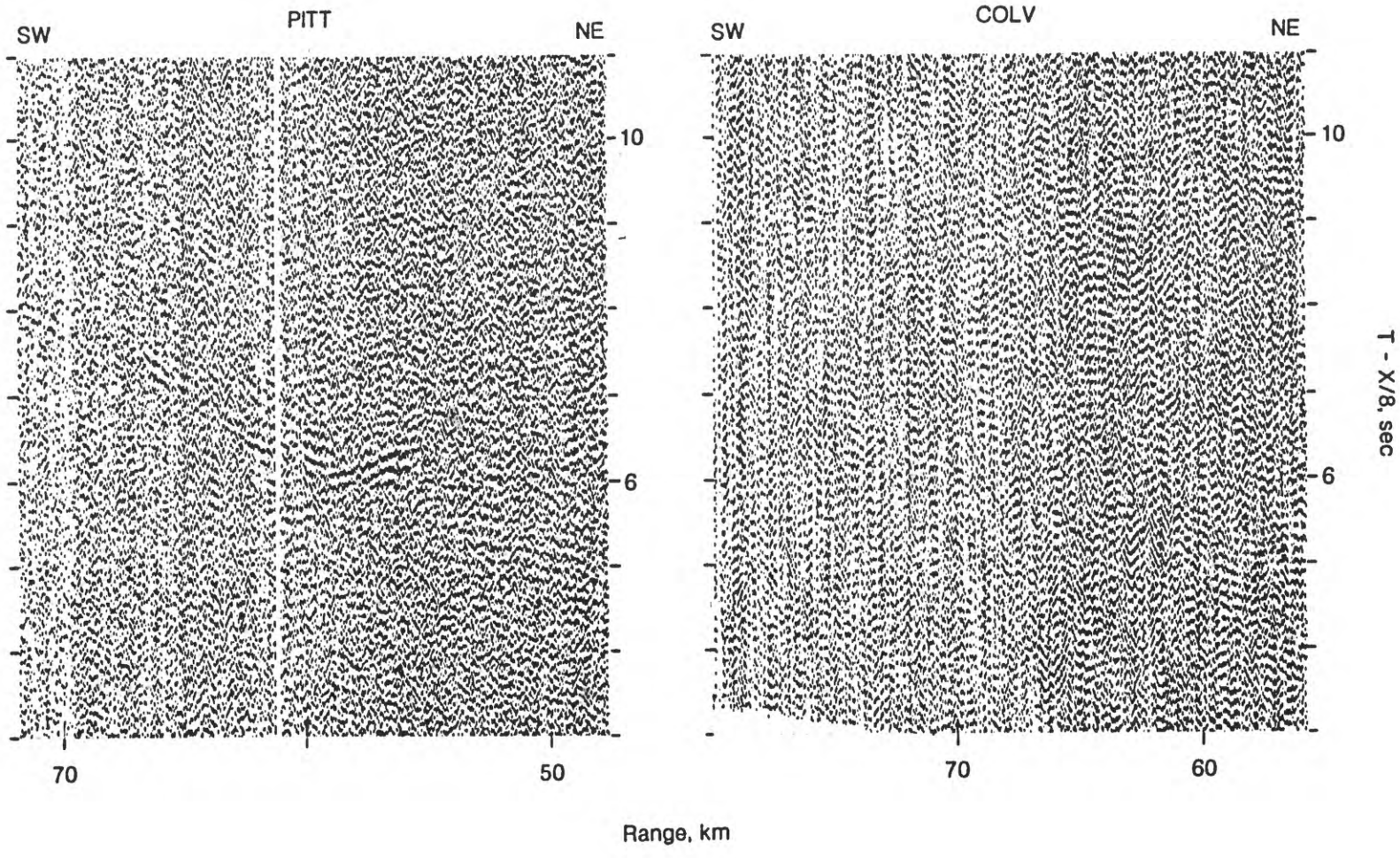

FIGURE 39. Receiver gathers for stations PITT and COLV from lines 201-202. The record sections have been linearly reduced using a velocity of 8 km/s and trace amplitudes have been scaled according to Range$^{0.7}$.

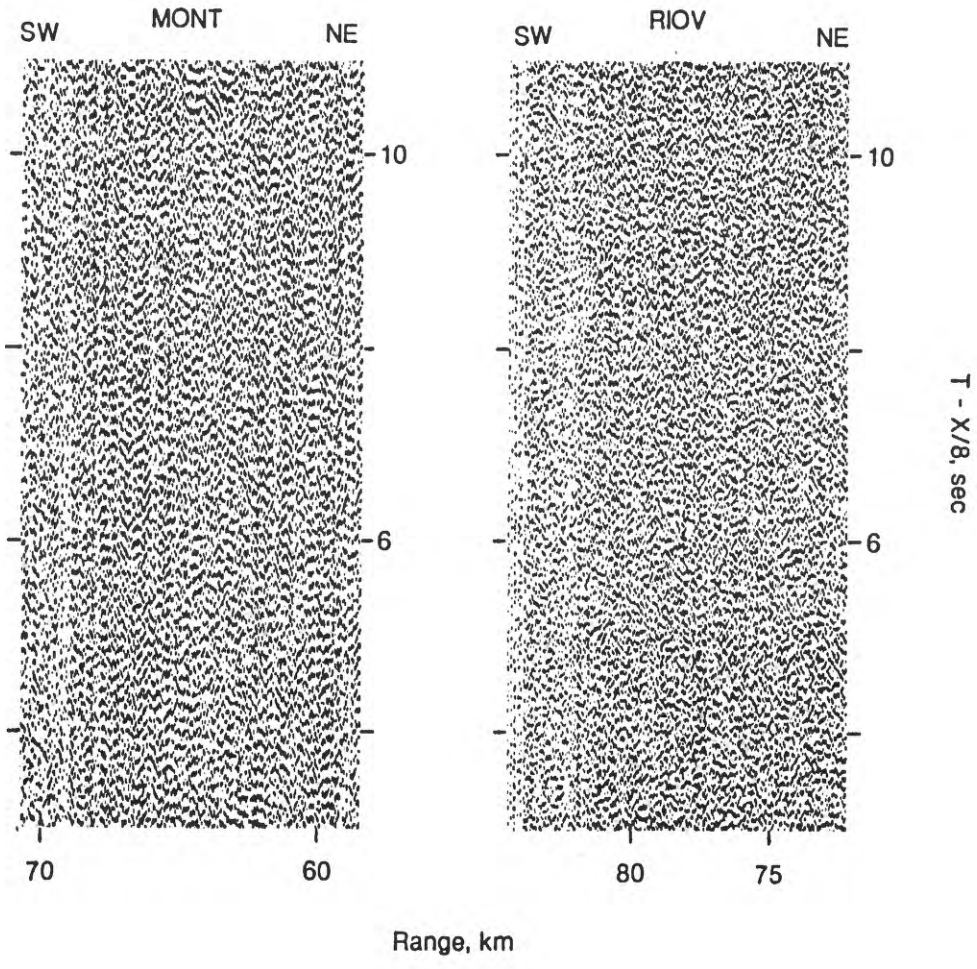

FIGURE 40. Deconvolved receiver gathers for stations MONT and RIOV from lines 201-202. The record sections have been linearly reduced using a velocity of 8 km/s and trace amplitudes have been scaled according to Range$^{0.7}$.

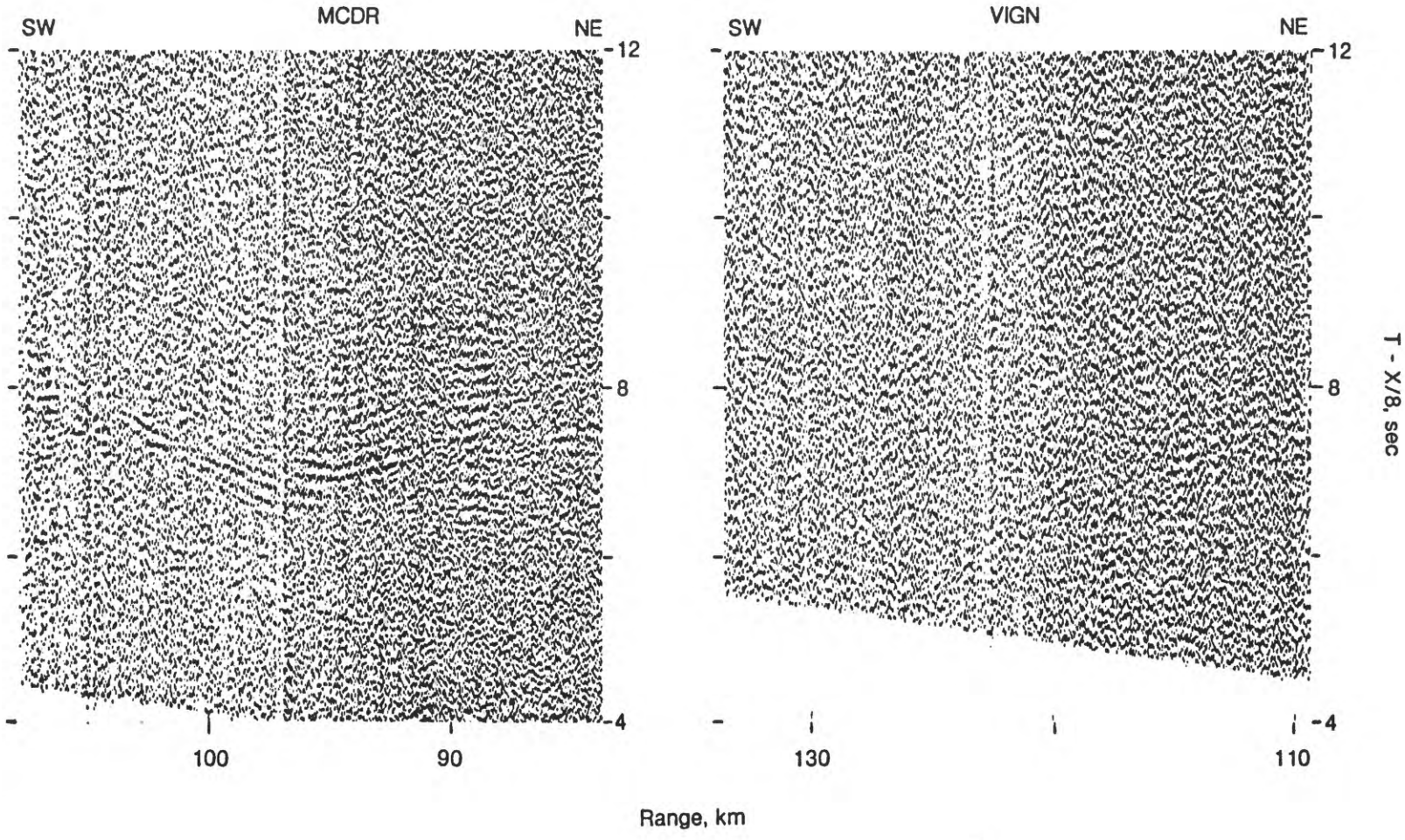

FIGURE 41. Receiver gathers for stations MCDR and VIGN from lines 201-202. The record sections have been linearly reduced using a velocity of 8 km/s and trace amplitudes have been scaled according to Range$^{0.7}$.

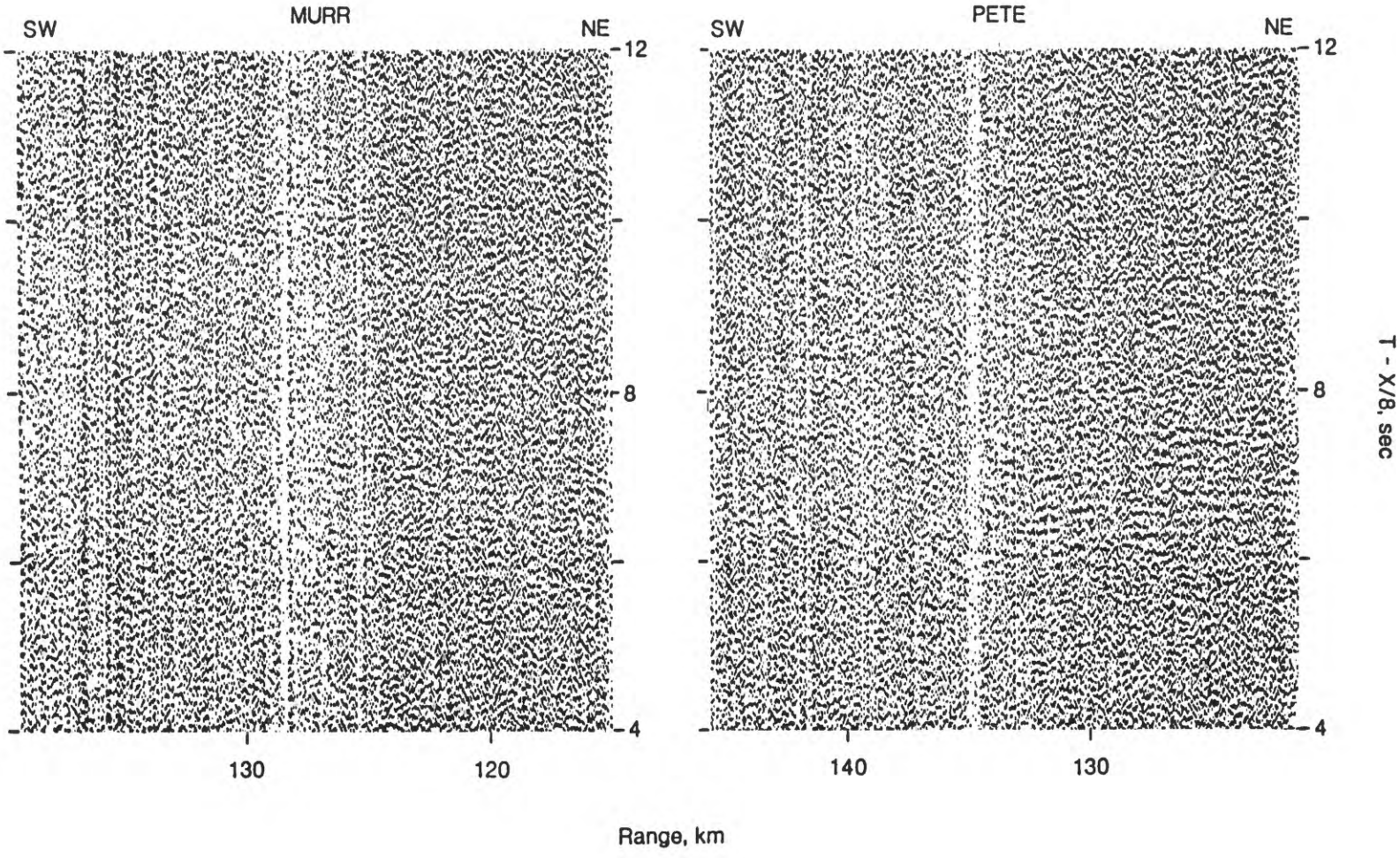

FIGURE 42. Deconvolved receiver gathers for stations MURR and PETE from lines 201-202. The record sections have been linearly reduced using a velocity of 8 km/s and trace amplitudes have been scaled according to Range$^{0.7}$.

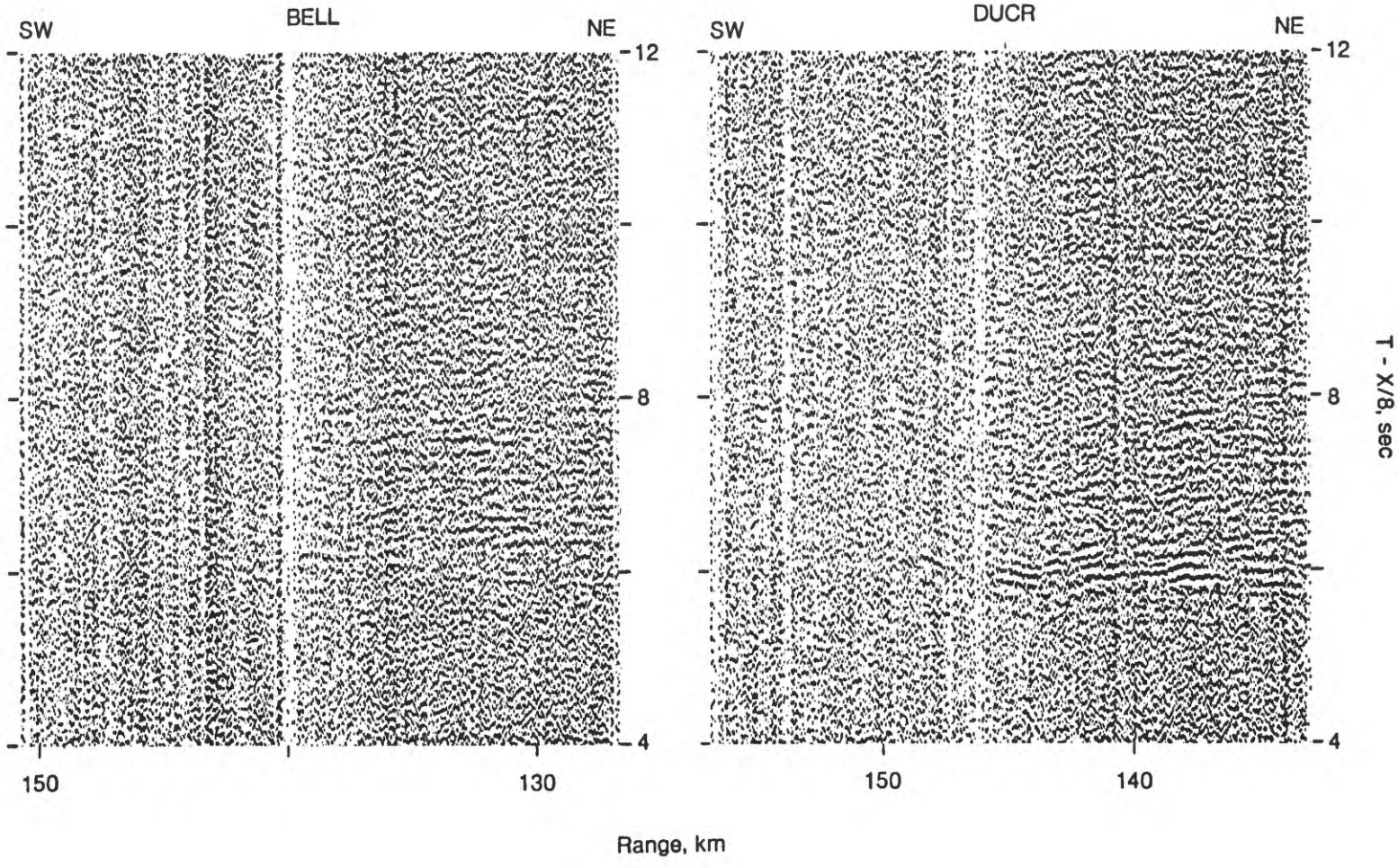

FIGURE 43. Deconvolved receiver gathers for stations BELL and DUCR from lines 201-202. The record sections have been linearly reduced using a velocity of 8 km/s and trace amplitudes have been scaled according to Range$^{0.7}$.

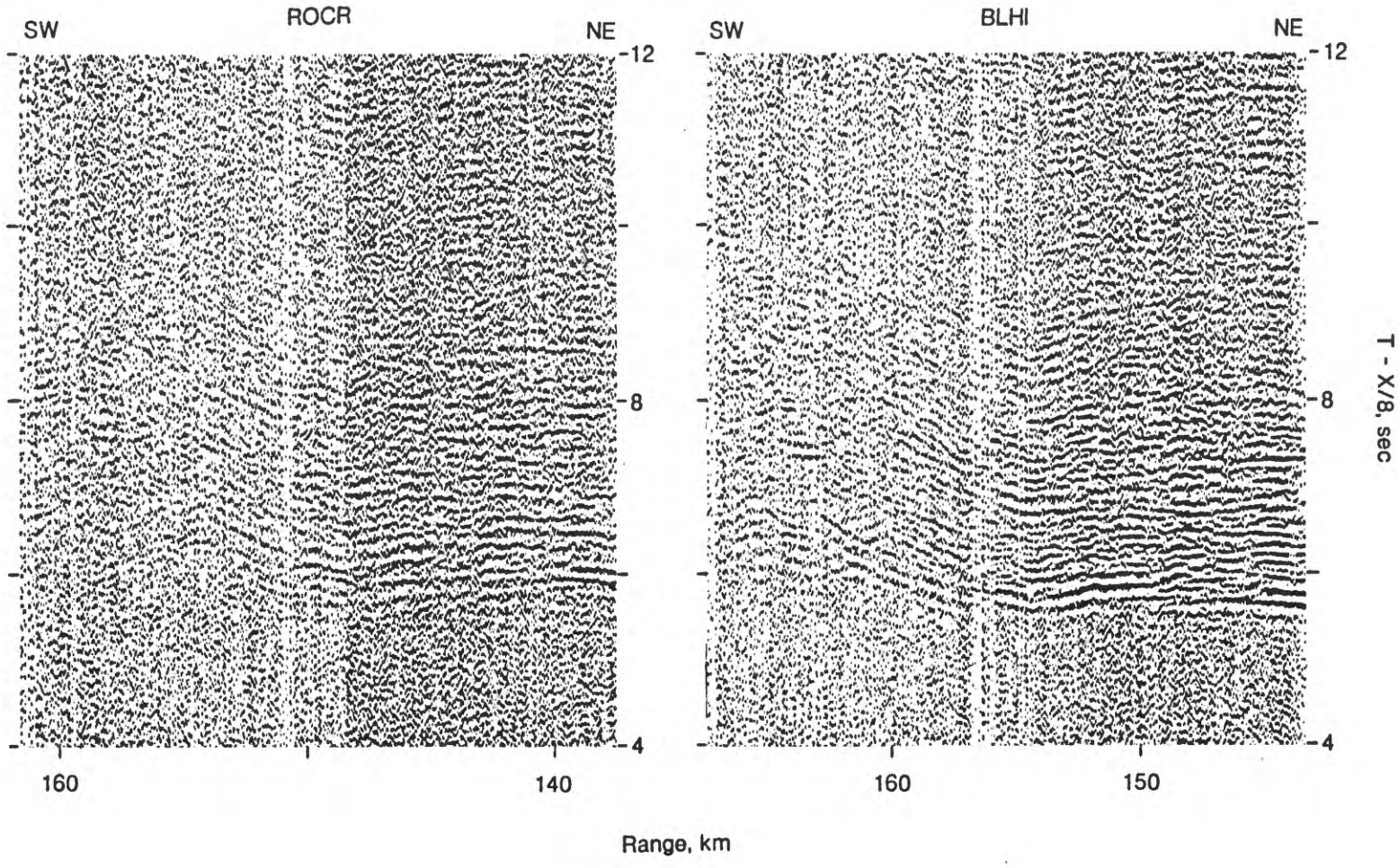

FIGURE 44. Deconvolved receiver gathers for stations ROCR and BLHI from lines 201-202. The record sections have been linearly reduced using a velocity of 8 km/s and trace amplitudes have been scaled according to Range$^{0.7}$.

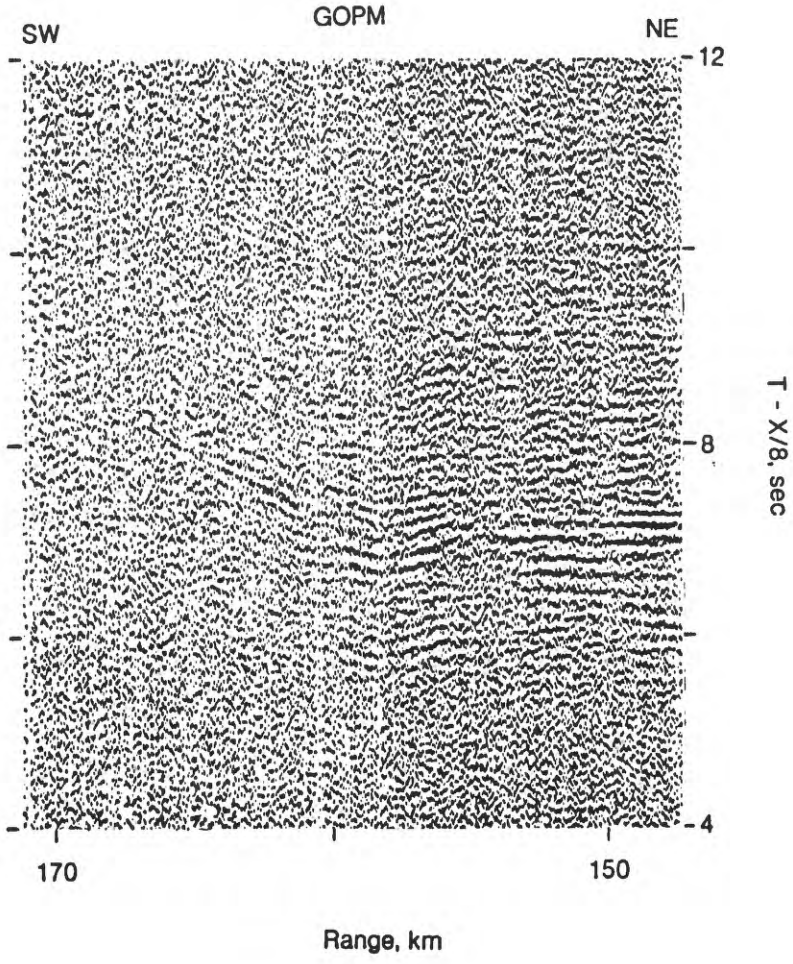

FIGURE 45. Deconvolved receiver gather for station GOPM from lines 201-202. The record section has been linearly reduced using a velocity of 8 km/s and trace amplitudes have been scaled according to Range$^{0.7}$.

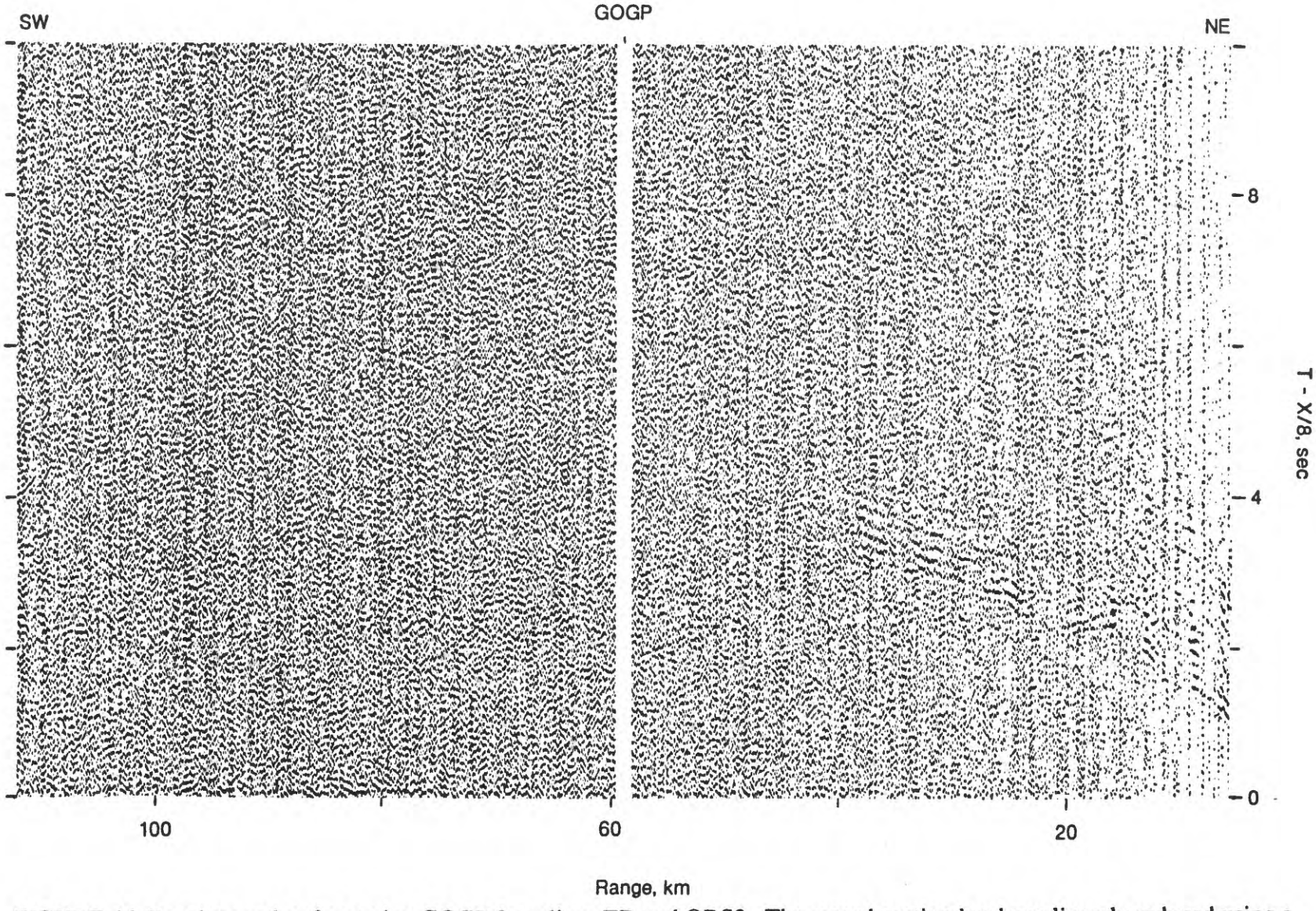

FIGURE 46. Receiver gather for station GOGP from lines TR and OBS2. The record section has been linearly reduced using a velocity of 8 km/s and trace amplitudes have been scaled according to Range$^{0.7}$.

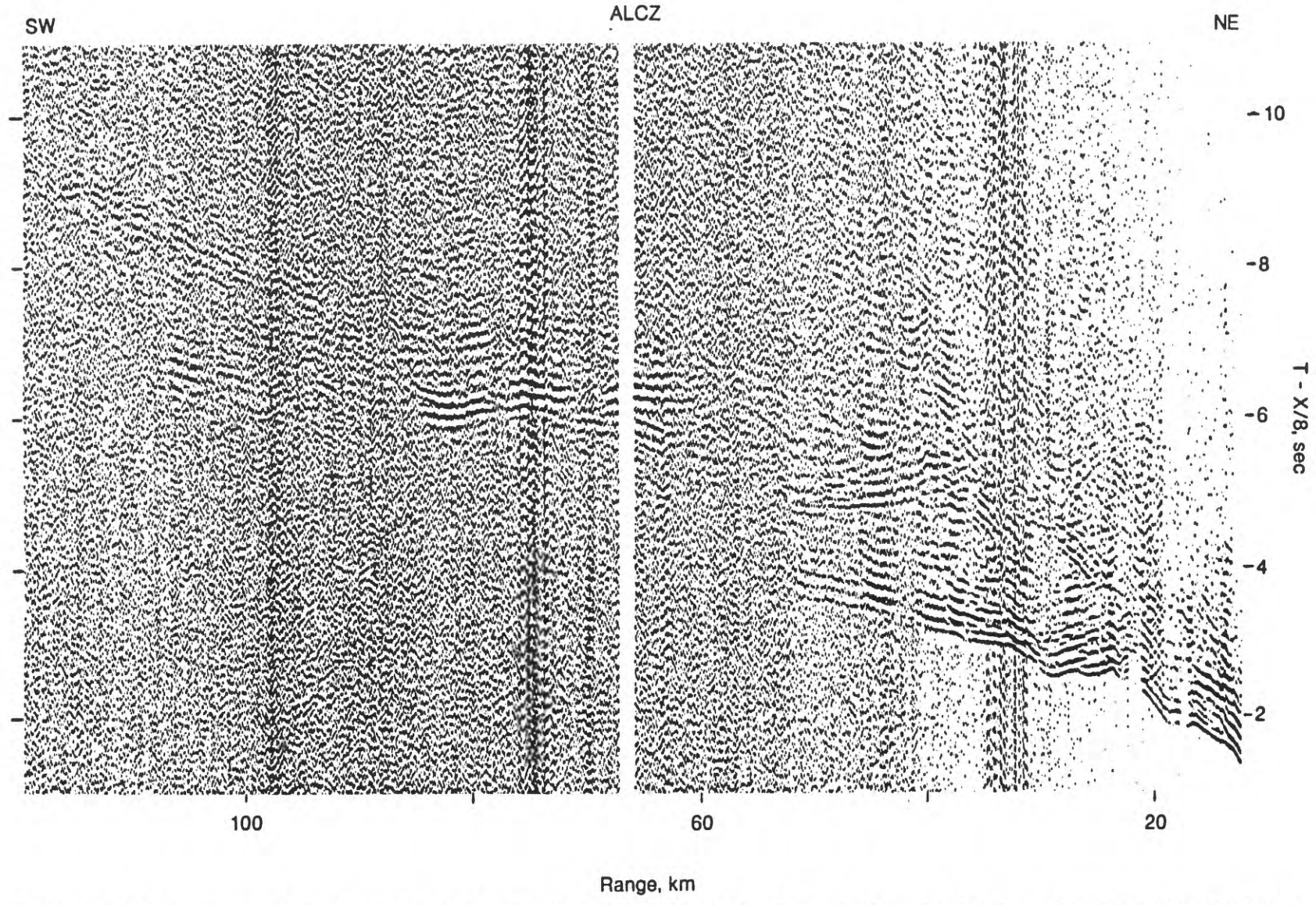

FIGURE 47. Receiver gather for station ALCZ from lines TR and OBS2. The record section has been linearly reduced using a velocity of 8 km/s and trace amplitudes have been scaled according to Range$^{0.7}$.

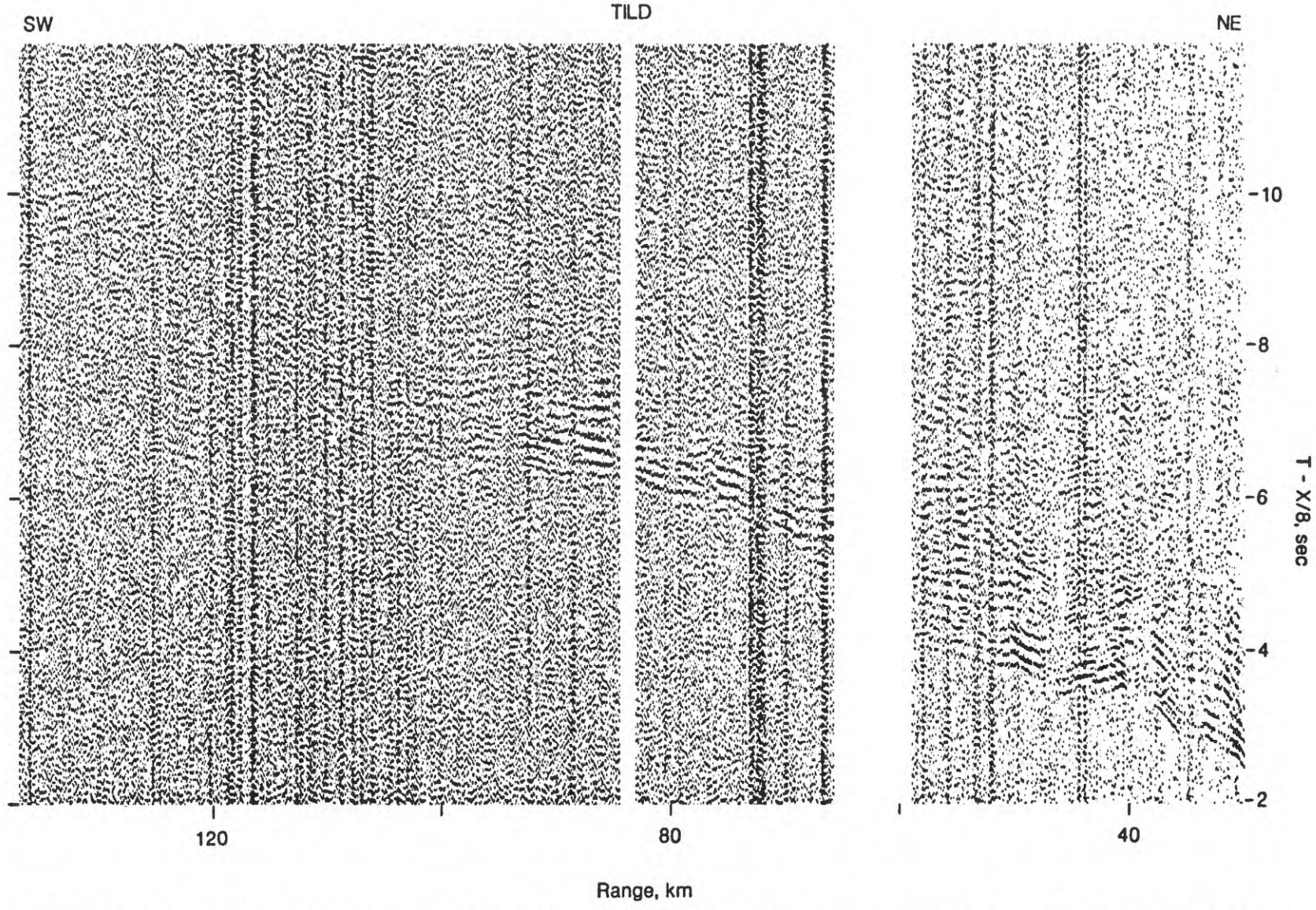

FIGURE 48. Receiver gather for station TILD from lines TR and OBS2. The record section has been linearly reduced using a velocity of 8 km/s and trace amplitudes have been scaled according to Range$^{0.7}$.

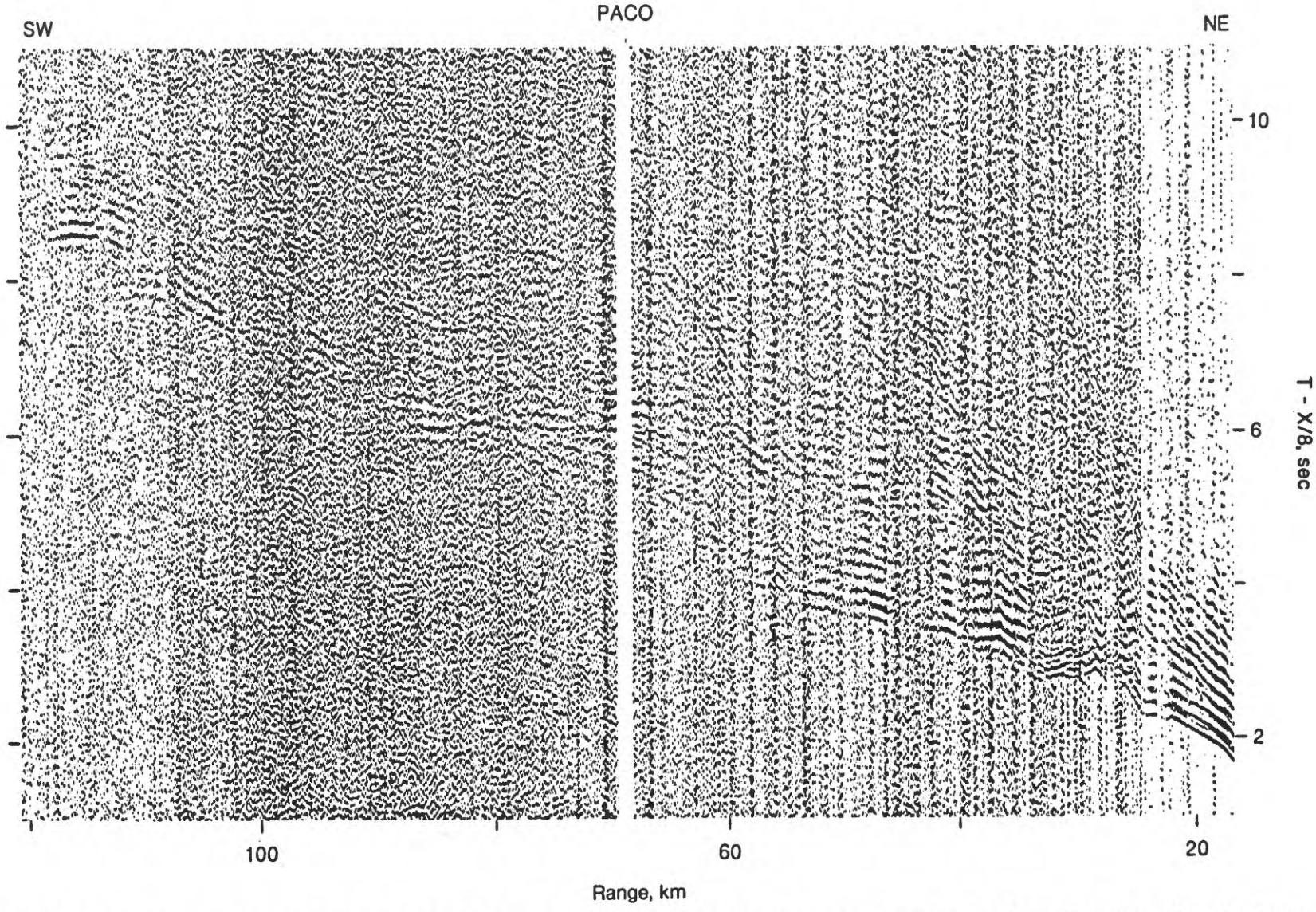

FIGURE 49. Receiver gather for station PACO from lines TR and OBS2. The record section has been linearly reduced using a velocity of 8 km/s and trace amplitudes have been scaled according to Range$^{0.7}$.

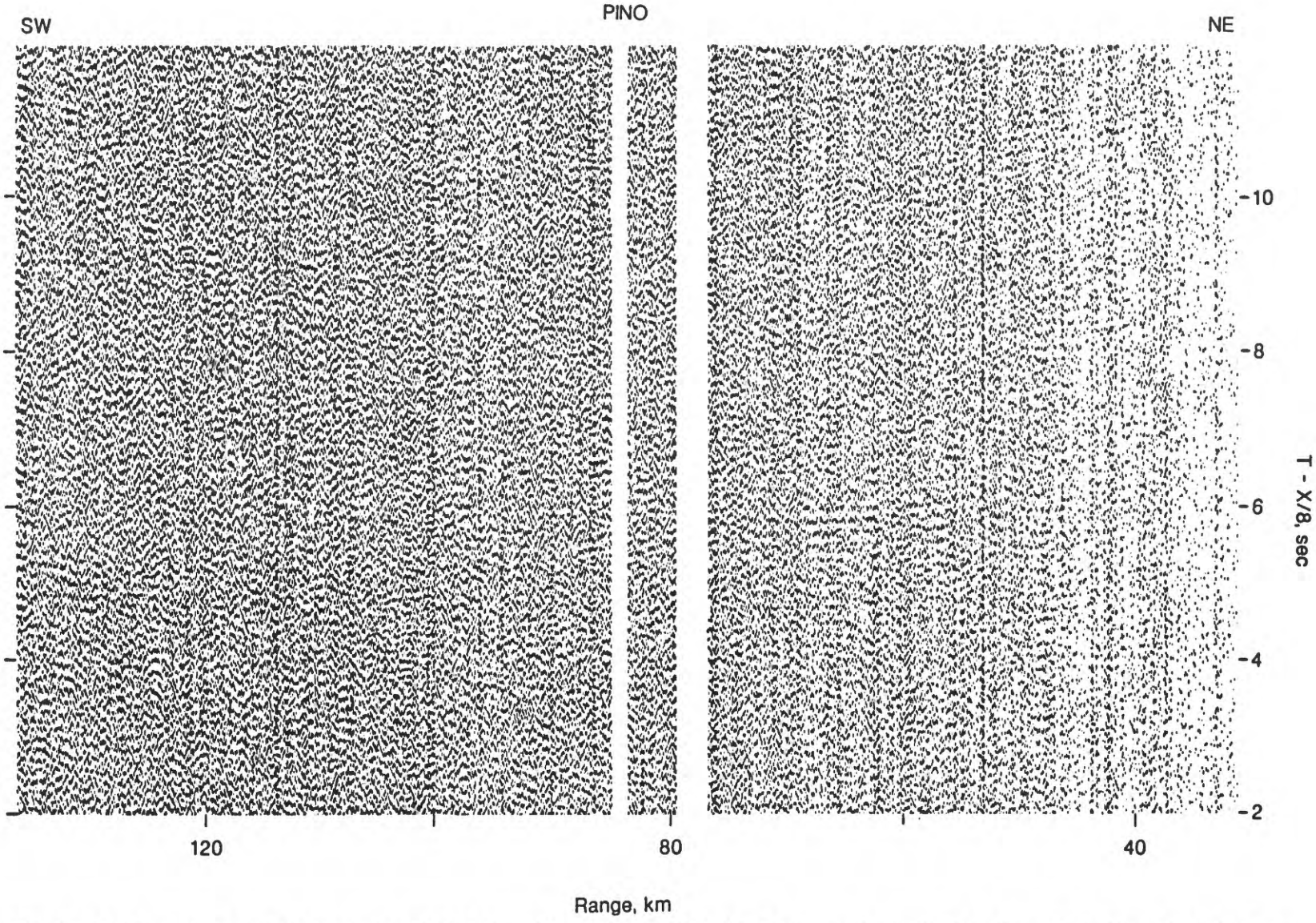

FIGURE 50. Receiver gather for station PINO from lines TR and OBS2. The record section has been linearly reduced using a velocity of 8 km/s and trace amplitudes have been scaled according to Range$^{0.7}$.

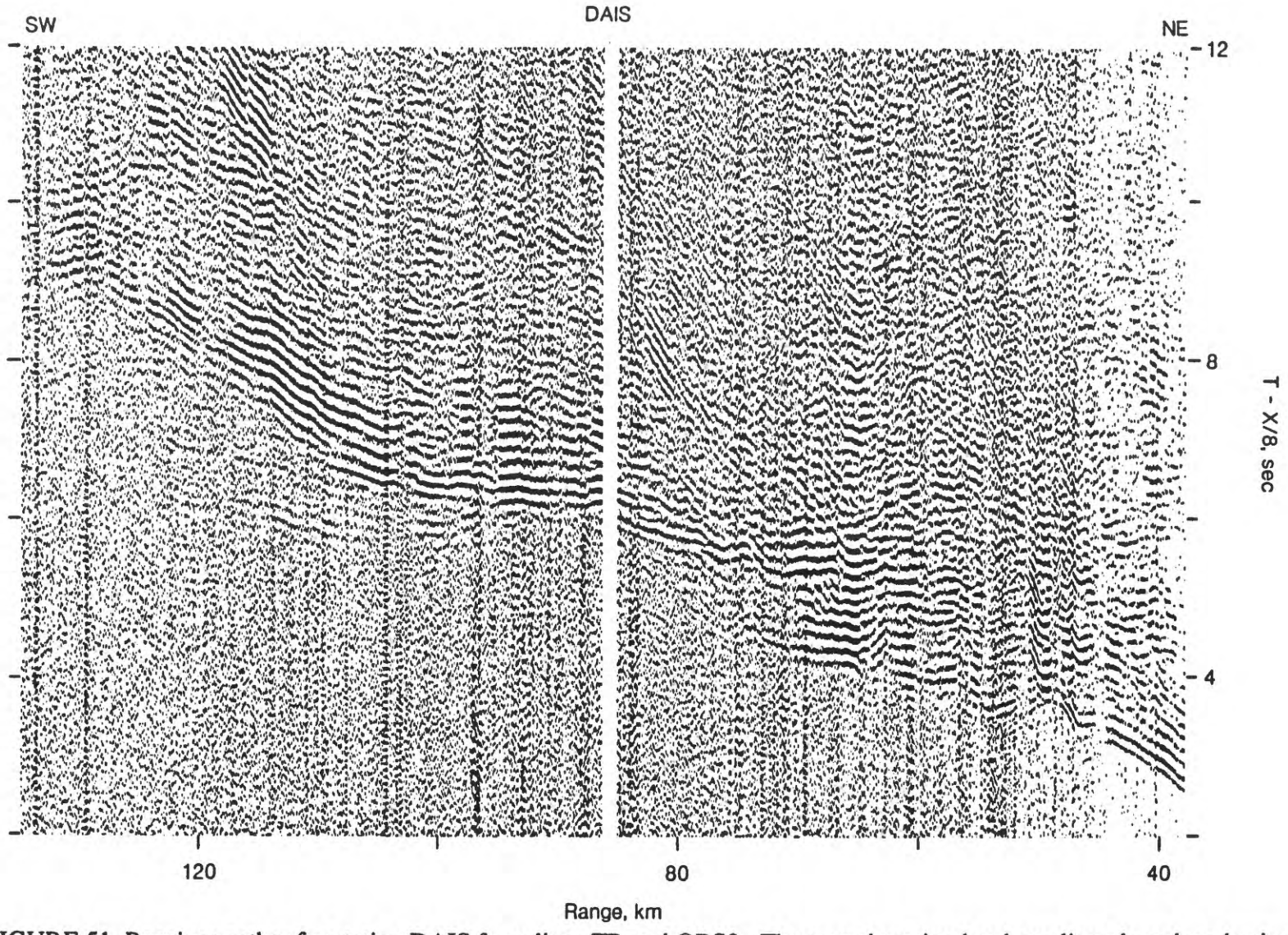

FIGURE 51. Receiver gather for station DAIS from lines TR and OBS2. The record section has been linearly reduced using a velocity of 8 km/s and trace amplitudes have been scaled according to Range$^{0.7}$.

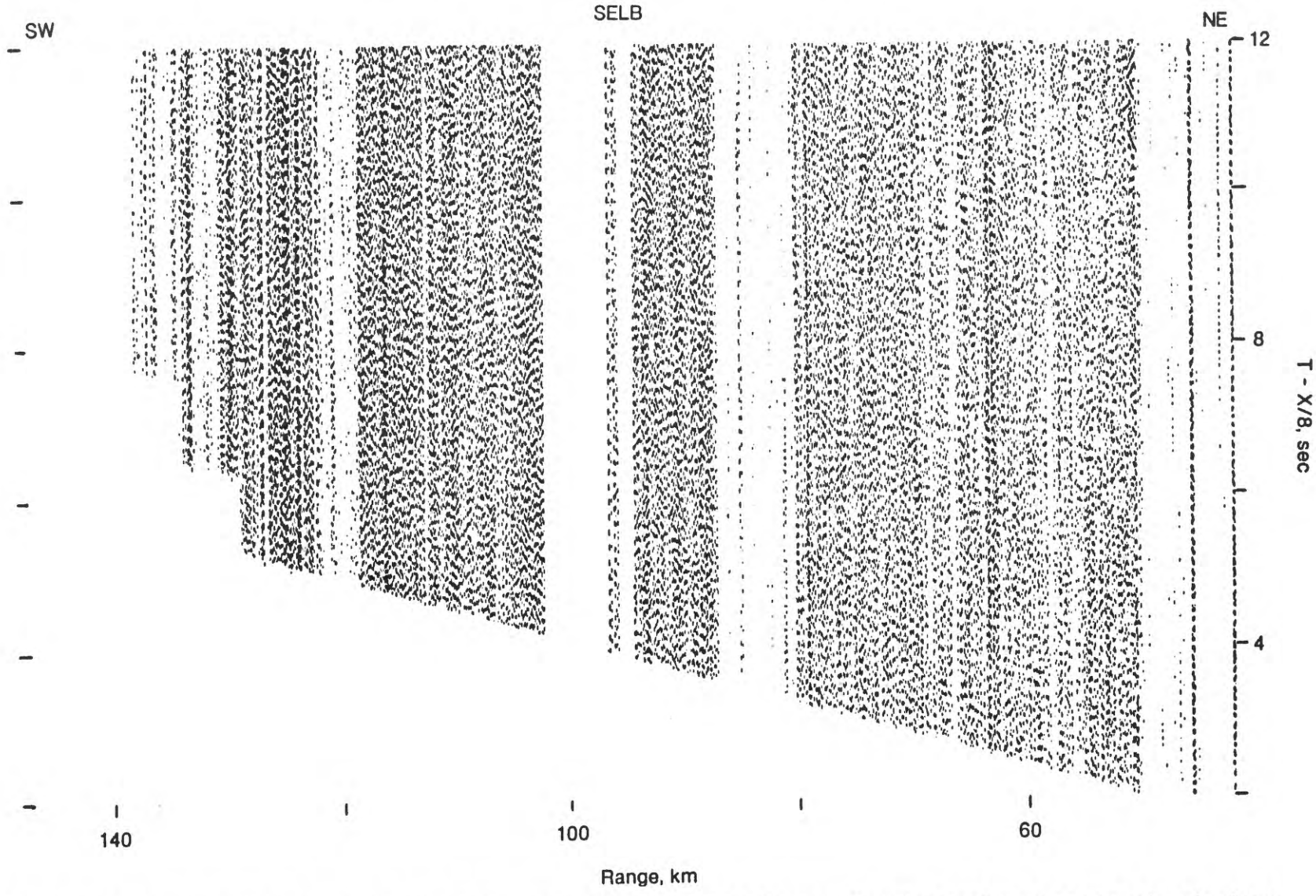

FIGURE 52. Receiver gather for station SELB from lines TR and OBS2. The record section has been linearly reduced using a velocity of 8 km/s and trace amplitudes have been scaled according to Range$^{0.7}$.

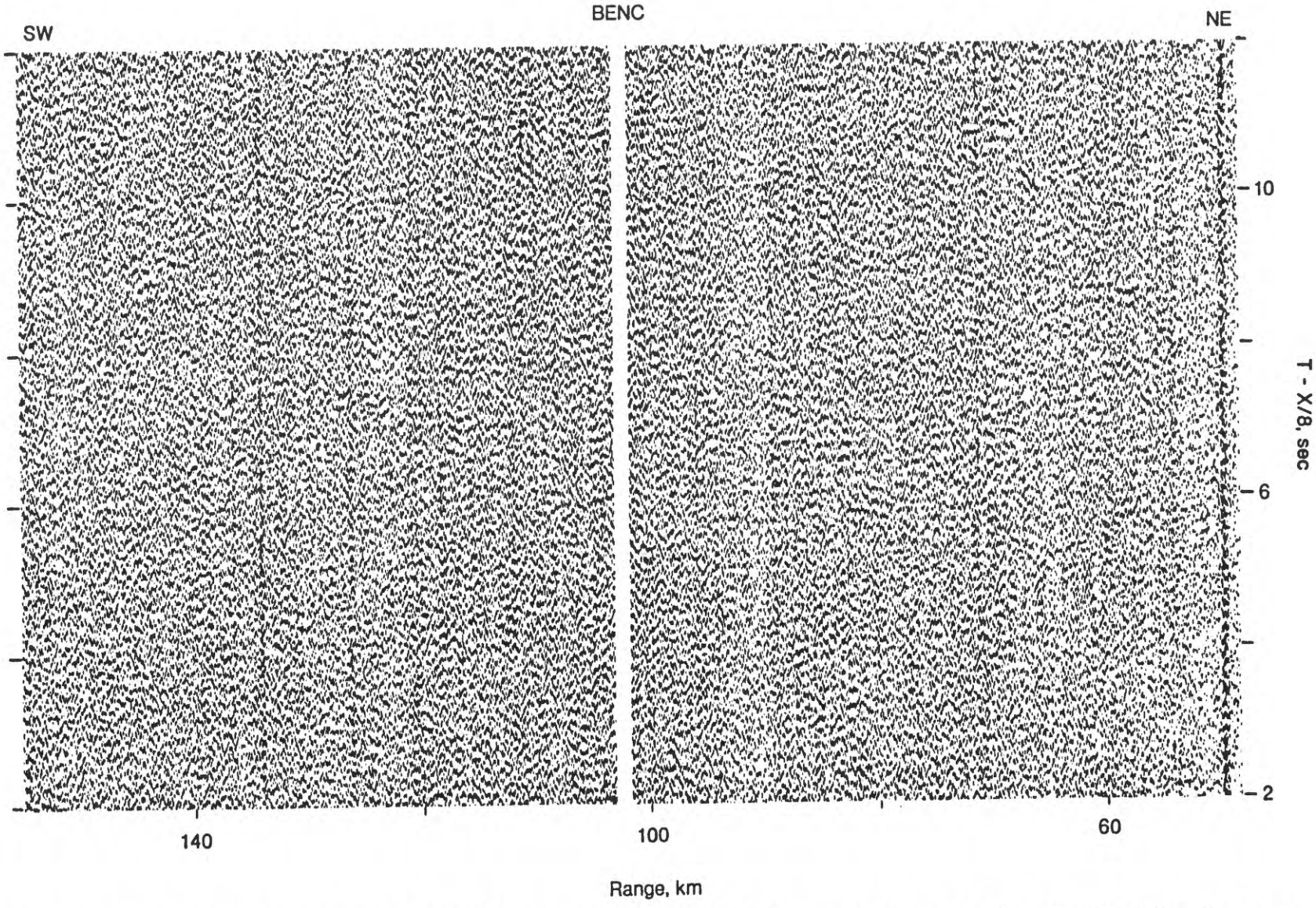

FIGURE 53. Receiver gather for station BENC from lines TR and OBS2. The record section has been linearly reduced using a velocity of 8 km/s and trace amplitudes have been scaled according to Range$^{0.7}$.

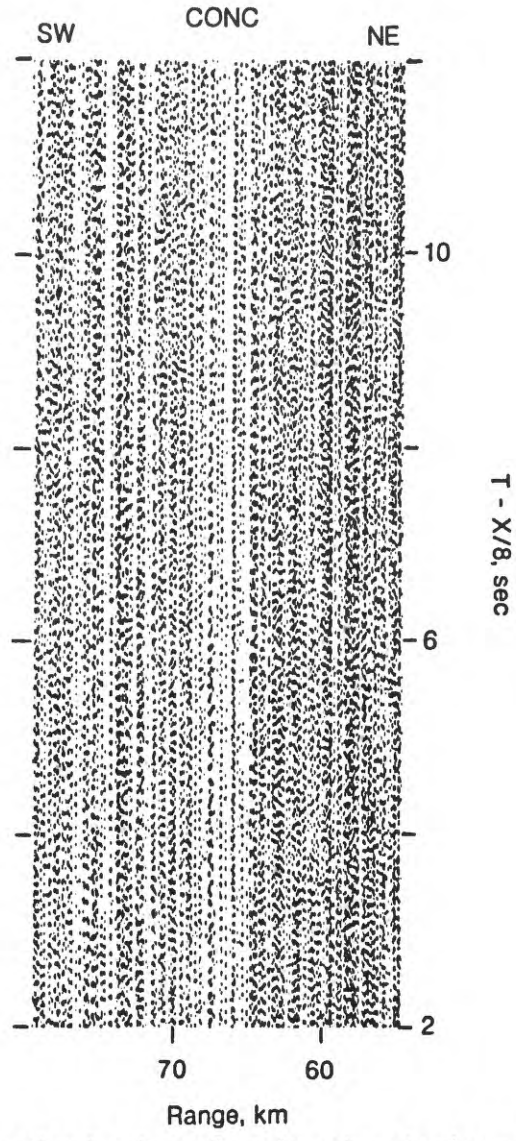

FIGURE 54. Receiver gather for station CONC from lines TR and OBS2. The record section has been linearly reduced using a velocity of 8 km/s and trace amplitudes have been scaled according to Range$^{0.7}$.

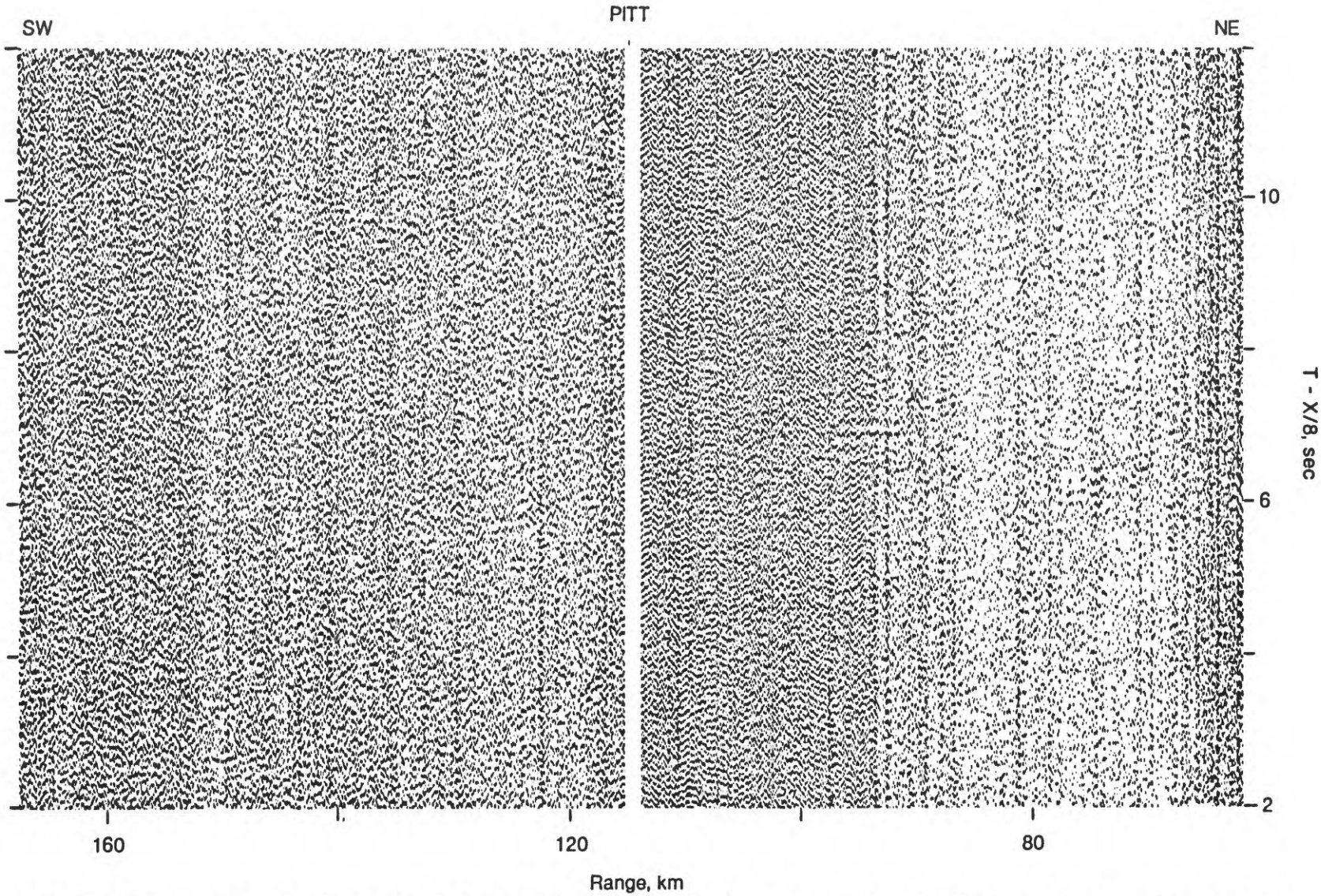

FIGURE 55. Receiver gather for station PITT from lines TR and OBS2. The record section has been linearly reduced using a velocity of 8 km/s and trace amplitudes have been scaled according to Range$^{0.7}$.

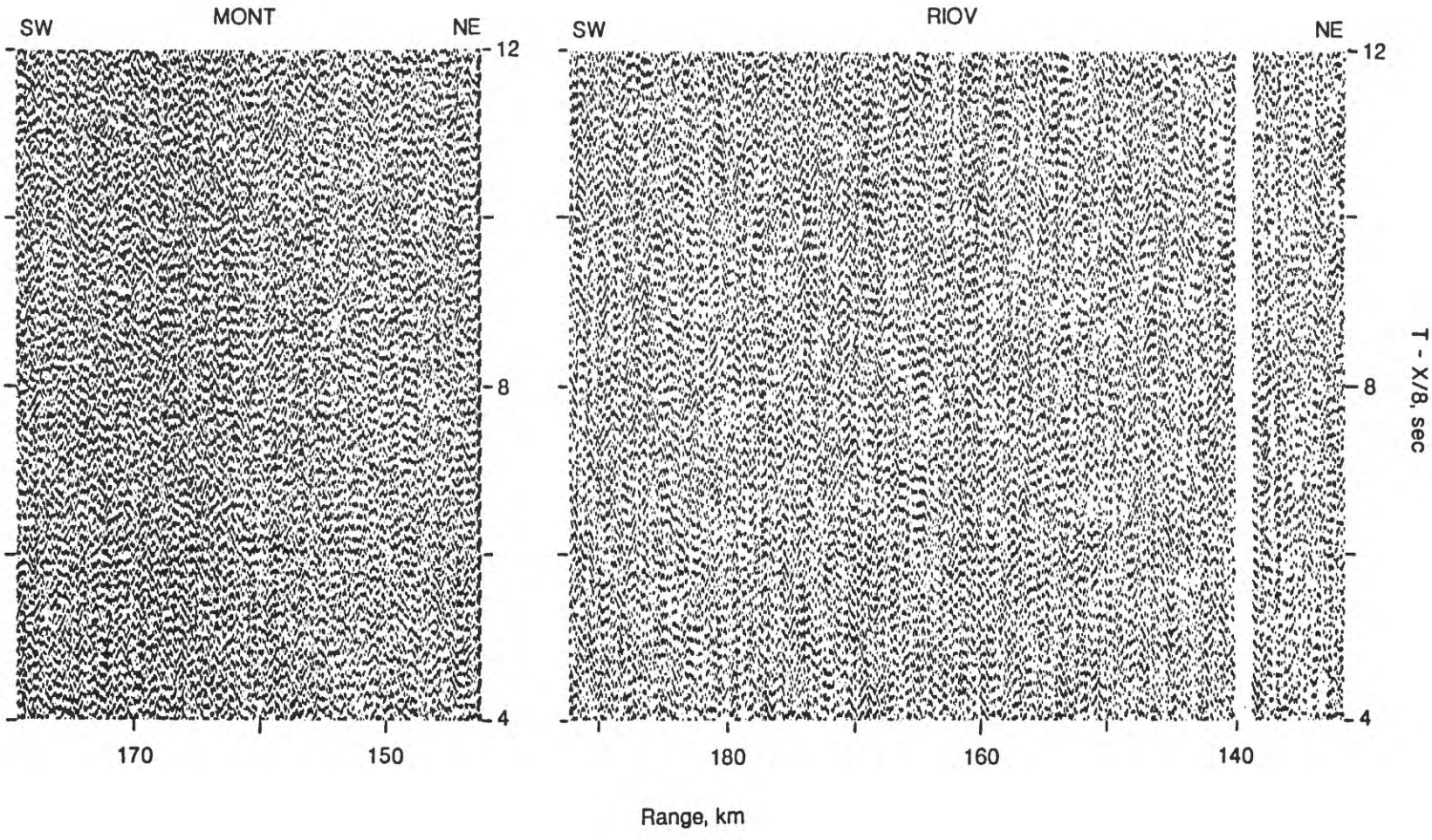

FIGURE 56. Receiver gathers for stations MONT and RIOV from lines TR and OBS2. The record sections have been linearly reduced using a velocity of 8 km/s and trace amplitudes have been scaled according to Range$^{0.7}$.

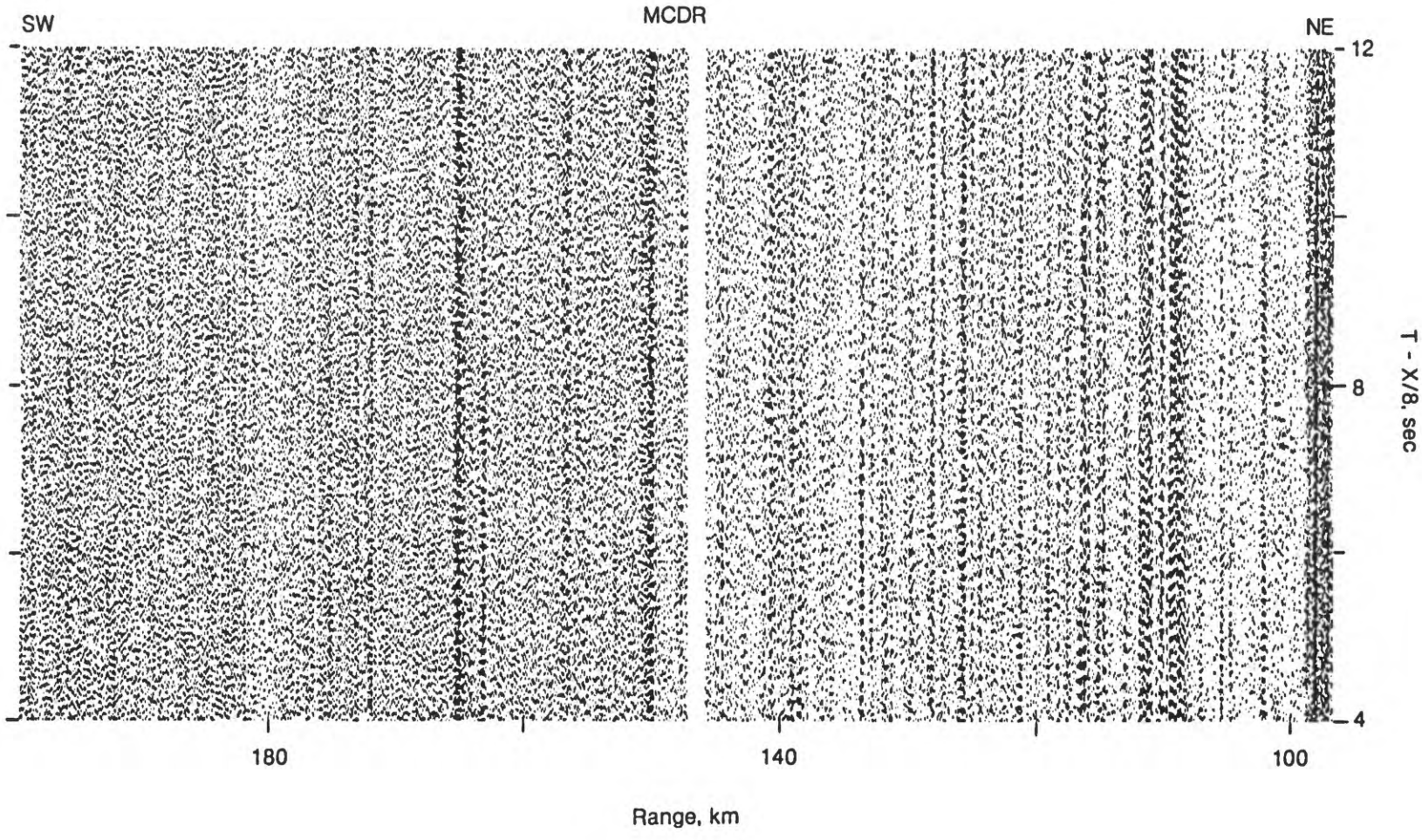

FIGURE 57. Receiver gather for station MCDR from lines TR and OBS2. The record section has been linearly reduced using a velocity of 8 km/s and trace amplitudes have been scaled according to Range$^{0.7}$.

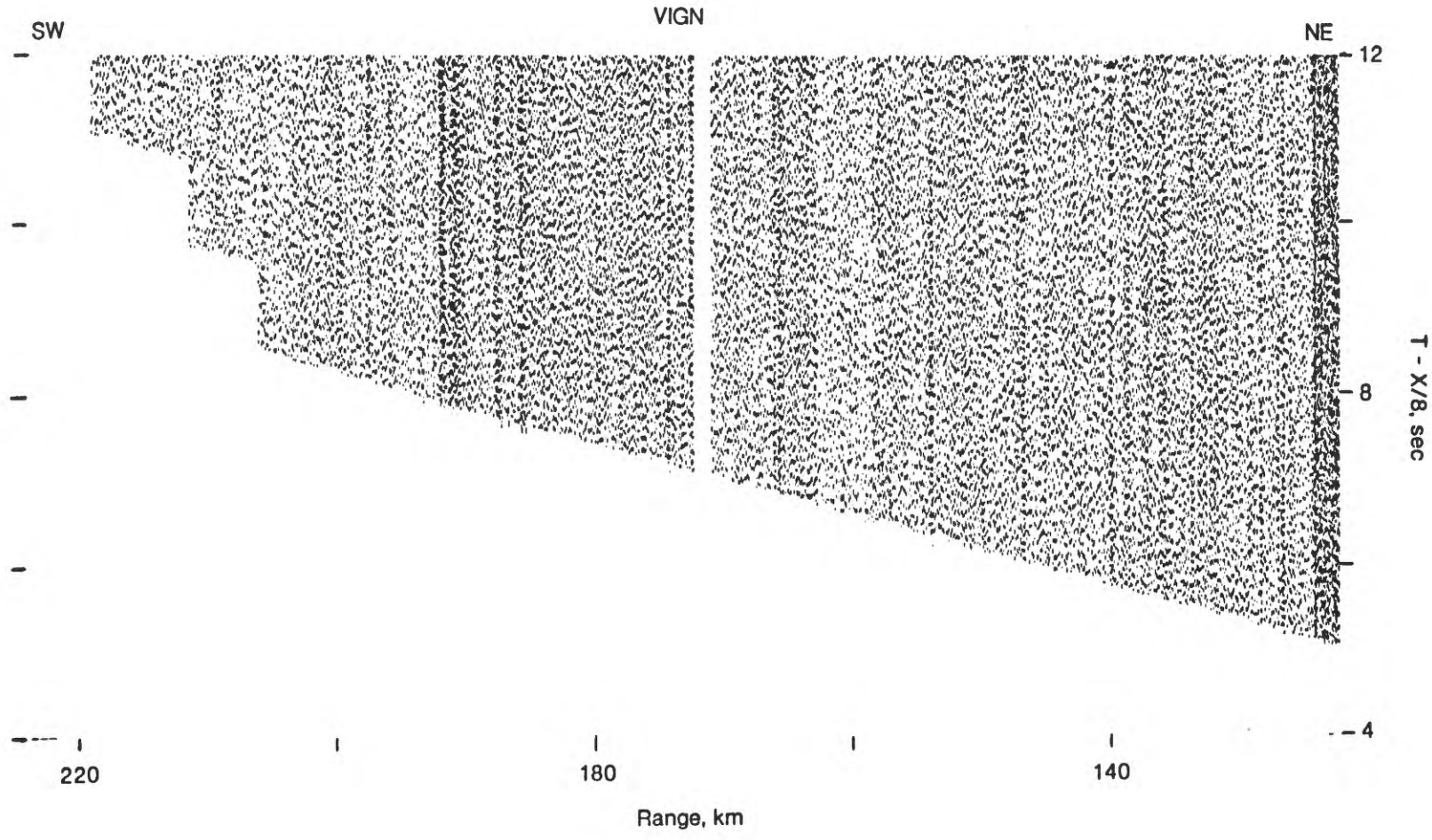

FIGURE 58. Receiver gather for station VIGN from lines TR and OBS2. The record section has been linearly reduced using a velocity of 8 km/s and trace amplitudes have been scaled according to Range$^{0.7}$.

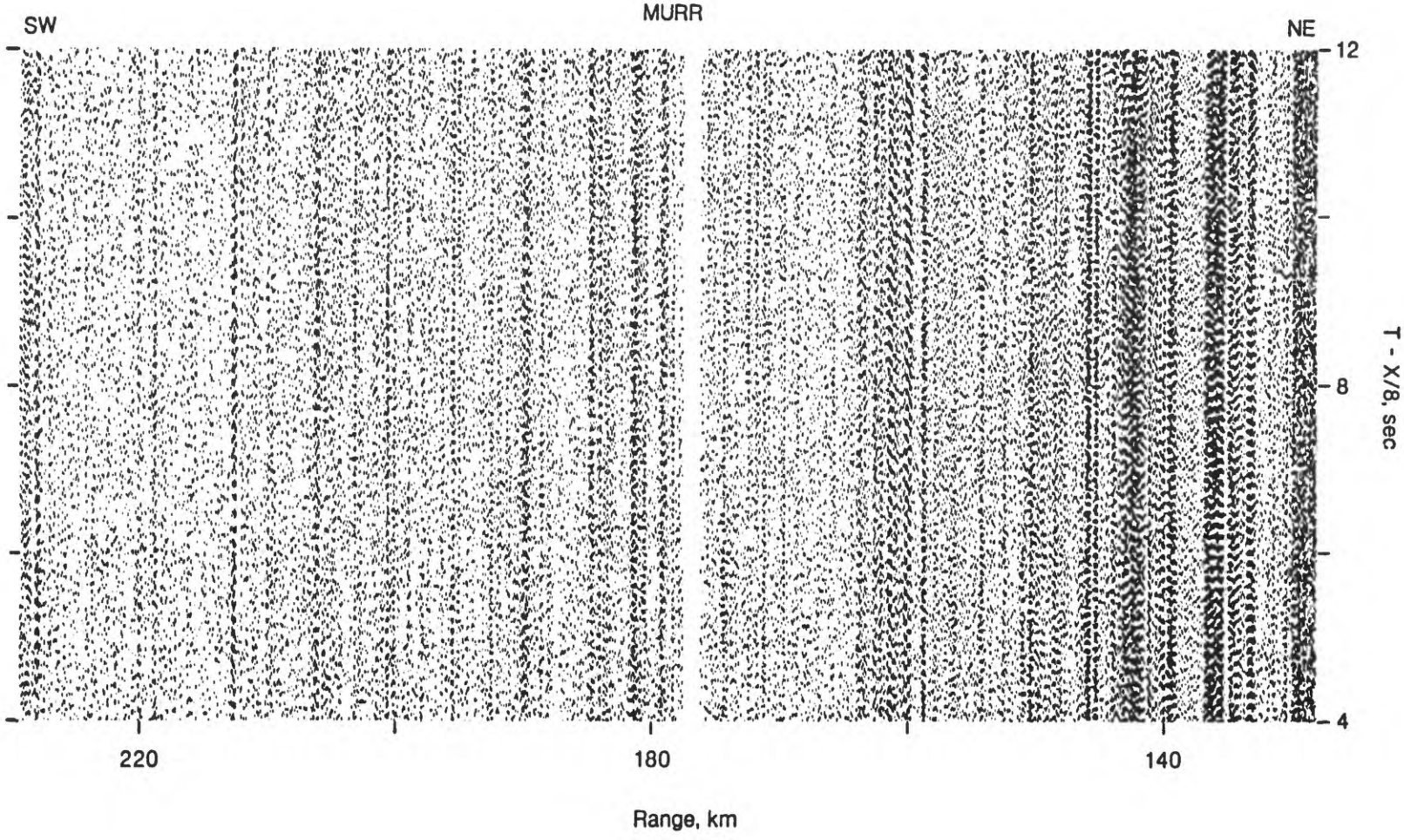

FIGURE 59. Receiver gather for station MURR from lines TR and OBS2. The record section has been linearly reduced using a velocity of 8 km/s and trace amplitudes have been scaled according to Range$^{0.7}$.

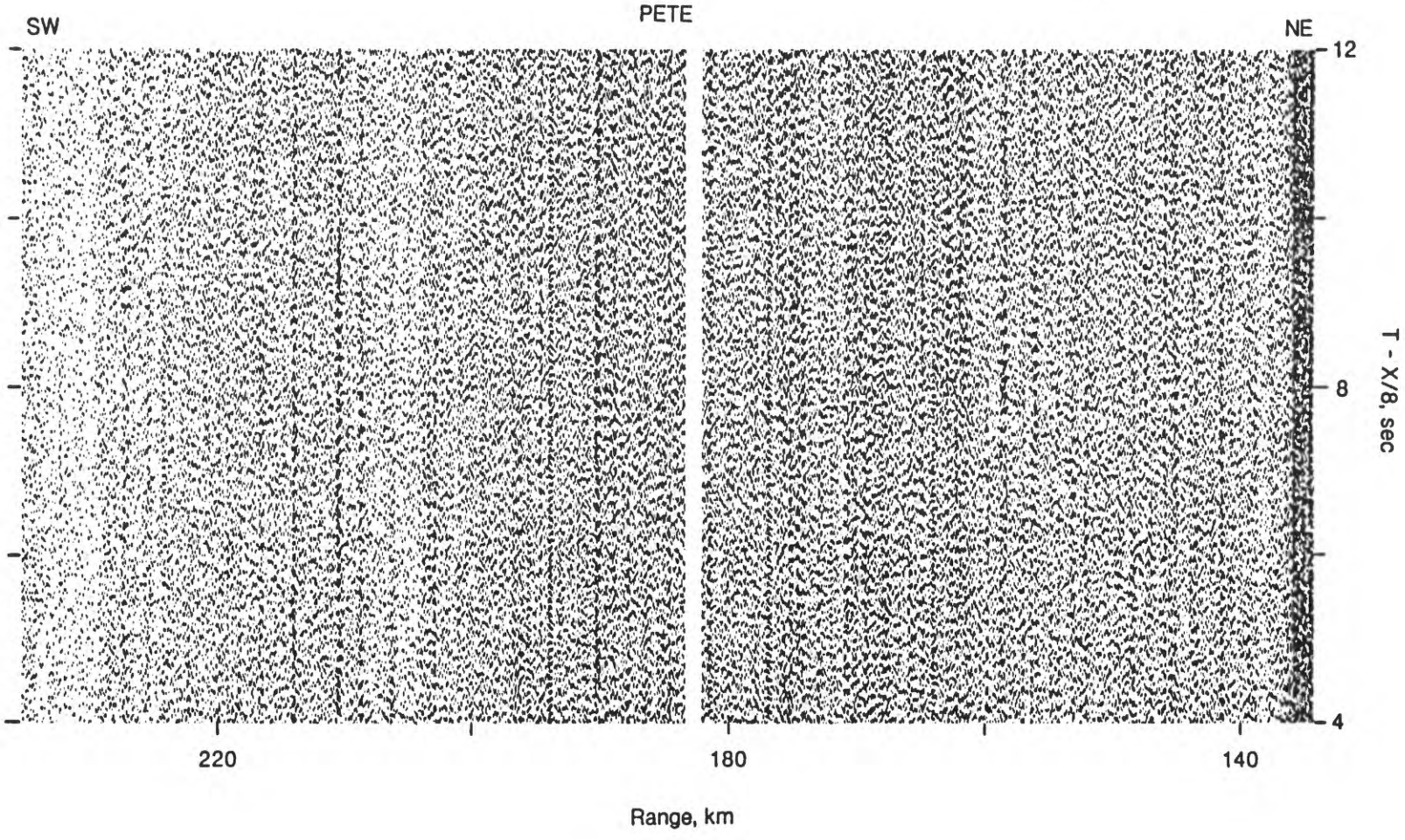

FIGURE 60. Receiver gather for station PETE from lines TR and OBS2. The record section has been linearly reduced using a velocity of 8 km/s and trace amplitudes have been scaled according to Range$^{0.7}$.

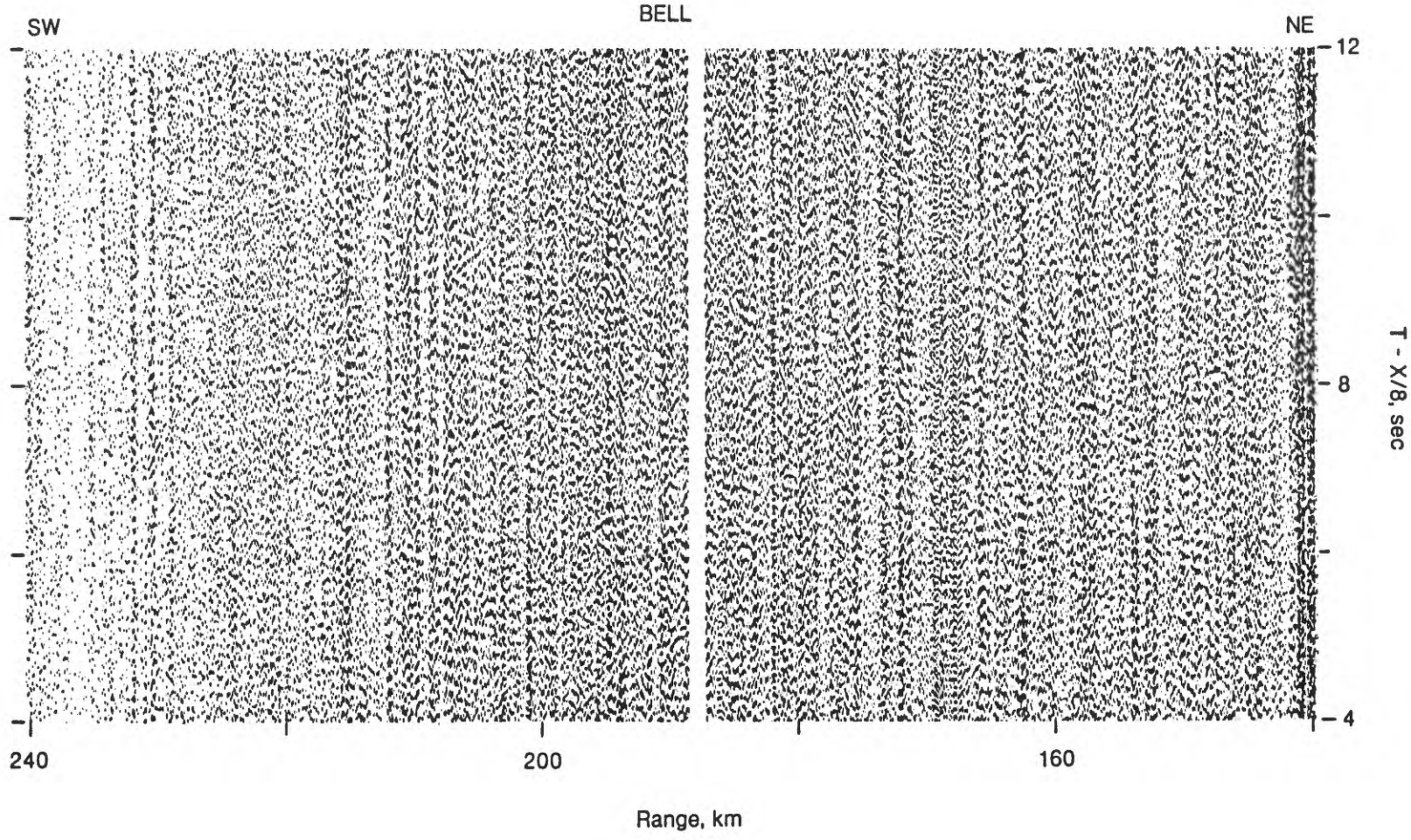

FIGURE 61. Receiver gather for station BELL from lines TR and OBS2. The record section has been linearly reduced using a velocity of 8 km/s and trace amplitudes have been scaled according to Range$^{0.7}$.

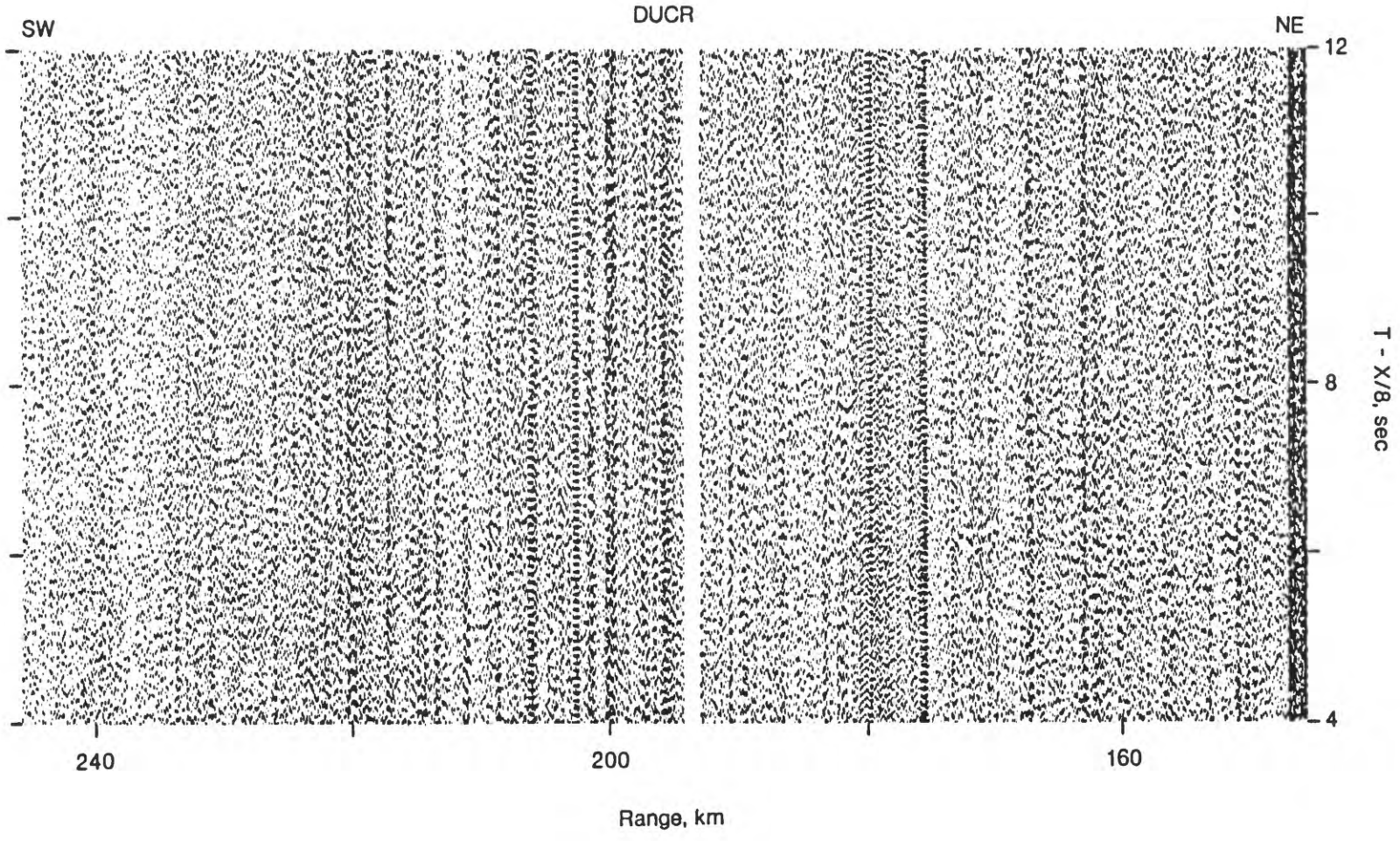

FIGURE 62. Receiver gather for station DUCR from lines TR and OBS2. The record section has been linearly reduced using a velocity of 8 km/s and trace amplitudes have been scaled according to Range$^{0.7}$.

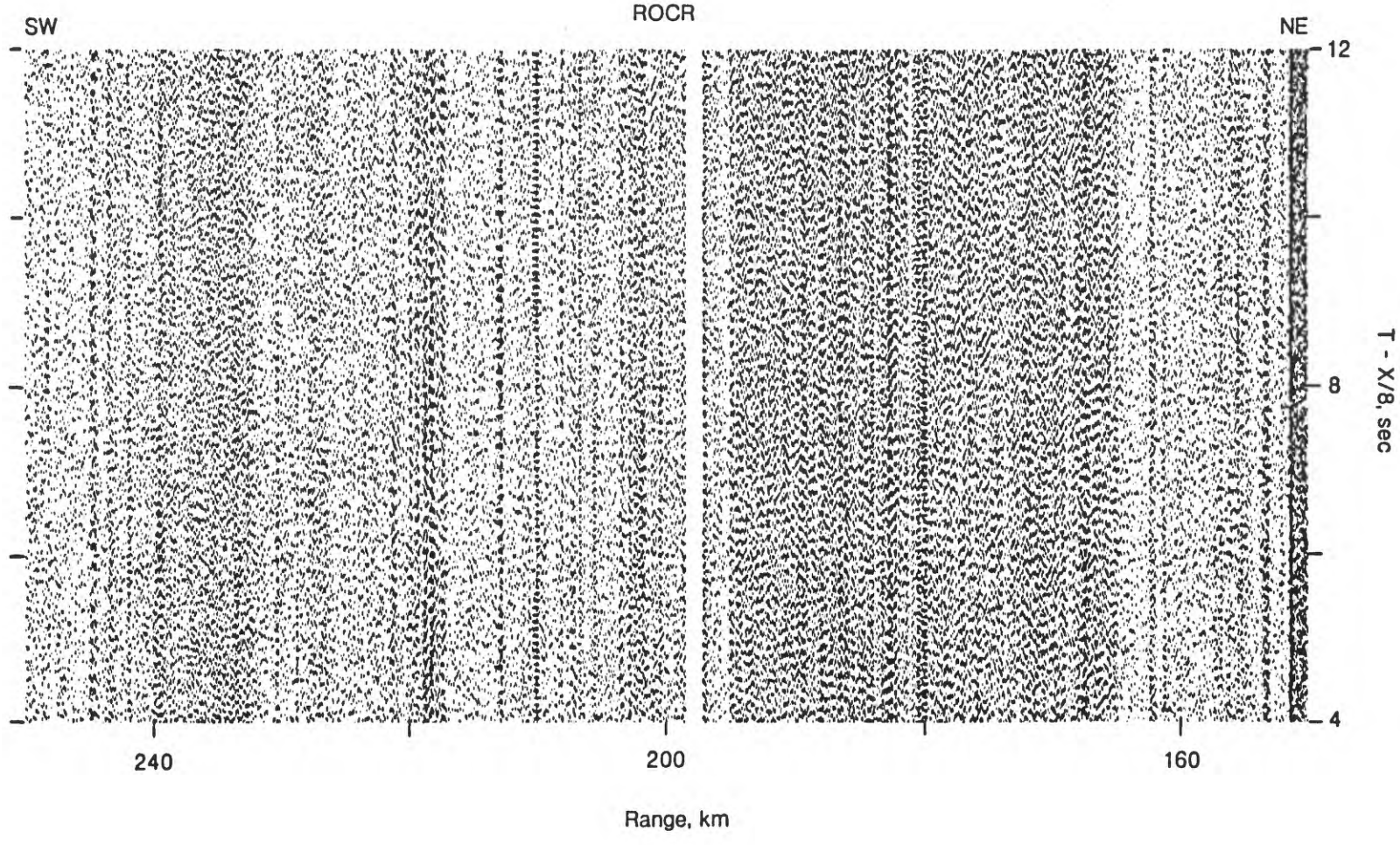

FIGURE 63. Receiver gather for station ROCR from lines TR and OBS2. The record section has been linearly reduced using a velocity of 8 km/s and trace amplitudes have been scaled according to Range$^{0.7}$.

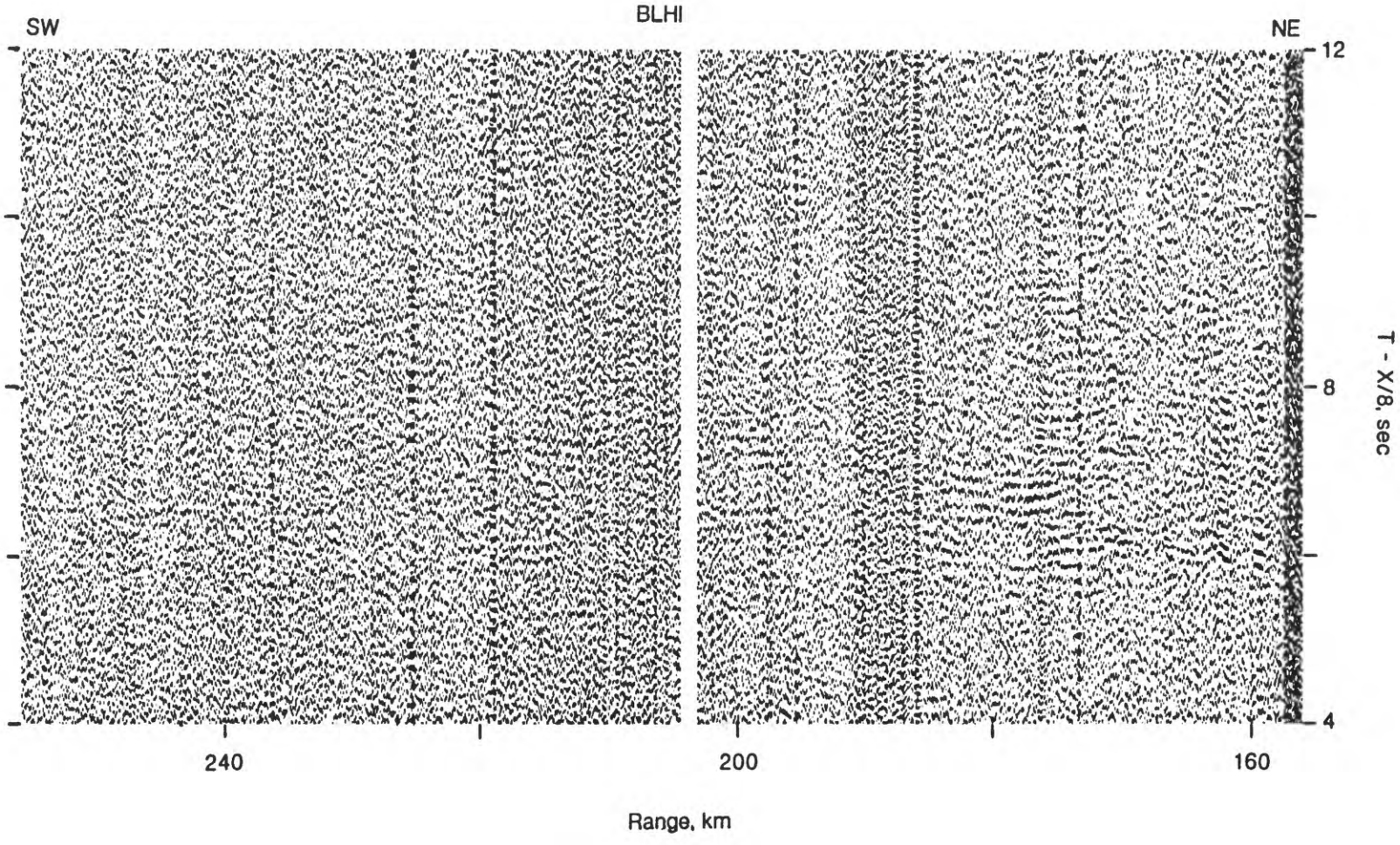

FIGURE 64. Receiver gather for station BLHI from lines TR and OBS2. The record section has been linearly reduced using a velocity of 8 km/s and trace amplitudes have been scaled according to Range$^{0.7}$.

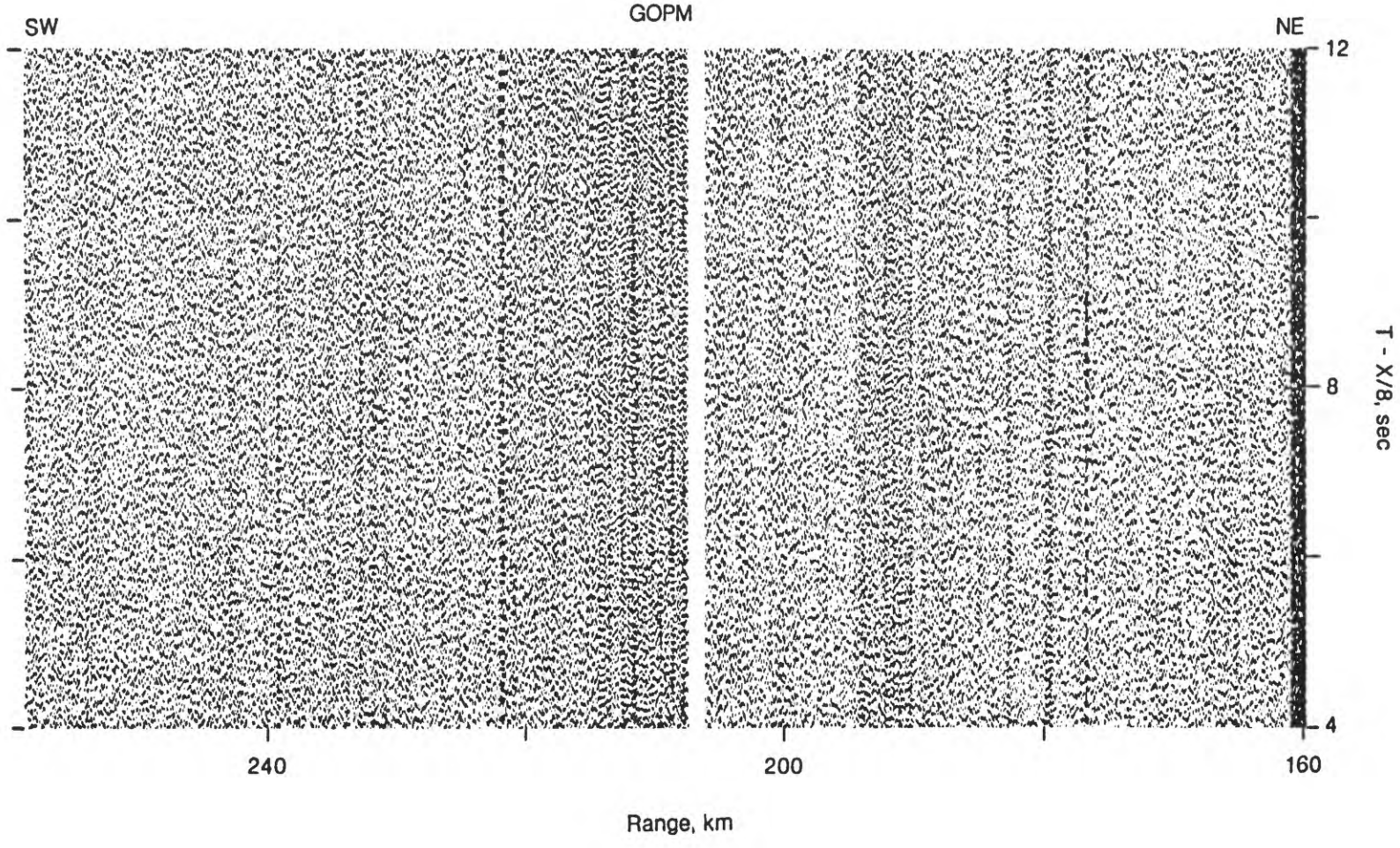

FIGURE 65. Receiver gather for station GOPM from lines TR and OBS2. The record section has been linearly reduced using a velocity of 8 km/s and trace amplitudes have been scaled according to Range$^{0.7}$.

ACKNOWLEDGEMENTS

We thank Jill McCarthy of the USGS for organizing and heading the BASIX project. Numerous private landowners kindly gave us permission to locate USGS 5-day recorders on their property. We thank Mr. Kevin Shea of East Bay Regional Park District, Mr. Barney Barrons of Golden Gate Park, San Francisco, and Mr. Brian Hunter and Mr. Jim Swanson of the California Department of Fish and Game for providing access to property under their jurisdiction. John Coakley, Dave Croker, and Gonzalo Mendoza of the USGS-Menlo Park deployed the 5-day recorders. We are pleased to acknowledge the able seamanship of the Captain and crew of the **S.P. Lee** and the technical assistance of the USGS Marine Facility for preparing and maintaining the airgun array. Jon Childs, Pat Hart, Walt Olson, and Kevin O'Toole provided valuable technical assistance onboard the R/V **S.P. Lee**. Steve Holbrook provided the USGS OBS locations, depths, and along track locations. Rick Clymer provided the University of California Berkeley recorder locations. Simon Klemperer provided station locations for the Stanford University Reftek recorders. Dan Pope and Vicki Goetcheus helped to digitize the five-day analog tapes. Willie Lee and Phil Dawson provided assistance in getting the new digitizing system working. Will Kohler, Jim Luetgert, and Peter Ward provided programming assistance. PASSCAL loaned Stanford University the Reftek recorders used during the BASIX experiment. Jim Luetgert and H.M. Iyer provided useful comments on an earlier draft of this report.

This work was supported by the National Earthquake Hazards Reduction Program.

REFERENCES CITED

Barry, K.M., D.A. Cravers, and C.W. Kneale, 1975, Recommended standards for digital tape formats: *Geophysics, v. 40,* p. 344-352.

Brocher, T.M., S.L. Klemperer, U.S. ten Brink, and W.S. Holbrook, 1991, Wide-angle seismic profiling of San Francisco Bay Area faults: Preliminary results from BASIX: *Eos (American Geophysical Union Transactions), v. 72,* p. 446.

Brocher, T.M., and M.J. Moses, 1990, Wide-angle seismic recordings obtained during the TACT multichannel reflection profiling in the northern Gulf of Alaska: *U.S. Geological Survey Open-file Report 90-663,* 40 pp.

Brocher, T.M., M.J. Moses, and S.D. Lewis, 1992, Wide-angle recordings obtained during seismic reflection profiling by the S.P. Lee offshore the Loma Prieta epicenter: *U.S. Geological Survey Open-file Report 92-245,* 63 pp.

Brocher, T.M., M.J. Moses, and S.D. Lewis, in press, Evidence for tectonic wedging west of the San Andreas fault based on onshore-offshore wide-angle seismic recordings: *U.S. Geological Survey Professional Paper.*

Catchings, R.D., and G.S. Fuis, 1991, Influence of crustal structure on the 1989 Loma Prieta earthquake and associated destruction: *Eos (American Geophysical Union Transactions), v. 72,* p. 338.

Criley, E., and J. Eaton, 1978, Five-day recorder seismic system: *U.S. Geological Survey Open-file Report 78-266,* 85 pp.

Ellsworth, W.L., 1990, Earthquake history, 1769-1989: *U.S. Geological Survey Professional Paper 1515,* p. 153-187.

Furlong, K.P., 1984, Lithospheric behavior with triple junction migration: An example based on the Mendocino triple junction: *Physics of the Earth and Planetary Interiors, v. 36,* p. 213-223.

Furlong, K.P., W.D. Hugo, and G. Zandt, 1989, Geometry and evolution of the San Andreas fault zone in northern California: *Journal of Geophysical Research, v. 94,* p. 3100-3110.

Furlong, K.P., J. McCarthy, and T. McEvilly, 1991, Geometry and kinematics of the Pacific-North American Plate Boundary in the San Francisco Bay Area: A testable model for BASIX: *Eos (American Geophysical Union Transactions), v. 72,* p. 445-6.

Hart, P.E., and R. Clymer, 1991, Geometry of San Francisco Bay Area faults: Preliminary results from BASIX: *Eos (American Geophysical Union Transactions), v. 72,* p. 446, 1991.

Hill, D.P., J.P. Eaton, and L.M. Jones, 1990, Seismicity, 1980-86: *U.S. Geological Survey Professional Paper 1515*, p. 115-151.

Holbrook, W.S., and U.S. ten Brink, 1991, San Francisco Bay and Margin Seismic Experiment: Ocean bottom seismometer operation, September, 1991: *Woods Hole Oceanographic Institution, Preliminary Cruise Report.*

Holbrook, W.S., and W.D. Mooney, 1987, The crustal structure of the axis of the Great Valley, California, from seismic refraction measurements: *Tectonophysics, v. 140*, p. 49-63.

Klemperer S.L., and BASIX Working Group, 1991, Bay Area Seismic Imaging eXperiment: Fan-profiling to image the maximum depth of penetration of the San Andreas, Hayward, and Calaveras faults: *Eos (American Geophysical Union Transactions), v. 72*, p. 446.

Kerr, R.A., 1990, Worse News for the Bay Area: *Science, v. 249,* p. 860.

Lewis, S.D., 1990, Deformation style of shelf sedimentary basins seaward of the San Gregorio fault, central California: *Eos (American Geophysical Union Transactions), v. 71*, p. 1631.

Luetgert, J., S. Hughes, J. Cipar, S. Mangino, D. Forsyth, and I. Asudeh, 1990, Data report for O-NYNEX the 1988 Grenville-Appalachian seismic refraction experiment in Ontario, New York, and New England: *U.S. Geological Survey Open-file Report 90-426*, 51 pp.

McCarthy, J., and P.E. Hart, 1993, Data report for the 1991 Bay Area Seismic Imaging Experiment (BASIX): *U.S. Geological Survey Open-file Report 93-301,* 27 pp.

Namson, J.S., and T.L. Davis, 1988, Seismically active fold and thrust belt in the San Joaquin valley, central California: *Geological Society of America Bulletin, v. 100,* p. 257-273.

Somerville, P., and J. Yoshimura, 1990, The influence of critical Moho reflections on strong ground motions recorded in San Francisco and Oakland during the 1989 Loma Prieta earthquake: *Geophysical Research Letters, v. 17,* p. 1203-1206.

Tottingham, D. M., and W. H. K. Lee, 1989, User manual for XDETECT, *in* W. H. K. Lee, editor, Toolbox for seismic data acquisition, processing, and analysis: *International Association of Seismology and Physics of the Earth Interior (IASPEI) Software Library Vol. 1,* p. 89-118.

U.S. Geological Survey staff, 1990, The Loma Prieta, California, earthquake: An anticipated event: *Science, v. 247*, p. 286-293.

Vuillermoz, C., A.J. Bertagne, and R. Delzer, 1987, Sacramento delta: new approach to seismic exploration in areas of near-surface problems: *Oil & Gas Journal, v. ?*, p. 63-66.

Ward, P. L., and F. Williams, 1992, The Seismic Unified Data System, Version 2.0: unpublished manuscript, 147 pp.

Zoback, M.D., and others, 1987, New evidence on the state of stress of the San Andreas fault system: *Science, v. 238*, p. 1105-1111.